PRECISE METHODS FOR PRE-CALCULATION OF CYCLOTRON CONTROL SETTINGS

By

Richard Eugene Berg

A THESIS

Submitted to
Michigan State University
in partial fulfillment of the requirements
for the degree of

DOCTOR OF PHILOSOPHY

Department of Physics and Astronomy

1966

ABSTRACT

PRECISE METHODS FOR PRE-CALCULATION
OF CYCLOTRON CONTROL SETTINGS

by Richard Eugene Berg

A computer program, SETOP, has been written which uses measured magnetic fields and a pre-computed set of ideal average fields to determine "operating points" for the MSU variable-energy, multi-particle cyclotron; to obtain a complete set of operating instructions, the experimenter need only specify the particle and energy of interest. Control settings are computed in a straightforward sequence of operations: (1) the fields at the desired excitation are synthesized by interpolation in the measured field data, (2) an average field is obtained using a modified least squares fit of the desired average field by the trim coils, and (3) the RF frequency is determined so as to minimize the energy spread of the beam in a single turn at the extraction energy. Independent numerical orbit studies were employed to investigate important features of the separated longitudinal equations of motion as used in SETOP, and several diagnostic procedures were investigated using numerical orbit integration to establish their validity under conditions obtained in the MSU cyclotron. Finally, the results of experimental measurements of several dynamical beam properties are presented which are in excellent agreement with pre-computed values.

ACKNOWLEDGMENTS

I should like to thank Dr. H. G. Blosser and Dr. M. M. Gordon for their guidance during this work. I am also grateful to T. I. Arnette, W. Joho, and D. A. Johnson for use of their computer programs in various phases of the numerical work.

A special word of thanks is also due Mr. Craig Barrows and Mrs. Judy Hilbert for their help in preparing the figures, and to Miss Wilma Sanders for her typing.

Finally, I am indebted to the National Science Foundation for the financial support without which this work would not have been possible—especially for an NSF Graduate Fellowship during the final year.

TABLE OF CONTENTS

LIST OF TABLES

LIST OF FIGURES

Figure Page

Figure | Page

Figure Page

Figure

Page

INTRODUCTION

The Michigan State University cyclotron is a multi-particle, variable-energy machine with a maximum proton energy of 56 MeV. The low-spiral magnetic field configuration, obtained through model magnet studies[1], minimizes saturation effects while optimizing the radial average field contour for the desired range of particles and energies. The RF system consists of two 134° dees, and can be operated in either push-pull or push-push modes over a frequency range of approximately 13.5 to 22 megacycles[2], allowing acceleration of particles on any harmonic. Maximum energies for typical particles are: 56 MeV protons, 28 MeV deuterons, 56 MeV alphas, 75 MeV $^{3}He^{2+}$ ions, and 75 MeV $^{12}C^{4+}$ ions; a more complete survey of expected energy ranges for various particles which can be accelerated using the MSU cyclotron is given in Fig. 1.

In the design of sector-focused cyclotrons, as well as in other areas of physics, the computer has come to be an indispensable tool. Indeed, a substantial amount of recent progress in cyclotron physics would not have been possible without the high-speed digital computer. Early sectored cyclotron work made use of numerical techniques to approximate the magnetic field of a given magnet configuration; later, numerical approximations were used to determine orbit properties in more detail[3]. In most cases, operation of these early machines was accomplished by relatively simple "knob-twiddling" techniques. However, with the increasing desire of cyclotron builders to obtain variable-energy and multi-particle features in a single

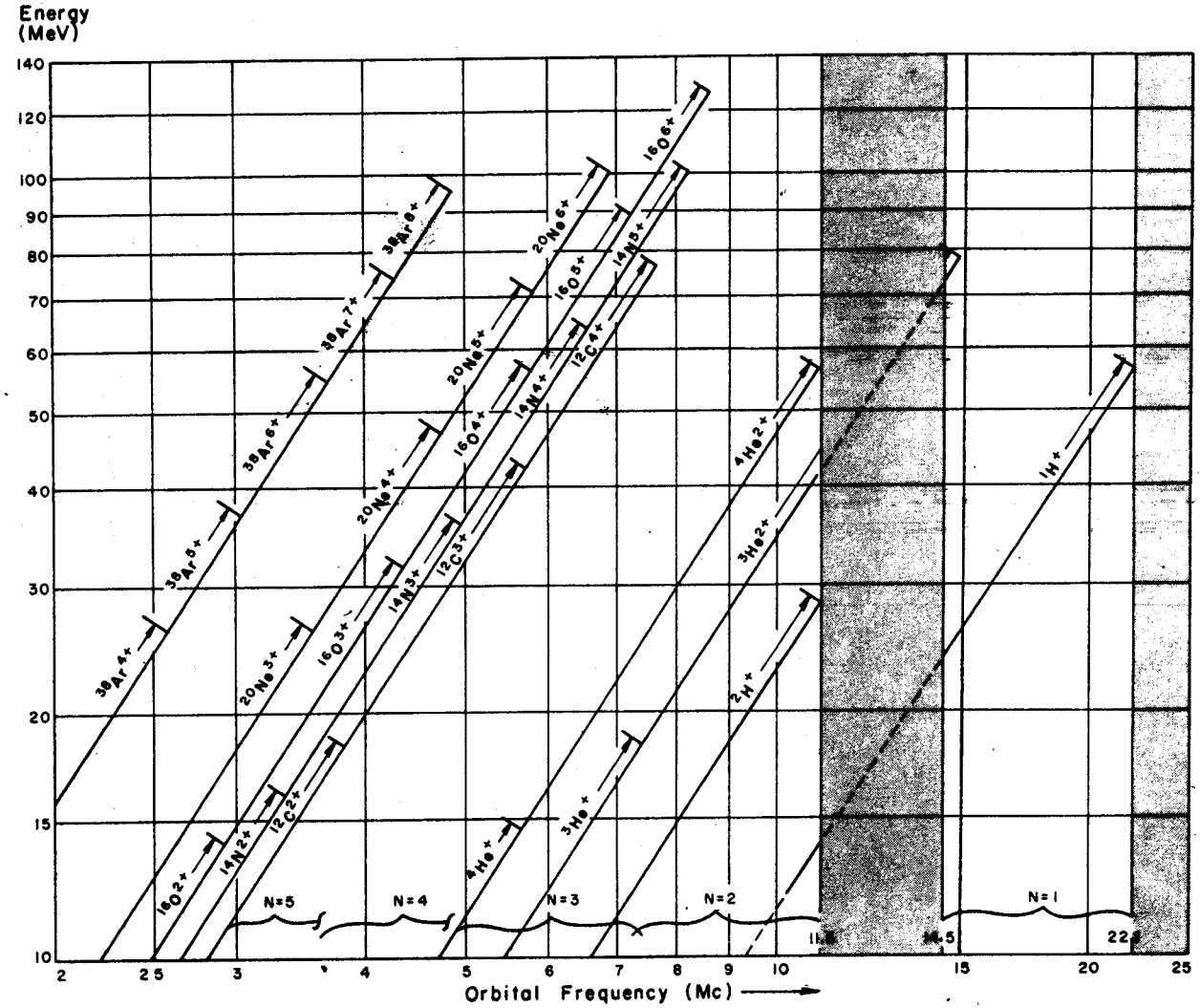

Figure 1. Energy versus orbital frequency for various particles which can be accelerated by the MSU cyclotron. Gray bands indicate areas outside the tuning range of the rf system; intermediate energy protons are obtained by using negative hydrogen ion acceleration with stripping extraction at partial radius.

machine, as well as the desire to obtain higher energies, a vastly more complicated program including model magnet measurements and detailed orbit computations became necessary to insure adequate operation of the final machine. Introduction of these diverse features and the concomitant complexity in the cyclotron hardware require extensive computer use both in the design of the cyclotron and in setting up the operation of the machine. With the powerful computer programs now available essentially all aspects of the behavior of orbits in cyclotrons can be observed and understood.

The computer has been used extensively at Michigan State University in the development of most of the basic cyclotron components, most notably in the central region, electrostatic deflector, magnetic channel, and beam handling system as well as the magnetic field[4,5,6,7]. In the case of the MSU cyclotron, the resulting control system includes roughly twenty variables which must be set with varying degrees of precision in order to obtain successful acceleration of particles to the extraction radius, namely main magnet excitation, trim coil excitations, RF frequency and voltage, valley coil first harmonic amplitude and phase, as well as parameters dealing with the central region and extraction system. In this paper techniques are presented for determining proper settings for all controls except those for the central region and extraction system, which have been discussed elsewhere[8,9].

Optimally, any calculation of operating values for the various controls should provide the best beam characteristics

possible within the limits of accuracy of the necessary measurements, where the best beam is defined as that with minimum energy spread at extraction possessing adequate optical properties. Computations predicting operating points for variable-energy cyclotrons have been performed previously, most notably those using a linear programming method through which trim coils, main field, and RF frequency and voltage may be simultaneously adjusted subject to constraints on various beam parameters such as axial and radial focusing frequencies and the phase of the particle with respect to the RF voltage[10]. This work deals with computation of cyclotron operating points for a multi-particle, variable-energy cyclotron such as the Michigan State University machine.

Preliminary to the final computations of operating conditions, an extensive set of magnetic field measurements was performed. A single computer program has been compiled which uses the measured magnetic field data and pre-computed ideal average fields to obtain operating points in a straightforward sequence of operations. Behavior of orbits in fields computed by the operating point program has been investigated theoretically with independent orbit integration programs, and the results of the two methods of computation are in good agreement. Results of a number of such studies are presented herein. Finally, beam dynamical properties have been experimentally measured and are found to be in excellent agreement with the computed values.

The approach toward computation of cyclotron operating points used at MSU is substantially different from the previous

work at other institutions; this difference in approach is partially a result of the desire to obtain single turn extraction[11] and the stringent requirements which this method of operation places on the various operating parameters.

With the MSU procedure a great deal of effort is invested in setting up an optimized average field called an "ideal field", previous to the actual operating point calculations. At each of the measured main field excitation values, a set of ideal average fields is pre-computed for each of the desired particles. The procedure used to obtain these ideal average fields is to first compute isochronous fields, then to introduce small deviations from isochronism to obtain desired beam properties for each field individually and collectively for each particle with respect to variable-energy operation. In setting up an operating point, the cyclotron field is adjusted or trimmed to conform to the ideal shape by a set of circular correcting coils. Required currents for the various coils are computed using a modified least squares procedure described in detail in Section 4. Results show that such a program for obtaining a fitted field yields beam properties for the fitted field which are essentially identical to corresponding properties in the ideal field.

Fields at intermediate excitation values at which magnetic fields have not been measured are obtained by interpolation in both measured fields and ideal fields. Criteria for an adequate interpolation scheme have been set up, and various schemes devised to meet the criteria have been investigated, and are discussed in Section 3. The scheme which best satisfies the re-

quirements is a double three-point Lagrangian interpolation with provision for a weighting factor which forces continuity of the first derivative of the magnetic field with respect to main magnet excitation.

Linear orbit properties of the fitted magnetic fields are investigated by computing sets of equilibrium orbits (using the MSU equilibrium orbit program) covering the entire energy range for that field. Inspection of the equilibrium orbit data reflects the adequacy of the interpolation and field fitting procedures in terms of the requirements on the radial and axial focusing frequencies and the phase history. Typical results are presented in Section 7. The extraction energy, obtained from the equilibrium orbit data, is defined by the geometry of the magnetic field in the edge region and the position of the entrance to the electrostatic deflector. With the energy set the dee voltage is fixed to yield a uniform 220 turn orbit geometry for all particles at all extraction energies.

Finally, using decoupled longitudinal equations of motion, an RF frequency correction is computed which minimizes the energy spread of the beam at the extraction energy. This procedure is quite similar to the more familiar computation of a frequency which balances the phase history curve about zero degrees[12], but has the advantage of more precisely minimizing the energy spread of the extracted beam. Also, for comparison with other calculations, the longitudinal equations of motion are integrated to obtain the phase-energy history of the beam as a function of turn number.

Detailed discussion of methods and procedures outlined

above are presented in following sections, along with other information pertaining to the operating point computation. Discussion of results of such calculations is presented both individually and collectively with particular emphasis on the attainment of an accurate method for continuous energy variation.

Section 8, in addition to surveying beam measurements, gives results of detailed comparison of computed and measured beam properties, with emphasis on use of the computer as a diagnostic tool.

I. MAGNETIC FIELD MEASUREMENTS

Magnetic field measurements on the Michigan State University cyclotron and analysis of the data obtained have been described in an MSUCP report[13], and will be summarized here to the extent necessary for understanding of subsequent material.

A thermoelectrically-cooled Hall probe with an accuracy of better than 5 parts in 100,000 was employed for the magnet measurements[14]. The Hall voltage was amplified, and digitized by a voltage-to-frequency converter and a frequency counter, and the resulting data punched automatically on cards; random error in the complete measuring system was kept below 1 part in 10,000. Using a deuteron NMR probe to monitor the field during all measurements, the magnet drift was observed to be less than 1 part in 10,000.

Measurements were made on a polar grid of points of one inch radial spacing at four degree azimuthal intervals[15]. The radial position was in most cases correct to within 0.001 inches, while the azimuthal position was controlled to about 0.005 degrees. The absolute azimuthal position was reproducible to within 0.005 degrees.

Variable-energy, multi-particle operation of a cyclotron imposes stringent demands on the accuracy with which the magnetic fields must be known over the entire excitation range of the magnet; magnetic field elements for the MSU machine consisted of the main magnet, eight pairs of concentric circular trimming coils, and a set of identical first harmonic coils located in each magnet "valley" near the position of the maximum average

field (or, equivalently, at the $\nu_r = 1$ resonance). It is necessary to measure the magnetic field at a number of excitations with spacing close enough to allow accurate interpolation of the field at intermediate excitations. The time required for a complete set of magnet measurements imposes a practical upper limit on the number of excitations at which the field can be measured. (In the case of the MSU measurements, one complete measurement scan——R = 0, 1, 2, ...46 inches, $\theta = 0^\circ, 4^\circ, 8^\circ,$ .....360°——required a minimum time of sixteen hours.) In the light of these requirements, the field of the main magnet was measured at seven approximately equally-spaced magnetic field intervals covering a range of average fields between 6 kilogauss and 15 kilogauss. The adequacy of this procedure was verified by interpolating to obtain the field at an excitation where it had also been measured. Differences between measured and interpolated field components are typically of the order of a few gauss out of 10,000 gauss, which is sufficient accuracy for present computations. (The accuracy should, in fact, improve, since the central interval for this check is twice that used in computing interpolated fields for orbit studies.)

A Fourier analysis was performed on the main field data at each measured radius, and the effective median plane magnetic field expressed in terms of the Fourier components $\langle B(r,\theta)\rangle$, $H_3(r)$, $G_3(r)$, $H_6(r)$, $G_6(r)$, $H_9(r)$, $G_9(r)$, $h_1(r)$, and $g_1(r)$, where:

$$B(r,\theta) = \langle B(r,\theta)\rangle + \sum_{n=1}^{3}[H_{3n}(r)\cos 3n\theta + G_{3n}(r)\sin 3n\theta] + h_1(r)\cos\theta + g_1(r)\sin\theta, \qquad (1\text{-}1)$$

or, alternatively, in terms of the Fourier amplitudes B_i:

$$B(r,\theta) = \langle B(r,\theta)\rangle + \sum_{n=1}^{3} B_{3n}(r)\cos 3n(\theta-\delta_{3n}(r)) + b_1\cos(\theta-\delta_1(r)), \quad (1\text{-}2)$$

where:

$$B_i(r) = \sqrt{H_i^2(r) + G_i^2(r)}, \quad (1\text{-}3)$$

and:

$$\delta_i(r) = \frac{1}{i}\,\mathrm{Arctan}\left|\frac{G_i(r)}{H_i(r)}\right| . \quad (1\text{-}4)$$

The seven sets of main magnet average field components $\langle B(r,\theta)\rangle$ were "smoothed" by a graphical procedure to within about 5 parts in 100,000; this procedure was chosen instead of a numerical device because it allowed discrimination against a known systematic error in the positioning device used in the measurements while rendering other data points unchanged. (See Reference 13 for details.) It was not necessary to apply any smoothing procedure to the flutter components since the effects on orbits due to the errors in the flutter smoothness are negligibly small. Studies showed that sufficient detail in the orbit properties could be obtained with a truncated Fourier representation consisting of only the average field, third, sixth, and ninth harmonics. Since the behavior of orbits in the vicinity of the $\nu_r = 1$ resonance depends very sensitively on the

magnetic field first harmonic and its derivative, it was necessary to carefully smooth these functions. The cosine and sine components of the first harmonic at each measured main magnet excitation were smoothed by least square fitting with Legendre polynomials, with a resulting RMS deviation between measured and fitted components of about 0.1 gauss. (The amplitudes of the first harmonic components are typically of order one gauss over the accelerating region of the magnetic field, while the average field varies from six to fifteen kilogauss.) The resulting smoothed average field, flutter amplitudes, and first harmonic components (alternating measured fields spanning the range of excitations) are shown respectively in Figs. 2, 3, and 4. The measured first harmonic data are also shown in Fig. 4 to show in detail the effect of the smoothing procedure.

Previous measurements have shown that the incremental magnetic fields of circular average field trimming coils such as those of the MSU cyclotron are strongly dependent on the main magnet excitation, or equivalently, on the degree of saturation of the magnet pole tips. Therefore, it is necessary to measure trim coil fields at several main magnet excitation values in order to obtain an adequate representation of the trim coil fields over the entire excitation range. However, since the average field profile of a given trim coil changes quite smoothly with main magnet excitation, and the total contribution of all trim coils together never exceeds about three percent of the final average field in the case of

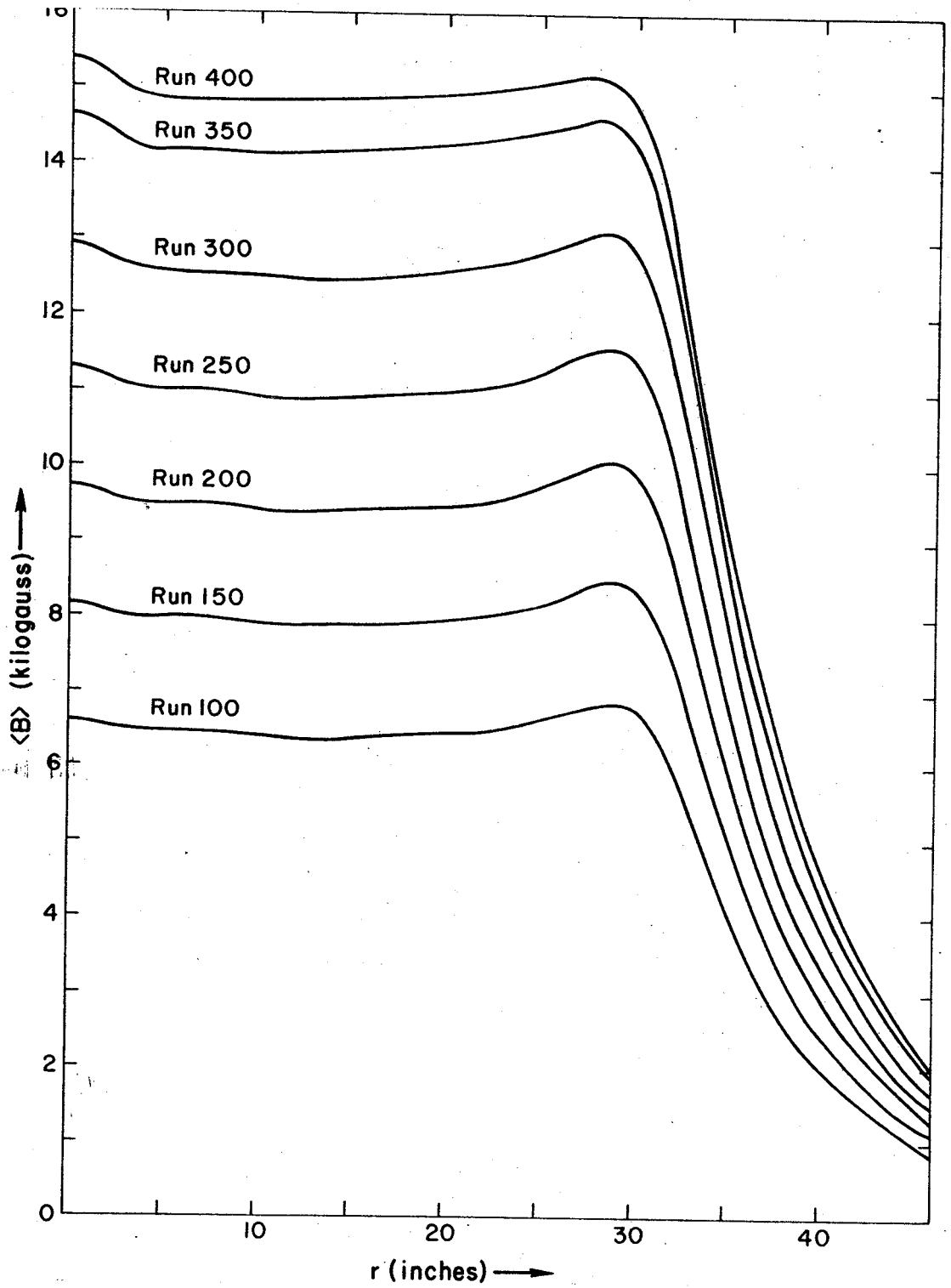

Figure 2. Azimuthal average of the magnetic field vs. radius for each measured excitation of the Michigan State University cyclotron.

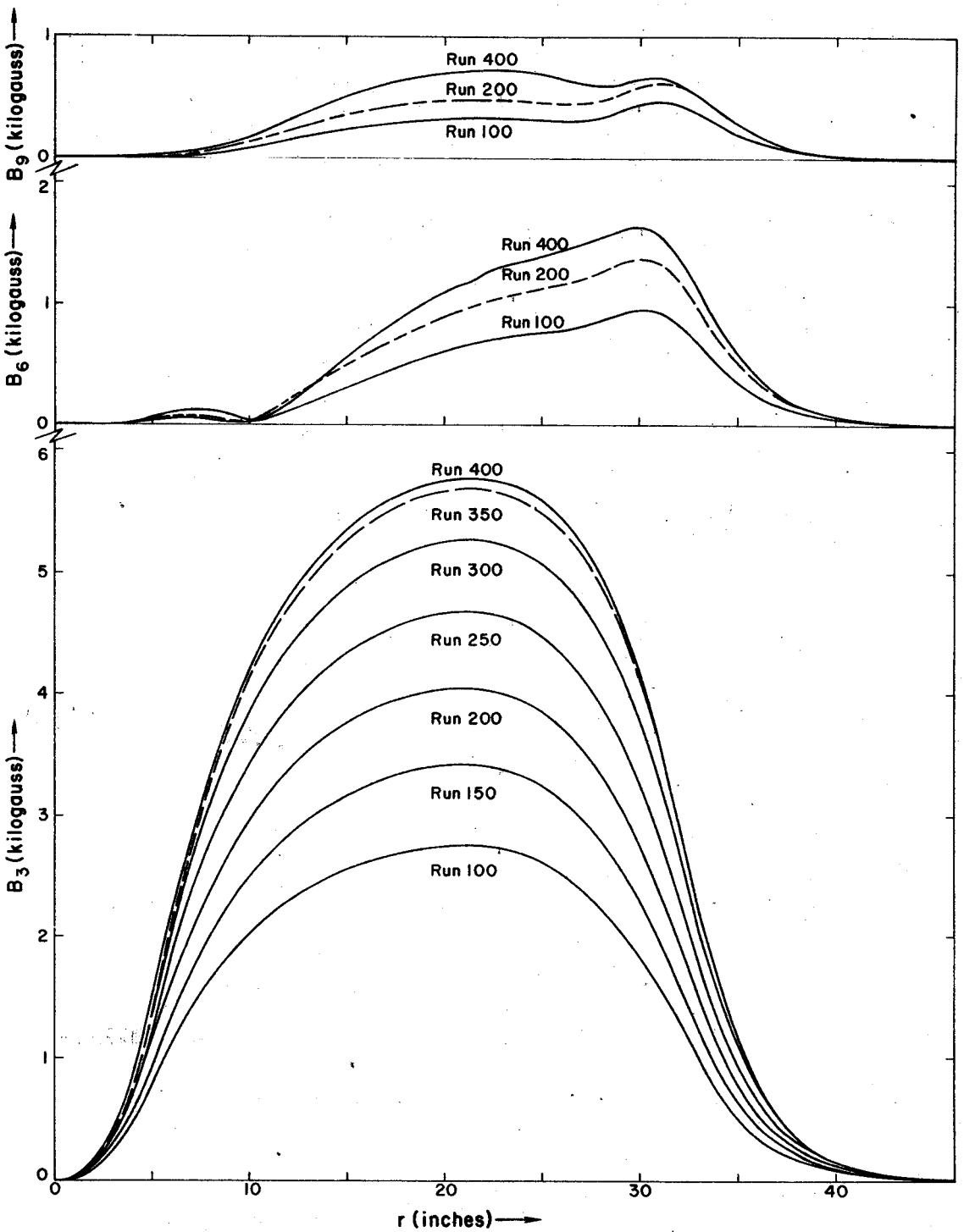

Figure 3. Amplitudes of the third, sixth and ninth field harmonics vs. radius for selected main field excitations of the Michigan State University cyclotron.

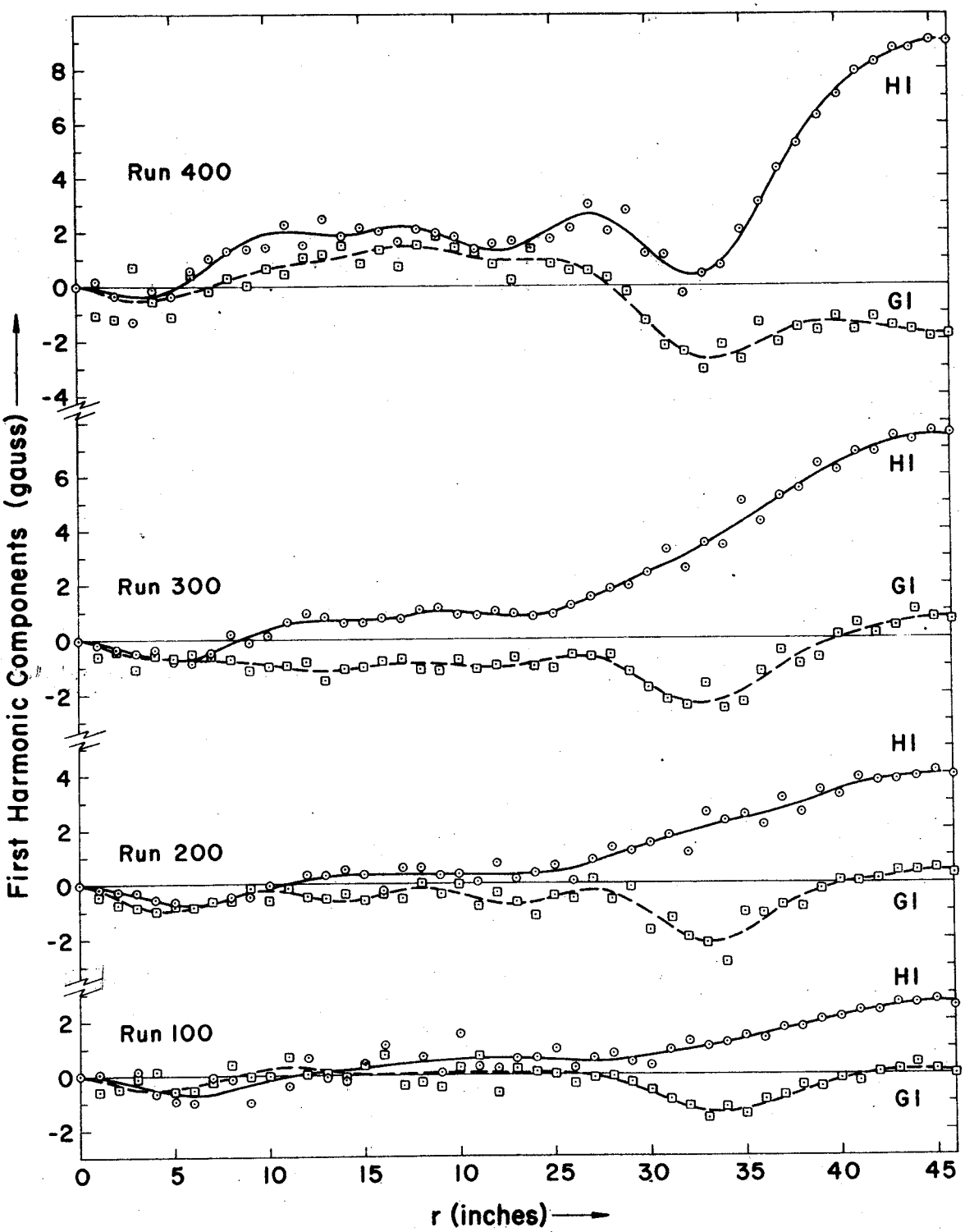

Figure 4. Magnetic field first harmonic sine and cosine Fourier components vs. radius for four main field excitations. Points show measured values; curves show result of smoothing computation. The large first harmonic at outer radii is due to main coil leads.

the MSU machine, it was not necessary to measure the trim coil fields at as many main field excitation values as were necessary for main field measurements. It was also determined to be unnecessary to perform measurements using combinations of trim coils, since coupling phenomena arising from changes in iron saturation due to trim coil fields are small compared to the fields themselves. A linearity check of the trim coil field as a function of current in the trim coil at a given main field excitation value showed that any non-linearity was undetectable with the measuring apparatus used over the entire current range of the trim coil power supply ($-200 \text{ amps} \leq I \leq 200 \text{ amps}$); therefore, each trim coil field was measured at only a single trim coil current setting. Trim coil fields were obtained at four main field excitation values using alternate single-sector (120°) field scans with the trim coil on and off respectively, and Fourier analyses performed on the incremental fields as a function of radius. Because the flutter components of the trim coil fields are small compared to the main field flutter and since introduction of trim coil flutter fields substantially complicates the computational procedure, flutter components of the trim coils were neglected in all ensuing calculations. (The amplitude of the third Fourier harmonic for any individual trim coil reaches a maximum of less than 1% of the main field third harmonic for typical values of trim coil current.) In a manner similar to the main field, the trim coil average fields were smoothed graphically to within about one gauss per 100 amps, where typical trim coil currents range, in

most cases, below 100 amps, as will be discussed later. Figures 5 and 6 show the incremental fields of the trim coils as a function of radius for each of the measured main field excitations.

In addition to the trimming coils which are concentric with the magnet pole, each valley of the magnet contains a small circular coil centered at a radius of 27 inches and used to control the first harmonic in the vicinity of the $\nu_r = 1$ resonance. The fields of these coils were found to closely approximate that of an air-core coil, with little change with main magnet excitation; thus it was deemed necessary to make field measurements for these valley coils at only two main magnet excitation values. A Fourier analysis of the incremental effect of the valley coil yielded the first harmonic sine and cosine components of its magnetic field. All other components were discarded; the coils are used with the algebraic sum of their currents equal to zero and thus produce no net average field component; other harmonics were found to be extremely small. Since the phase angle δ_1 of the first harmonic is relatively constant, a simplifying procedure was introduced in describing the valley coil first harmonic by a cosine component centered about the azimuthal position of the coil and thus possessing no spiral component, with a radial profile given by the measured cosine component. The data were smoothed graphically to within a few tenths of one gauss per 100 amps in the valley coil; the resulting radial profile of the valley coil first harmonic at both of the measured main field excitations is given in Fig. 7.

The resultant data were combined with ideal average fields,

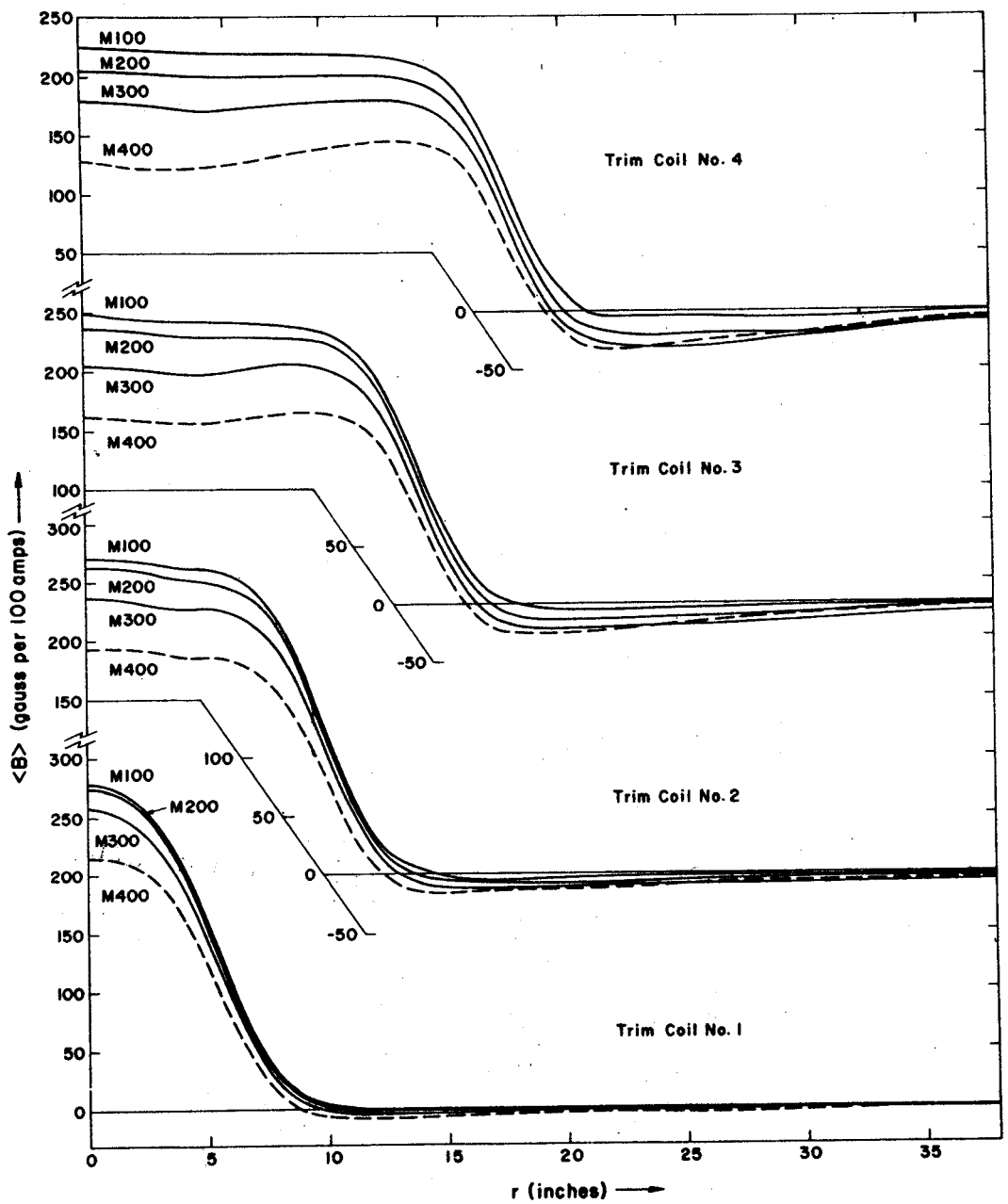

Figure 5. Average magnetic field vs. radius for trim coils 1-4 of the MSU cyclotron. Curves are shown for each trim coil for each of the four main field excitations at which the trim coil fields were measured.

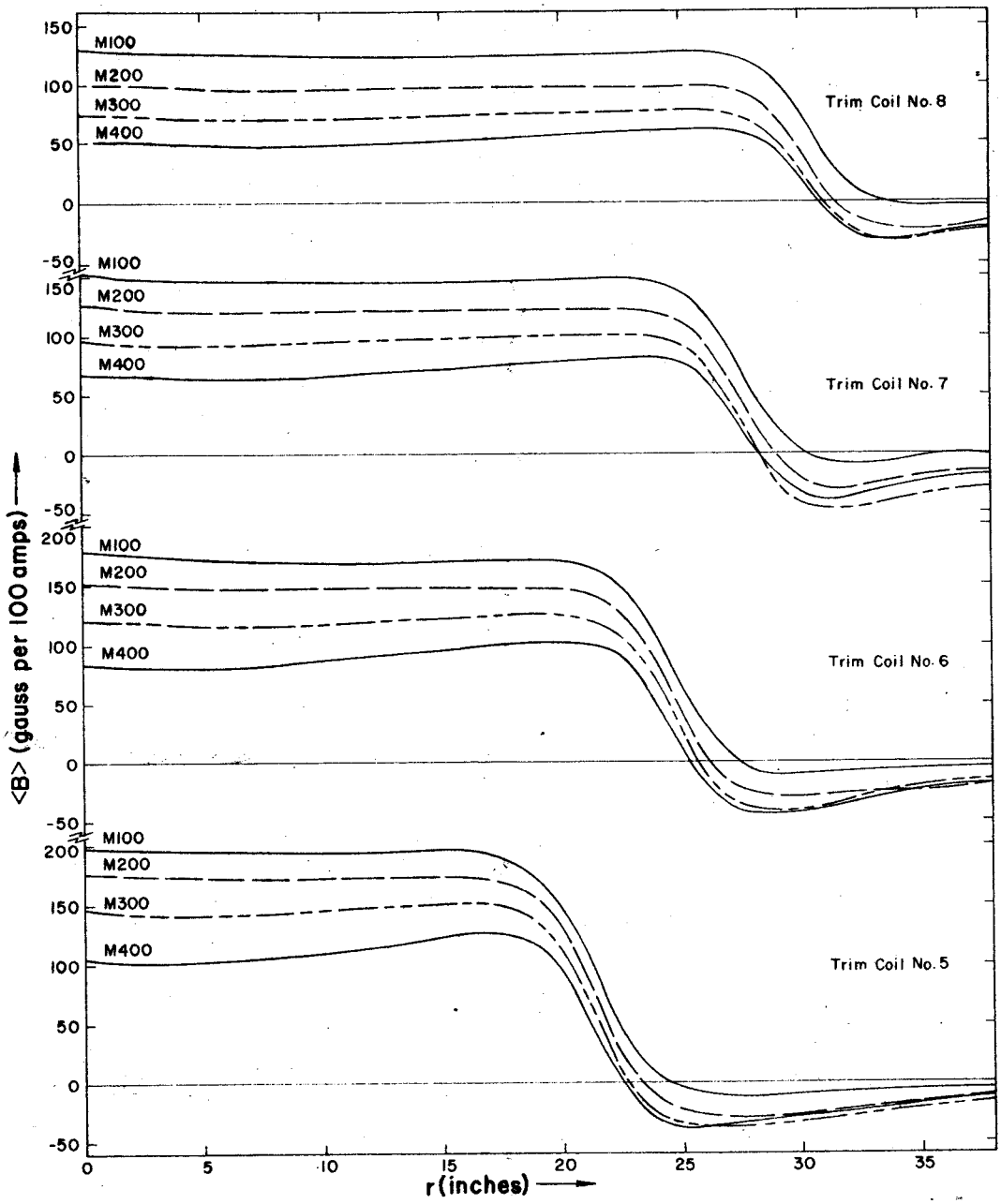

Figure 6. Average magnetic field vs. radius for trim coils 5-8 of the MSU cyclotron. Curves are shown for each trim coil for each of the four main field excitations at which the trim coil fields were measured.

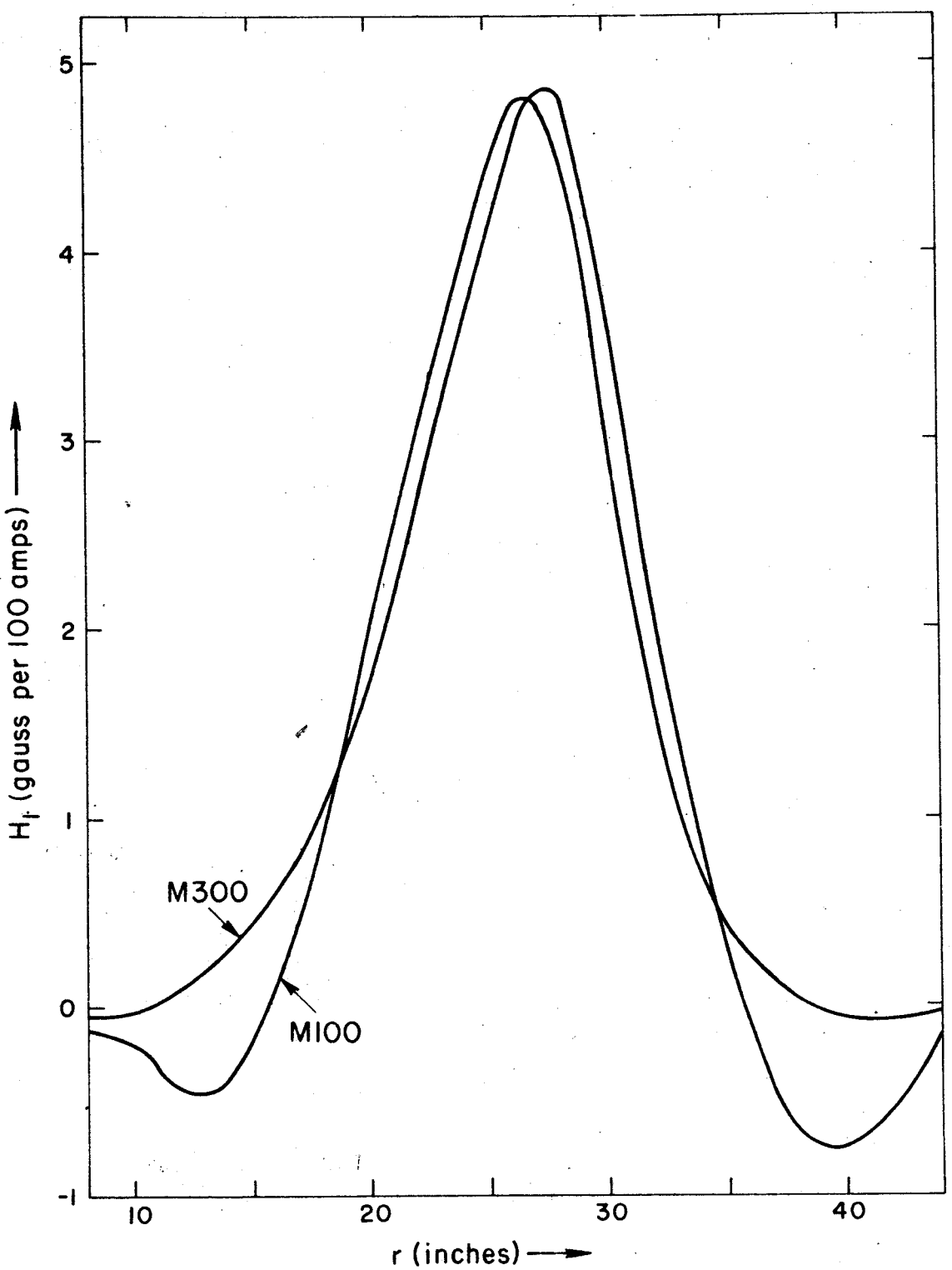

Figure 7. Smoothed magnetic field first harmonic amplitude vs. radius for one of the MSU cyclotron valley coils for both of the two main field excitations at which valley coil field was measured.

obtained as described in the following section, to yield a "master" field deck, the data appearing as follows:

(1) Main magnetic field data at each of the seven measured main field excitations:

(a) Proton ideal average field.

(b) Deuteron ideal average field.

(c) $^{12}C^{4+}$ ideal average field.

(d) $^{3}He^{2+}$ ideal average field.

(e) "Heavy ion" ideal average field.

(f) Main magnet raw average field.

(g) Flutter field Fourier components H_3, G_3, H_6, G_6, H_9, G_9.

(h) First harmonic Fourier components h_1, g_1.

(2) Trim coil data: average field of each trim coil at each of the four main field excitations at which it was measured.

(3) Valley coil data: first harmonic components of one valley coil at each of the two main field excitations at which it was measured.

II. COMPUTATION OF IDEAL AVERAGE FIELDS

In order to use the method described herein for the computation of operating points, it is necessary to obtain ideal average fields which possess good beam properties; this section outlines the aims and general procedures involved in the computation of ideal average fields, then describes in detail the methods used.

Ideal fields can be defined in terms of their focusing properties, and their ability to keep the particles in phase with the RF accelerating voltage over the entire acceleration range; the focusing properties are described primarily by the small amplitude radial and axial focusing frequencies. These frequencies, ν_r and ν_z, are related to the magnetic fields and their derivatives by the approximate formulas[16]:

$$\nu_r^2 = \left(\frac{\omega_r}{\omega}\right)^2 = 1 + \frac{R}{\langle B\rangle}\frac{d\langle B\rangle}{dR}, \qquad (2\text{-}1)$$

$$\nu_z^2 = \left(\frac{\omega_z}{\omega}\right)^2 = -\frac{R}{\langle B\rangle}\frac{d\langle B\rangle}{dR} + F(1+2\tan^2\alpha), \qquad (2\text{-}2)$$

where ω_r and ω_z are the angular frequencies of the small radial and axial oscillations, ω is the particle orbital angular frequency, R is the average radius, α is the magnetic field spiral angle, given by:

$$\tan\alpha = R\frac{d\delta}{dR}, \qquad (2\text{-}3)$$

where δ is the angle of the peak hill field, and F is the flutter function, defined by:

$$F = \frac{\langle B^2 \rangle - \langle B \rangle^2}{\langle B \rangle^2} = \frac{1}{2} \sum_{i=3,6,9} \left(\frac{B_i}{\langle B \rangle} \right)^2 , \qquad (2\text{-}4)$$

where $\langle B \rangle$ is the average magnetic field Fourier component and the B_i are the magnetic field Fourier amplitudes defined by equation (1-3). The phase history of an accelerated particle may be related to the magnetic field (see Section 8 for more complete derivation) by the approximate equation:

$$\sin\phi(R) = \sin\phi(o) + \frac{2\pi q \omega_o}{E_1} \int_o^R [B_I(R) - \langle B(R) \rangle] R dR , \qquad (2\text{-}5)$$

where the phase ϕ is defined by:

$$\phi = \theta_{RF} - \theta_{Particle} , \qquad (2\text{-}6)$$

and q is the particle charge, ω_o is the RF angular frequency, E_1 is the maximum energy gain per turn and $B_I(R)$ is the isochronous average field.

Equations (2-1), (2-2), and (2-5) are given here only as approximate guides to aid in understanding the procedure used to obtain ideal fields. In practice, numerical integration of the complete equations of motion is used to obtain precise values of these functions, as is described later.

From equations (2-1), (2-2), and (2-5) one notes that the

radial and axial focusing frequencies depend dominantly on the average field gradient whereas the phase history is determined dominantly by the average field alone. For the MSU cyclotron the following general criteria are placed on these functions:

(1) axial focusing frequency: ν_z should rise as rapidly as possible from the center of the machine to a value of about 0.2 and remain relatively constant over the acceleration range, until the field edge begins. In no case should ν_z dip below a value of 0.1.

(2) radial focusing frequency: ν_r should rise above unity as rapidly as possible from the center of the machine. In the edge region ν_r should drop rapidly through the $\nu_r = 1$ resonance to prevent excessive growth of radial amplitude and allow a well-controlled resonant extraction system. Also, to simplify extraction the radial dependence of the radial focusing frequency in the edge region should be constant as a function of main field excitation thus yielding uniform orbit precession in the extraction region, which greatly eases difficulties in computing extraction parameters[9].

(3) phase history: The phase should in general be kept as small as possible. However, it is acceptable to allow phase excursion up to about 45° when necessary to obtain adequate axial focusing and the desired extraction energy.

The steps used to obtain fields satisfying these requirements can be summarized as follows:

(1) Noting that the flutter is a fixed property of the pole

face configuration (in the absence of flutter coils), the isochronous average field for a given ion is unique and can be calculated. Since the isochronous field automatically satisfies criterion (3) above, a first approximation to the desired ideal field was taken to be the isochronous average field, joined smoothly to the edge field at the radius of the peak average field. Given this first approximation field, the focusing frequencies were computed and inspected.

(2) For all fields, it was deemed desirable to increase the axial focusing at the center of the cyclotron more rapidly than could be obtained due to the rise in flutter alone. This problem had been anticipated in designing the pole tips, which were arranged to provide a focusing gradient in the average field in the central region. (See Fig. 2.) This natural focusing shape of the average field, conventionally referred to as a field "cone"[17], was effectively included in the ideal fields by the simple device of omitting the region of radius less than 5 inches from the fitting process. Such a cone results in a relatively large phase shift per turn, but this is acceptable because of the small number of turns in this region. Furthermore, the phase shift is useful in that it introduces desirable behavior into the phase history on the first few turns—to obtain large first order electric focusing on the early turns, it is customary[18] to start the particles at a phase of between 30° and 40°; the cone then shifts the phase to a value favorable for acceleration. (The cone also introduces a dip in the radial focusing frequency followed by a rise

through $\nu_r = 1$. It has, however, been observed in computer studies and later experimentally with the cyclotron beam that passage through this resonance is not harmful to the beam if orbit centering is correct and the traversal occurs in a relatively small number of turns[17].)

(3) For proton fields of 40 MeV final energy and higher, axial focusing was inadequate from about 25 to 27 inches. (This problem resulted from the extension of the maximum energy from 40 to 55 MeV by increasing the effective radius after the flutter had been fixed for 40 MeV maximum energy.) For these high-energy protons the flutter was insufficient to compensate for the strong axial defocusing term introduced by the rapidly rising isochronous average field. It was, therefore, necessary to introduce carefully gauged deviations from isochronism in these fields to reduce the defocusing average field gradient.

(4) Finally, it was necessary to vary the ideal fields at some excitations to obtain the desired uniform radial focusing frequency in the edge region (to simplify the calculation of extraction parameters).

The remainder of this section will describe in detail the computations necessary to obtain a complete set of ideal average fields.

2.1 Computation of Isochronous Fields

For each of the measured main magnetic fields, an isochronous field was computed for each of the standard particles mentioned[19]. This isochronous field is computed out to the radius of the peak average field (see Fig. 2), where it is joined smoothly to the field in the edge region. The fact that the isochronous average field is joined to the main magnet average field in this manner considerably reduces the load on the trim coils while allowing an extremely accurate fit, since the magnitude of the resulting field correction required from the trim coils is in general a monotonically decreasing function of radius, with no changes of sign, going to zero at the position of peak average field.

The isochronous fields are calculated with the computer program "POLICY" using an analytical procedure which requires only knowledge of the flutter fields and the charge and mass of the desired particle. The method (developed by M. M. Gordon) makes use of the fact that the isochronous average field $B_I(R)$ as a function of radius can be expressed in terms of the momentum through the relation:

$$\frac{qRB_I(R)}{M_o c} = p\left(1 - \frac{\delta_2}{p^2}\right), \qquad (2\text{-}7)$$

where q and M are the particle charge and mass respectively, p is the momentum in units of $M_o c$, and δ_2 is a function of the flutter field and its derivatives. Another useful relation is:

$$v = R\omega\left(1 + \frac{\delta_1}{p^2}\right) , \qquad (2\text{-}8)$$

where v is the particle velocity, ω is the orbital angular frequency, and δ_1 is a function of the flutter field. The isochronous field is normalized by choosing its value to be the value of the peak average field at the radius where the peak occurs. Equation (2-7) is used to obtain the momentum p, which is used in turn in equation (2-8) to obtain ω. The isochronous frequency is taken to be this frequency, and a set of self-consistent "cyclotron units" defined[20]: frequency unit ω_o; length unit $a = c/\omega_o$; magnetic field unit $b = \frac{M_o c}{qa} = \frac{M_o \omega_o}{q}$. These units are primarily used internally in some program results. The RF frequency, in particular, is related to the frequency unit: $\omega_{RF} = h\omega_o$ where h is the RF harmonic number.

The isochronous field is computed working inward: p is evaluated by solving equation (2-8), and the resulting value used in equation (2-7) to obtain $B_I(R)$. The central field is taken to be equal to the cyclotron field unit b. To insure a smooth transition between isochronous field and edge field, the field at the transition radius is re-computed using four-point Lagrangian interpolation in the four neighboring points.

Sets of isochronous fields for the standard particles are shown in Figs. 8 and 9 along with main magnet average fields for two widely varied main field excitations (25 MeV and 52 MeV protons). Analytical error in the isochronous field computation results in a phase lag or lead per revolu-

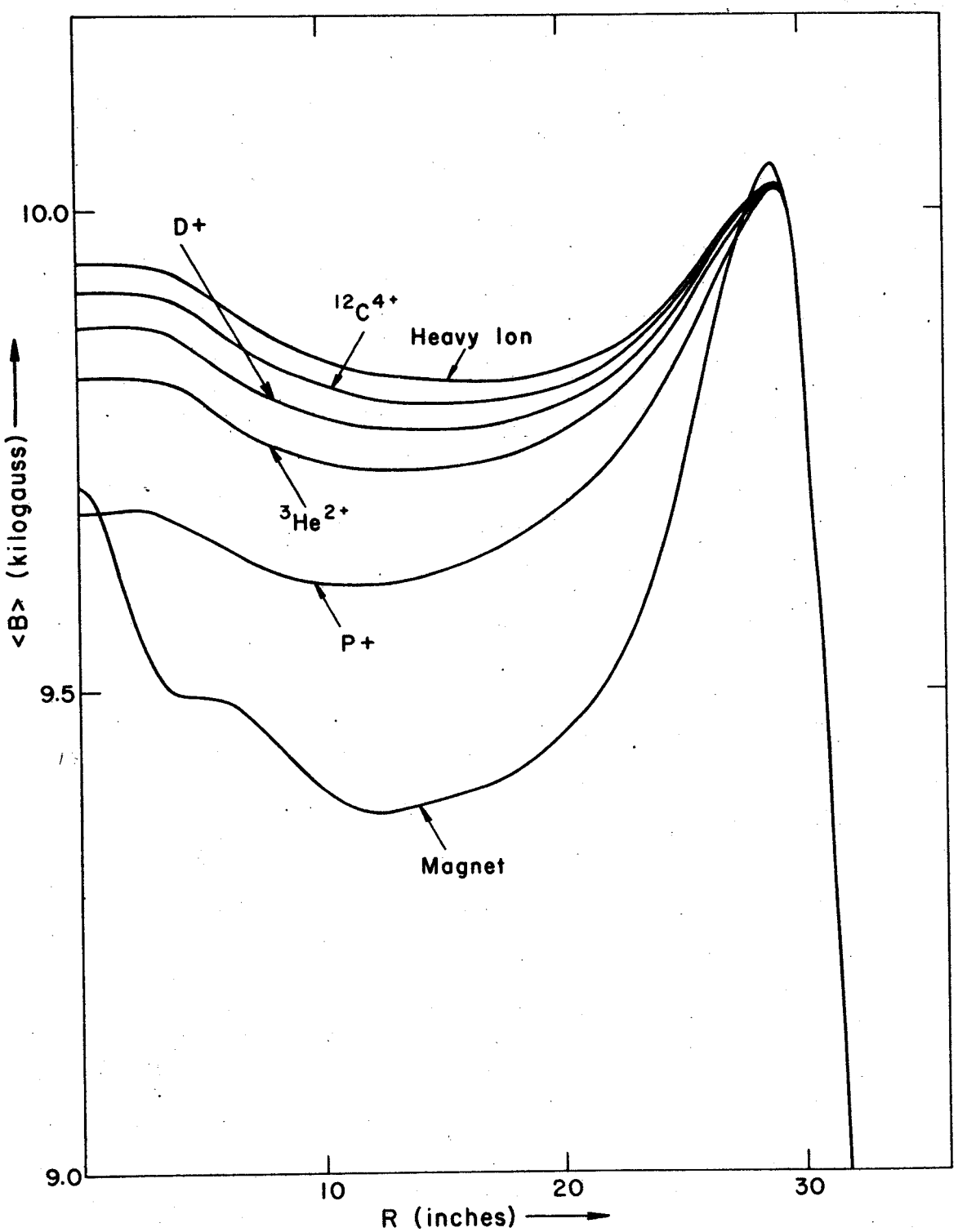

Figure 8. Isochronous average fields vs. radius for protons, deuterons, $^{3}He^{2+}$ ions, $^{12}C^{4+}$ ions and the "heavy ions", with main magnet average field for Run 200 (25 MeV protons).

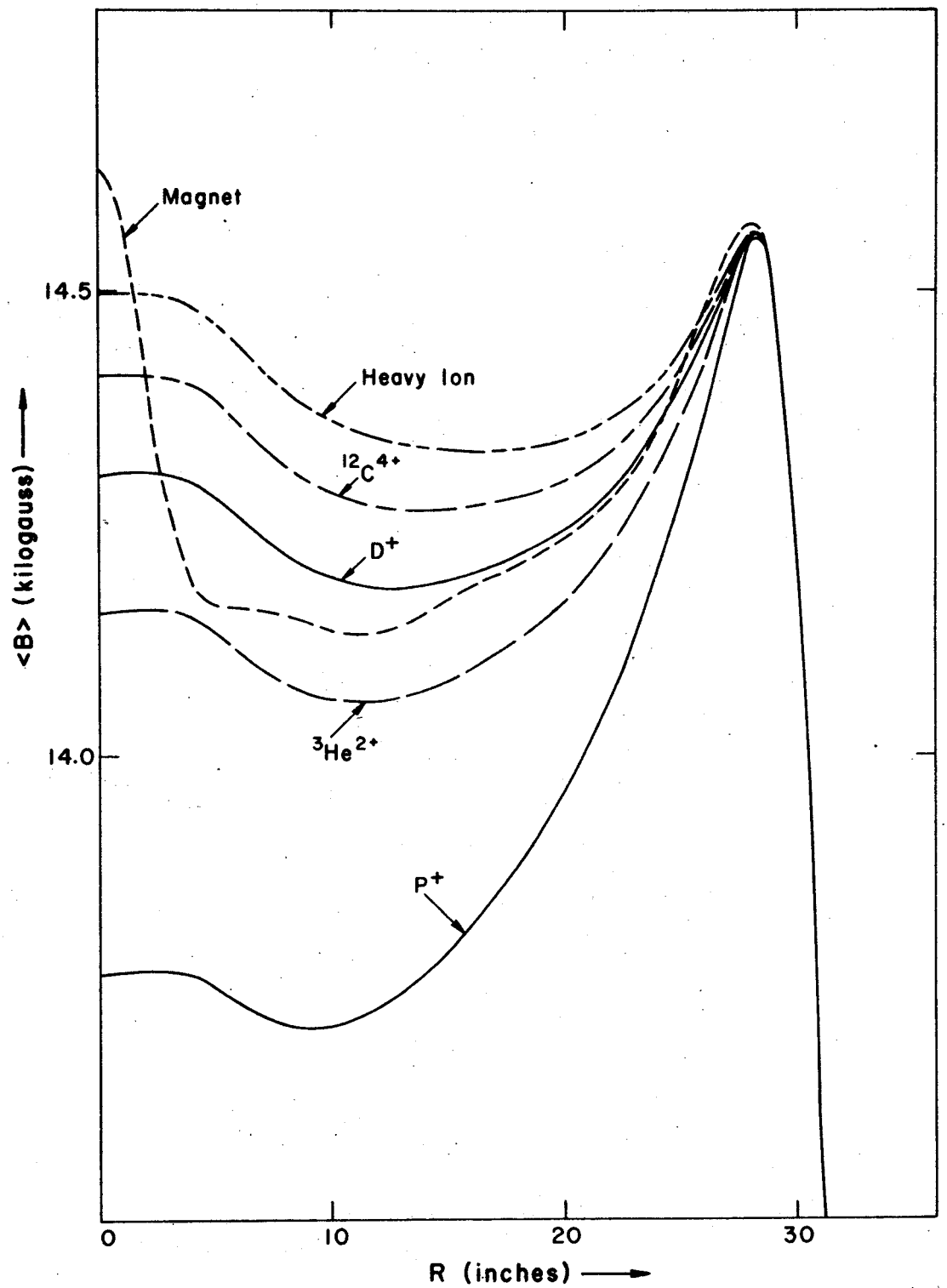

Figure 9. Isochronous average fields vs. radius for protons, deuterons, $^3He^{2+}$ ions, $^{12}C^{4+}$ ions, and the "heavy ion", with main magnet average field for Run 350 (52 MeV protons).

tion which is typically less than two parts per 10,000 over the field region which is isochronized. Note that the main magnet has been designed to possess an average field whose increase with radius lies between the extremes needed for acceleration of the various particles thereby reducing overall trim coil loads. Also, note that the isochronous field in the central region decreases with radius due to higher order effects involving the flutter gradient; this drop extends over half radius in the case of the heavy ions.

2.2 Axial Focusing Correction

For the high-energy proton fields it was necessary, as indicated previously, to de-isochronize the field to obtain axial focusing. The following equations are given as a guide to aid in understanding the method used. Approximations are used to initially obtain the average field correction; the validity of the approximations is then checked by exact computations using the equilibrium orbit code.

From before:

$$\nu_z^2 = - k(R) + F(R)[1+2\tan^2\alpha(R)], \qquad (2\text{-}2)$$

where:

$$k(R) = \frac{R}{\langle B\rangle}\frac{d\langle B\rangle}{dR} . \qquad (2\text{-}9)$$

The isochronous average field can be approximated by the function:

$$\langle B(R)\rangle = \frac{b}{\sqrt{1-v^2/c^2}}\,, \qquad (2\text{-}10)$$

where v is the velocity of the accelerated particle and b is the cyclotron field unit. For high-energy particles the isochronous average field rises so rapidly with radius that ν_z becomes imaginary, i.e., the field is axially defocusing. This unacceptable feature can be corrected either through use of flutter coils or by reduction of the average field gradient from the isochronous value. Because flutter coils are costly and difficult both to install and to operate, as well as adding additional complexity to the necessary magnetic field measurements and computations, a change of the average fields was preferred for these cases. The limits placed on such a procedure are that the de-isochronization must not be so severe as to yield large phase deviations (greater than $\pm 45^{\circ}$). Since in the first approximation the axial focusing frequency depends on the gradient of the average field, while the condition of isochronism depends on the average field alone, relatively large variations can be made in the axial focusing frequency while producing less significant changes in orbital frequency.

The following procedure for adjusting ν_z was devised and programmed by M. M. Gordon and W. Joho[21]. Assuming that the flutter is, in the first approximation, independent of average

field, equation (2-2) may be written as:

$$\nu_z^2 = - k(R) + \frac{\Delta(R)}{\langle B \rangle^2} \quad , \tag{2-11}$$

where $\Delta(r)$ is independent of average field. Defining $u = \langle B \rangle^2$, and using primed variables to indicate the desired values for ν_z and the average field gives:

$$\frac{d}{dR}(u'-u) = - \frac{2}{R}\left[\nu_z'^2(u'-u) + u(\nu_z'^2-\nu_z^2)\right] . \tag{2-12}$$

This can be rewritten as:

$$\frac{dy}{dR} = p(R)y + q(R) \tag{2-13}$$

where p(R) and q(R) are known functions of the old and new axial focusing frequencies. Solution of the differential equation for $y = u'-u = \langle B' \rangle^2 - \langle B \rangle^2$ gives the correction to the average field necessary to produce the desired ν_z. A corrected field was calculated over the range of radii where the axial focusing was insufficient. Smooth connection of the corrected average field to the isochronous average field was accomplished at the outer radius by means of the starting conditions chosen for the integration. The average field below the corrected region was joined smoothly to the corrected region by scaling the isochronous field for all radii inside the corrected region.

An example of such a calculation is shown in Fig. 10 for

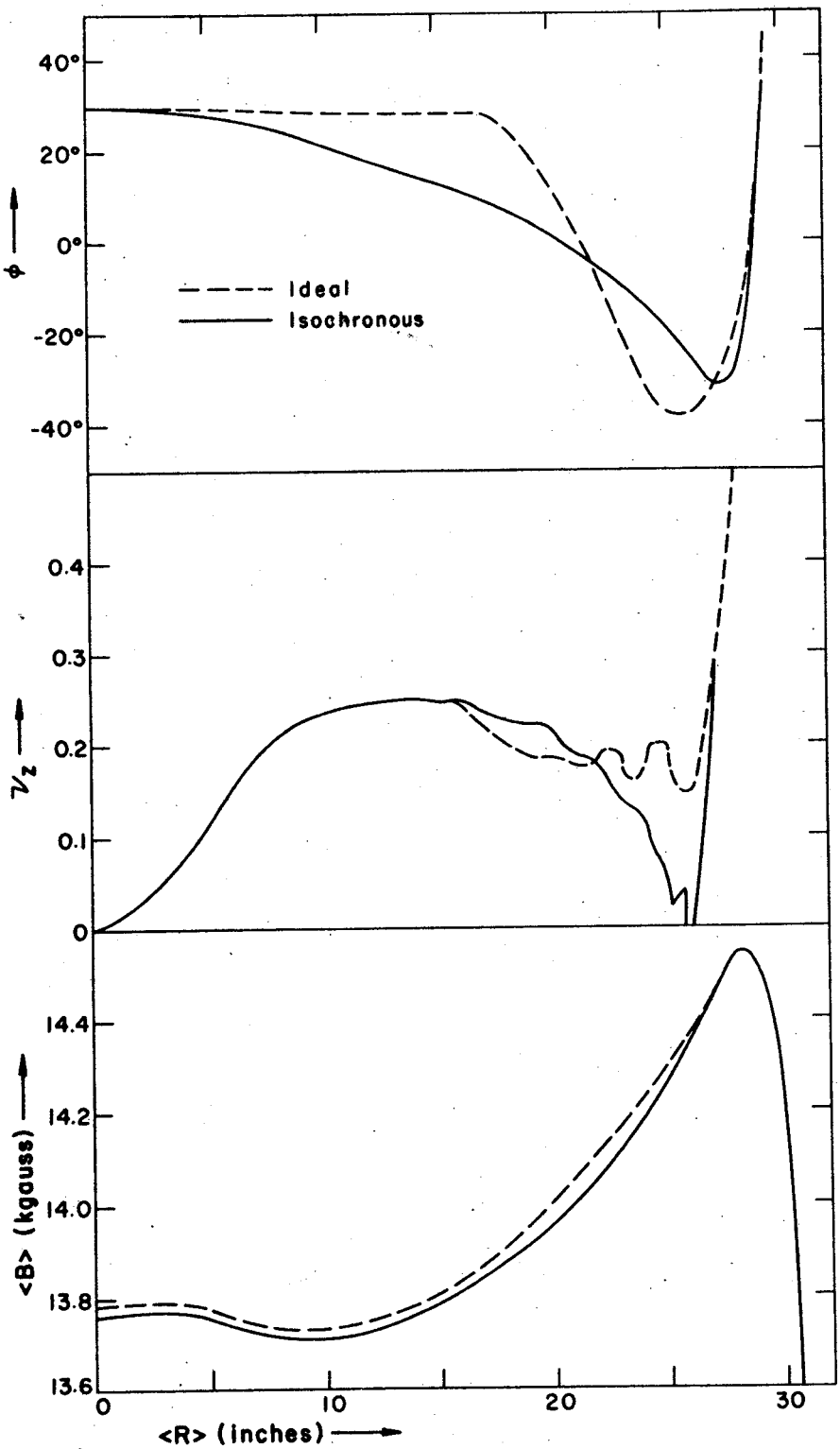

Figure 10. <B>, ν_z, and ϕ vs. radius for the 52 MeV proton field (Run 350) before and after correction of isochronous average field to obtain an ideal average field providing adequate axial focusing in the region from 25 inches to 27 inches.

the case of 52 MeV protons: part (a) shows the isochronous average field and the new average field resulting from correction of the axial focusing frequency of the isochronous field; part (b) shows the axial focusing frequency of the isochronous field and that of the corrected field; part (c) shows the sine of the phase slip of an accelerating particle versus radius for a starting phase of + 30° for both the isochronous field and the corrected field. The RF frequency in each case has been adjusted to minimize the energy spread in the beam at the extraction energy of 52 MeV. Both the axial focusing frequencies and the phase history data were obtained from the equilibrium orbit code.

The results indicate that this relatively simple procedure is quite adequate as an alternative to the use of flutter coils. The resulting field is satisfactory as regards all of the criteria stated in Section 2; in addition, the energy spread at extraction is kept within desired design limits and the phase of the particles with respect to the RF voltage at the extraction energy is kept small enough to retain ideal extraction properties.

2.3 Radial Focusing Correction

It is convenient in determining extraction parameters for the radial oscillation frequency to be a "similar function" of radius in the edge region for the entire range of

magnetic field excitations. This feature yields similar orbit geometry for all final energies as the beam passes through the $\nu_r = 1$ resonance, rapidly gains a large coherent radial oscillation, and continues to accelerate and precess out to the radius of the electrostatic deflector. Although the magnet was designed to minimize this variation in field shape with excitation, it is desirable to obtain more exacting control over ν_r in the edge region than results from the first approximation ideal fields.

As the excitation is increased, slight saturation of the magnet pole face causes the peak position of average field to move inward, which results in an earlier drop of ν_r through the $\nu_r = 1$ resonance. The rapid decrease in ν_r with radius is increased by the fact that the field gradient is higher at the higher excitations. This situation is illustrated in Fig. 11, which shows ν_r as a function of radius in the edge region for the seven measured magnetic fields, using the first approximation ideal fields. It was desired to extract where $\nu_r = 0.8$; however, the variation in radius of $\nu_r = 0.8$ in these fields is greater than 1/2 inch. At the same time the position of peak field, and thus the position of the $\nu_r = 1$ resonance, varies by over one inch. Because extraction problems are more severe at higher energies, the extraction system was designed on the basis of the high fields; lower fields were then varied so that the ν_r curves obtained properties similar to those of the higher fields. This choice possesses the further advan-

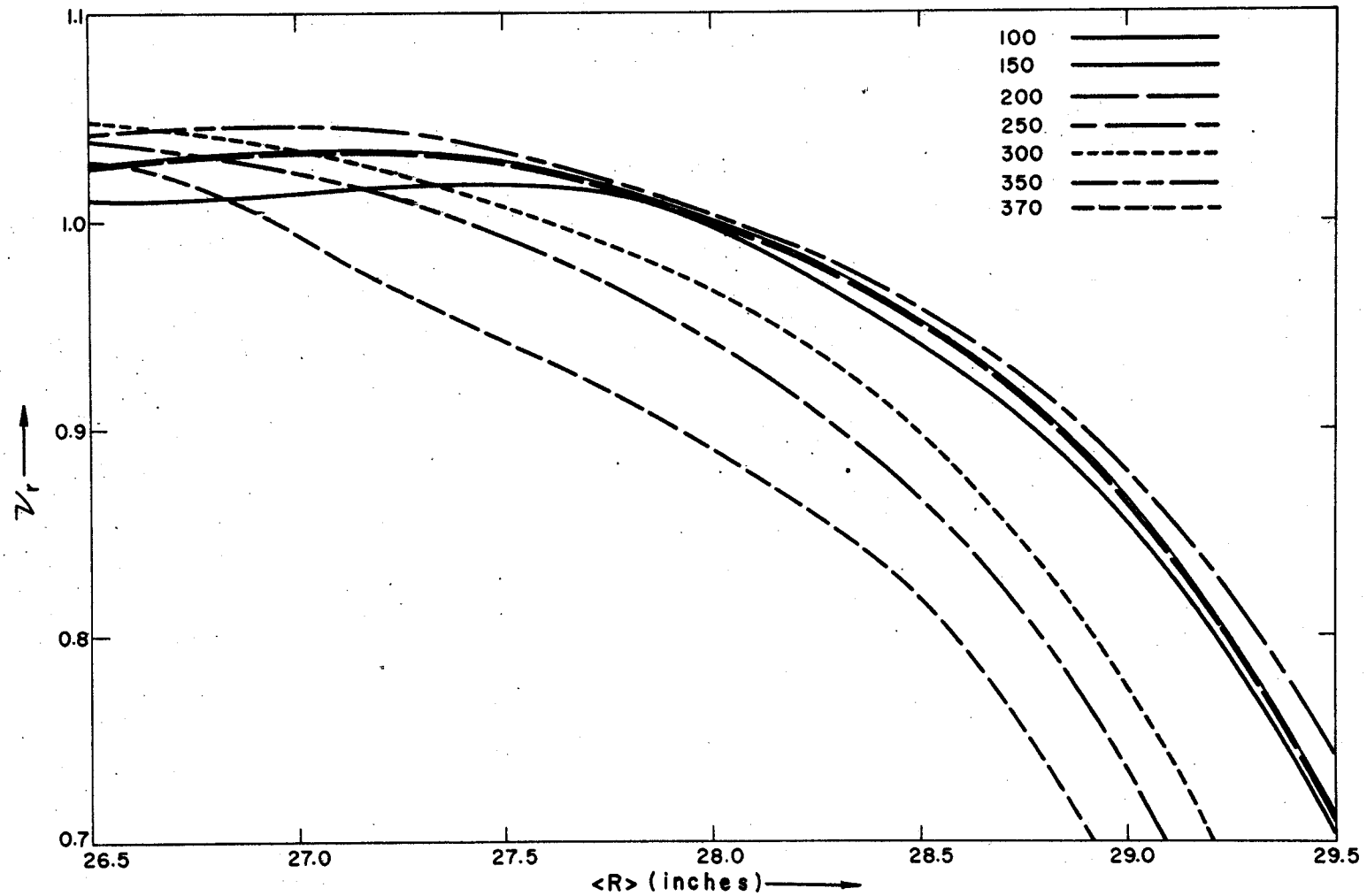

Figure 11. ν_r vs. radius for the set of proton isochronous average fields (corrected to provide axial focusing for energies above 42 MeV) at the measured main field excitation values.

tage that the additional load on the trim coils is more easily produced at lower excitations, where the field per unit current is substantially greater.

Two approaches were attempted to obtain this correction. The first trial involved using the trim coils to force the average field to drop more rapidly in the edge region. However, this leads to the undesirable feature of a crossover in the sign of the desired trim coil field. This is both extremely difficult to fit and costly in terms of the trim coil power needed. Within the limits placed on the trim coil currents, it was not possible to accomplish a detailed fit such as is necessary to lower ν_r to the desired value of 0.8 at the extraction radius without substantially decreasing the radius of the $\nu_r = 1$ resonance as well.

It was possible, however, to obtain the desired behavior by another device. Using the trim coils, the average field can be raised slightly above its isochronous value uniformly over the range of acceleration, then allowed to drop off sharply with radius slightly before the natural turnover of the average field. In practice the new ideal average field was obtained by scaling the interior average field, allowing it to drop off before the natural turnover, joining smoothly to the edge field. This retained the desirable feature of having no changes of sign in the trim coil fields while increasing the over-all trim coil load only slightly. An example of such a field variation is shown in Fig. 12 for the case of 25 MeV protons. The isochronous average field is

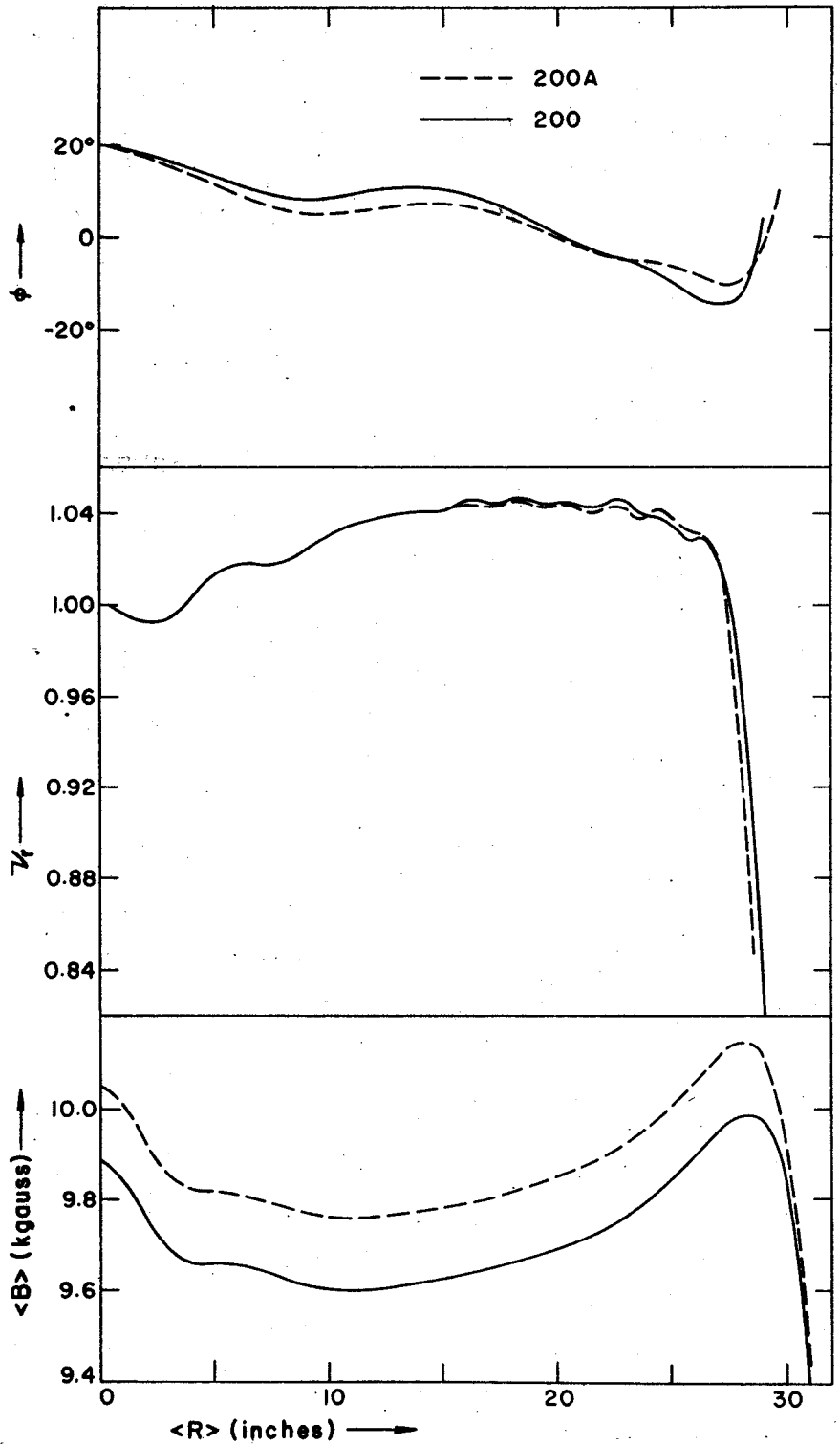

Figure 12. <B>, ν_r, and ϕ for fitted fields before (200) and after (200A) correction of ideal average field to provide uniformity of ν_r in the edge region.

shown along with the new average field, and the resulting ν_r curves for each. This change reduced ν_z slightly by raising the average field, and effectively redefined the frequency, but in no case did resulting properties violate any of the criteria of Section 2. Another result of this field change in this case was increase of the final energy to about 25.5 MeV. Figure 13 shows the resulting ν_r vs. R curves for the corrected fields, corresponding to those of Fig. 11 for the uncorrected fields.

Extraction studies have been made on the resulting fields, and data for 25 MeV and 52 MeV protons have been published[9]. These results show striking uniformity in all respects, vastly simplifying the process of computing desirable extraction parameters.

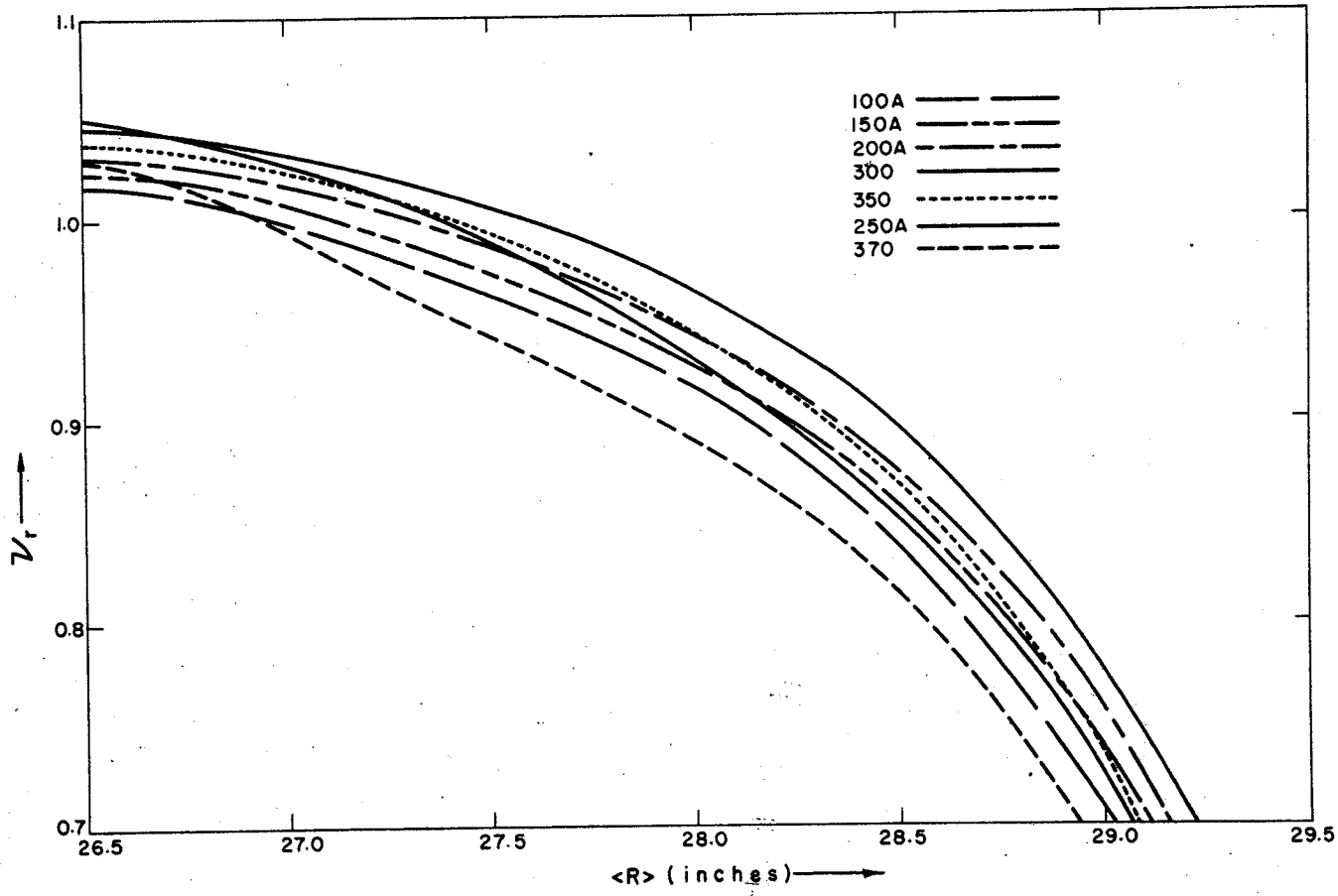

Figure 13. ν_r vs. radius for the ideal proton fields shown in Figure 11 after correction of the ideal average fields for main magnet excitations 100, 150, 200, and 250 (less than 33 MeV protons) to render ν_r in the edge region a similar function to that of field 350 (52 MeV protons).

III. MAGNETIC FIELD INTERPOLATION

In order to obtain continuously variable final energy, it is necessary to use interpolation to obtain fields intermediate to the measured magnetic field data; the interpolated fields at each excitation are then used to obtain an operating point at that excitation.

The following general criteria were considered in obtaining an acceptable method of interpolation:

(1) The median plane fields and their derivatives should be continuous and monotonic functions of excitation. The resulting field curves should be free of the "wiggles" characteristic of polynomial interpolations.

(2) Optimum use should be made of the accuracy with which the measured field data are known. An interpolation scheme should not change the known field data beyond their known errors; preferably it should render known values unchanged.

(3) The resulting fields should provide good orbit properties for accelerating particles; in particular, the interpolated ideal fields should meet the criteria stated and discussed in Section 2 for radial and axial focusing and phase excursion.

(4) The interpolated fields should correspond as closely as possible to the behavior of the actual magnetic fields. If possible, it is desirable to have independent computational checks of the resulting fields as well as experimental means of ascertaining the accuracy of an interpolation scheme.

(5) The resulting scheme should be as simple as possible; it should be fast and well-adapted for use on a computer due to the large number of interpolations which must be performed for each set of fields.

It also seems desirable that as little of the data as possible should be used in defining a particular intermediate result—due to the complex dependence of the saturation of the iron as a function of excitation, it seems reasonable to suppose that use of the data for low excitations, for example, would be of little aid in determining fields at the high excitation values.

Among the procedures considered were various order Lagrangian polynomial interpolations, various types of spline interpolation[22], and interpolation using polynomials obtained from fitting the data, which redefines the measured points as well as intermediate values by passing the best least squares curve through the data. Unfortunately, strict Lagrangian polynomial interpolation results in appearance of the ubiquitous polynomial wiggles, especially when high-order interpolation is used. For example, use of four-point Lagrangian interpolation to obtain trim coil average fields often results in distinct wiggles characteristic of a cubic polynomial, thereby introducing both unphysical field data at intermediate excitation values as well as discontinuities in the field derivatives at the measured field points. Therefore, it is desirable to reduce the number of points used in such a procedure as much as possible.

Use of fitting procedures to "smooth" measured data as a function of excitation yields an arbitrarily smooth curve, but results in the objectionable feature of changing the measured data. Although there are certain errors in the measured field data, and other methods both retain these errors and propagate them in the interpolated results, it seems questionable that fields corrected by introducing a low-order smoothing procedure are better than the measured data as far as corresponding to physical reality. Furthermore, such a procedure is both space-consuming and time-consuming since it introduces additional variables into the calculation.

Various types of spline interpolation were rejected since, because they are relatively sophisticated smoothing procedures, in general they introduce unnecessary complication into the calculation, with questionable improvement in the accuracy of the interpolated data when the accuracy of the measured data is considered.

In the light of the given objectives, the chosen scheme (suggested by M. M. Gordon) was a double three-point Lagrangian interpolation formula, with added provision for forcing continuity of the field derivatives with respect to excitation. Given the function $f(x_i)$ for $i = 1, 2, 3, 4$, the function $f(x)$ for an arbitrary x lying between x_2 and x_3 can be calculated as:

where $f_{lower}(x)$ and $f_{upper}(x)$ are given by three-point Lagrangian interpolation:

$$f_{lower}(x) = \sum_{i=1,2,3} \prod_{\substack{j=1,2,3 \\ j\neq i}} \left(\frac{x-x_j}{x_i-x_j}\right) f(x_i) \ , \qquad (3\text{-}2)$$

$$f_{upper}(x) = \sum_{i=2,3,4} \prod_{\substack{j=2,3,4 \\ j\neq i}} \left(\frac{x-x_j}{x_i-x_j}\right) f(x_i) \ . \qquad (3\text{-}3)$$

One limitation on this procedure is that it cannot be used in the extreme intervals of the measured data points. Therefore, straight three-point Lagrangian interpolation has been used in these regions in order to join the data smoothly while introducing a minimum of interpolation error. In practice no noticeable discontinuity resulted, nor were interpolation problems observed. Several of the Lagrangian polynomial methods were checked by computing difference tables for field functions obtained by interpolation using each method; the double three-point continuous derivative formula was found to yield the smoothest function over the entire range in that it gave the smoothest difference functions.

Choice of the particle extraction energy as the independent variable for interpolation was dictated by practicality and simplicity in labeling resulting fields. In each of the measured fields, an operating point was computed, where for each field the extraction energy was determined on the basis of orbit properties in the extraction region, which will be discussed later. (See Section 6.) Assigning this extraction

energy to each measured field as its "label", new fields could be computed using extraction energy as independent variable. This procedure is desirable in that the label used for the field possesses meaning to the user; it also provides a rough check on the adequacy of the interpolation scheme, as follows.

If the interpolation scheme is exact, and fitting errors small, the energy obtained in the interpolated field from orbit considerations should be the same as that used as independent variable in the interpolation to obtain the magnetic fields. Typical differences between energy used for interpolation and final energy are, for example, of the order of 20 keV over the entire range for 20 to 56 MeV protons. If this difference can be attributed to field errors resulting only from interpolation inaccuracy, an over-all field error of order 5 gauss is implied. In fact, deviations of this order can be introduced by other factors such as discontinuities in the fitting procedure and resulting small changes in orbit geometry in the extraction region. Thus it is reasonable to assume the interpolation procedure given here to be accurate to within less than 5 gauss over the entire excitation range.

To obtain a field description at an arbitrary excitation, sets of Fourier coefficients giving the fields of each of the magnetic elements are computed using the given interpolation scheme; the interpolated trim coil average field data are then used to fit the interpolated ideal average field, and the ef-

fective field at that excitation is synthesized by summing the Fourier data.

Other results of the interpolation method used as they apply to over-all operating point computations are discussed in Section 7.

IV. AVERAGE FIELD FITTING

For an arbitrary magnetic field excitation, the effective field is synthesized by adding trim coil average field contributions to the field of the main magnet, which consists of flutter and an average field component. Trim coil currents are obtained by fitting the difference field between ideal average field and the main magnet average field with the trim coil average fields.

An acceptable field fitting procedure must, of course, give resulting fields whose orbit properties are acceptable according to the criteria previously discussed. In addition, it is desirable that the method used produce smooth variations in the operating parameters as a function of excitation (or final energy); if such smooth behavior is obtained, it is possible to obtain essentially a continuum of final energies using a limited number of actual operating point calculations. This interpolation could then be performed and the cyclotron controls set by a much smaller computer than required for the original computation. (Such a system is now in the process of installation at the Michigan State University cyclotron laboratory.)

Two well-known methods have been used by other workers to accomplish this fitting, namely, least squares fitting and linear programming.

Linear programming methods, particularly as introduced and utilized by the Berkeley group[10,23], are capable of simul-

taneously adjusting trim coil currents, main field excitation, and RF frequency and voltage, subject to arbitrary constraints on the phase excursion, final energy, ν_r and ν_z. The method uses approximate equations to compute the phase and the betatron frequencies, so that no previous calculation is necessary to obtain ideal fields. In the limit, this extremely powerful method can be used to adjust any cyclotron parameter which can be expressed in an appropriate mathematical form.

Because of the versatility of the linear programming method, it is necessarily complex; therefore, if a problem in orbit properties arises, it is quite difficult to isolate the cause of such a problem and work on this problem independently. Furthermore, while results for the various parameters for any given operating point yield acceptable orbit properties for the given field, when taken in total, discontinuities in the various operating points occur over small excitation intervals.

A total operating point calculation using least squares fitting to obtain trim coil currents was chosen for several reasons. Although it is necessary to carefully pre-determine ideal fields, the fits obtained using least squares are extremely accurate, and field errors giving rise to differences between orbit properties in ideal and fitted fields are generally kept below the accuracy with which the magnetic fields are known. Therefore, since ideal fields possessing good beam properties are specified, fitted fields, as well, possess these desirable properties. Adjustment of RF frequency can be

accomplished at a later point in the calculation, thus eliminating the need to insert either RF frequency or main field variation into the fitting procedure. It is also possible to introduce arbitrary minimum and maximum current limits into the least squares procedure with no significant increase in complexity of the calculations. In addition, a step-by-step process such as the one described here offers the cyclotron designer greater opportunity to understand the procedure in total, and by separating the various computations allows the possibility of isolating individual problems in beam behavior, enabling more effective diagnostic work.

Reduced computing time is also obtained with the least squares procedure: using available programs, a linear programming field fitting alone required approximately five minutes of computer time, while a complete operating point calculation as described in Section 6 required less than two minutes.

In the light of these considerations, the following modified least squares method is employed for the fitting. For an arbitrary magnetic field excitation, given the average fields of the eight trim coils and the average field of the main magnet, all obtained by interpolation in the measured values, and the ideal average field obtained by interpolation in the set of pre-calculated ideal average fields, a best fit in the least squares sense of trim coil average fields to the difference field between the ideal average field and the average field of the main magnet is performed, yielding the desired

set of trim coil currents.

Given the average fields per unit ampere of the N trim coils at L radii $b_n(r_\ell)$, the ideal difference average field $E(r_\ell)$, and an arbitrary weight factor $\rho(r_\ell)$, the quantity δ can be formed, where:

$$\delta = \sum_{\ell=1}^{L} \rho(r_\ell) \sum_{n=1}^{N} [a_n b_n(r_\ell) - E(r_\ell)]^2, \qquad (4\text{-}1)$$

where the a_n are the desired trim coil currents. The least squares criterion may then be stated as calculation of the a_n such that δ is minimized, or as a set of N simultaneous linear equations:

$$\frac{\partial \delta}{\partial a_i} = \sum_{\ell=1}^{L} \rho(r_\ell) b_i(r_\ell) \sum_{n=1}^{N} [a_n b_n(r_\ell) - E(r_\ell)] = 0 \ , \qquad (4\text{-}2)$$

for i = 1. . .N. This can be reduced to the matrix equation:

$$\underline{X}\ \underline{A} = \underline{B} \ , \qquad (4\text{-}3)$$

where $\underline{X}$ is the N x N dimensional matrix:

$$\underline{X}_{in} = \sum_{\ell=1}^{L} \rho(r_\ell) b_i(r_\ell) b_n(r_\ell) \ , \qquad (4\text{-}4)$$

$\underline{B}$ is the N-dimensional column vector:

$$\underline{B}_i = \sum_{\ell=1}^{L} \rho(r_\ell) b_i(r_\ell) E(r_\ell) \ , \qquad (4\text{-}5)$$

and $\underline{A}$ is the N-dimensional column vector of the desired trim

coil currents. The trim coil currents can then be obtained by inversion of the matrix X:

$$\underline{A} = \underline{X}^{-1} \underline{B} \, . \qquad (4\text{-}6)$$

Matrix inversion is accomplished by the method of Gauss-Jordan-Rutishauser, an extremely compact and fast method derived specifically for use on automatic computers[32]. The method uses as storage only the given matrix and two row vectors and can be written in about ten FORTRAN statements.

In order to take account of upper and lower current limitations, after each field fitting computation all trim coil currents were inspected to assure compliance with the maximum limit. If the absolute value of any current exceeded its limit, its value was set to the maximum and the corresponding field subtracted from the original ideal field. If any current was in absolute value lower than its minimum, its value was set to zero. If more than one current was outside its specified limits, that one which exceeded its maximum by the greatest amount, or, if none, that one which was the lowest of those lower than its minimum, was eliminated, and another fitting calculation performed using the remaining coils. The procedure was repeated until the resulting currents all lay within their respective limits. Arbitrary and independent minima and maxima could be inserted for each coil.

The radius range over which the fitting was performed extended from 5 inches through 28 inches. As mentioned pre-

viously, the central region (0-5 inches) is omitted in order to preserve the field "cone" of the untrimmed fields and thereby increase ν_z in the first turns. The maximum radius was set at 28 inches which is both the maximum radius of useful orbits and also the radius beyond which the difference field between the ideal average field and the main magnet average field is essentially zero. Through this choice of radii, the field fitting was concentrated in the region where most of the acceleration occurs, while allowing the contribution of the trim coils to fall off naturally in the edge region, where the coils inherently have little effect. (See Figs. 5 and 6.)

Provision was also included for introduction of weighting factors which could be used to provide greater fitting accuracy in any desired radius region. However, in a test of this device, a weighting factor which weighted each radius by the turn density in that region was introduced with essentially negligible effect. This can be attributed to the fact that the fit is in any case exceedingly good, and a relatively large weighting factor is required to significantly effect the fit in any region.

A pleasant feature of the fitting in actual practice was a lack of large approximately equal currents of opposite sign in neighboring coils, which often are obtained in least squares fitting; this is partially a result of the fact that the fields that the trim coils are fitting are smooth, monotonic functions of radius with no sign changes.

Examples of results of this field fitting procedure are

given in Figure 14 for 25 MeV and 52 MeV protons, respectively. Typically such a least squares fit is capable of fitting the ideal difference field to within $\pm$ 5 gauss over the radius range used; errors as large as 10 gauss appear in a few cases and are a result of large gradients in the edge fields of the trim coils.

Figures 15 and 16 show a comparison of the radial and axial focusing frequencies and the phase excursion between the ideal and fitted field for the 25 MeV and 52 MeV fields previously discussed. The good general agreement reflects the excellent fitting results; the effect of the field cone on the axial focusing frequency for the fitted field can be easily seen, as can the property of the cone of restoring the high starting phase to a value more favorable to acceleration.

Further discussion of the results of the fitting procedure is given in Section 7, particularly as regards the continuum of operating points.

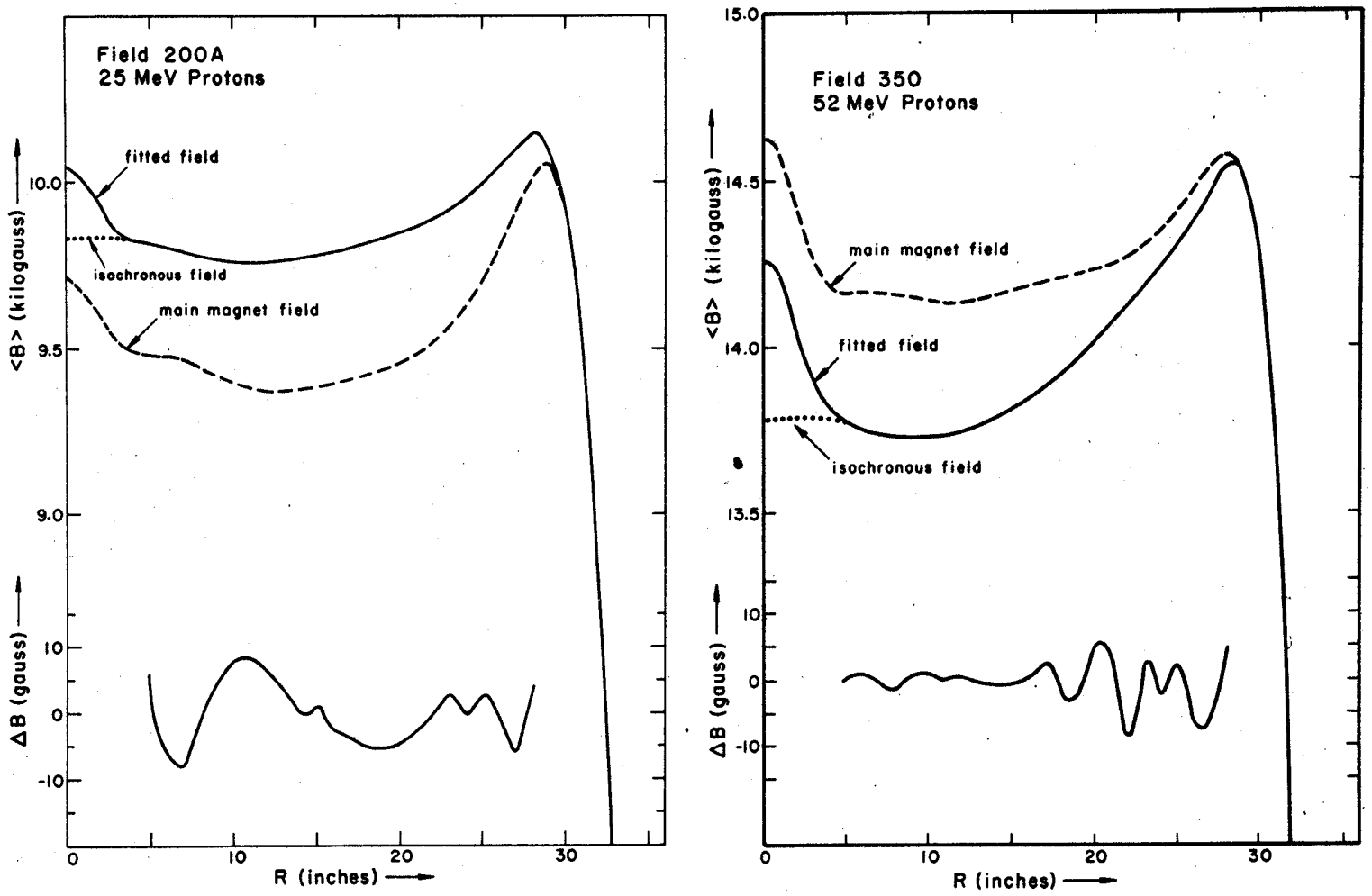

Figure 14. Average fields obtained by the modified least squares procedure for 25 and 52 MeV protons. Ideal average fields, main magnet average fields and fitted average fields are shown, along with the resulting error fields in the interval over which the fit was performed.

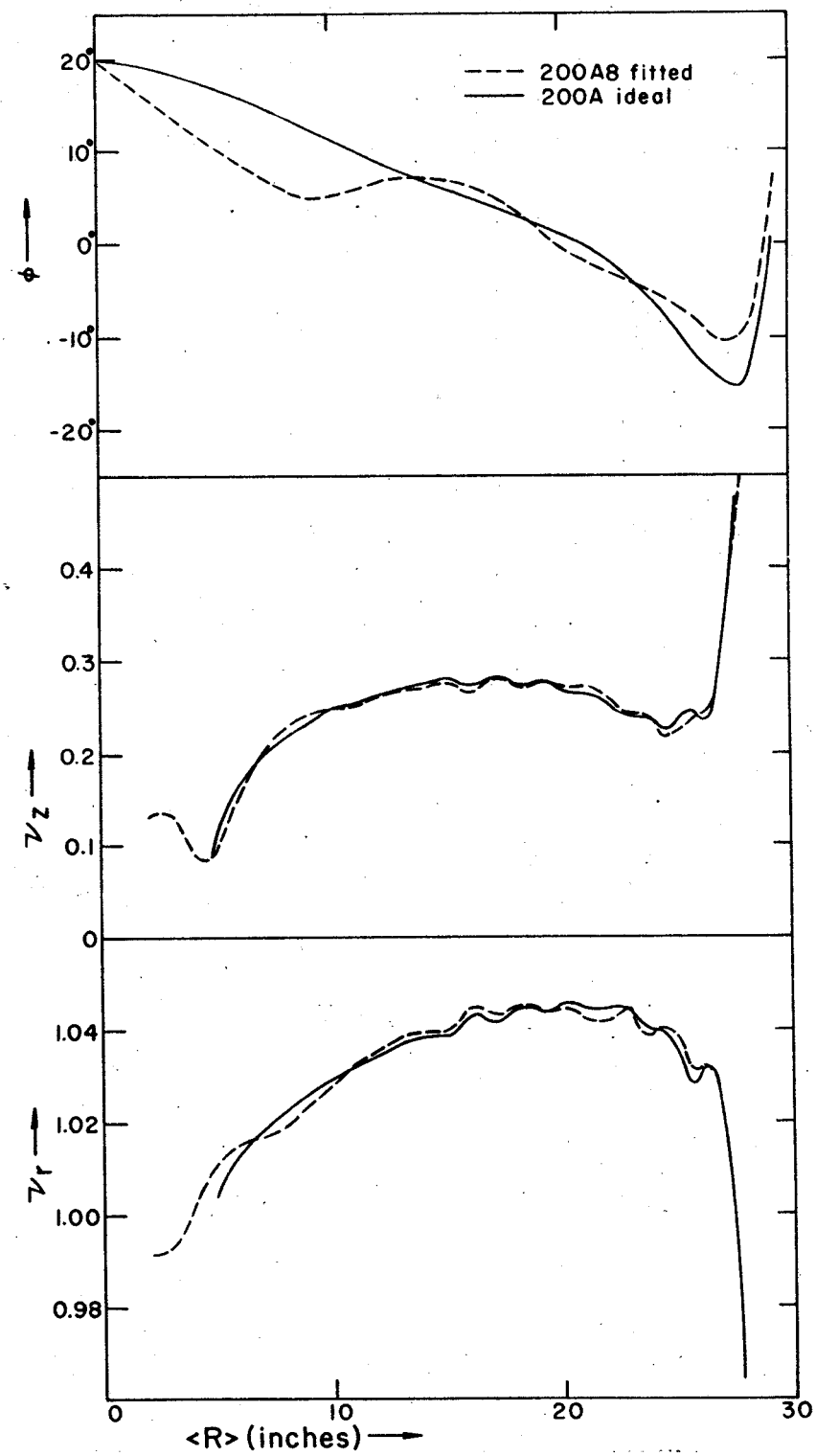

Figure 15. Comparison of ν_r, ν_z, and ϕ vs. radius with ideal average fields and fitted average fields for 25 MeV protons.

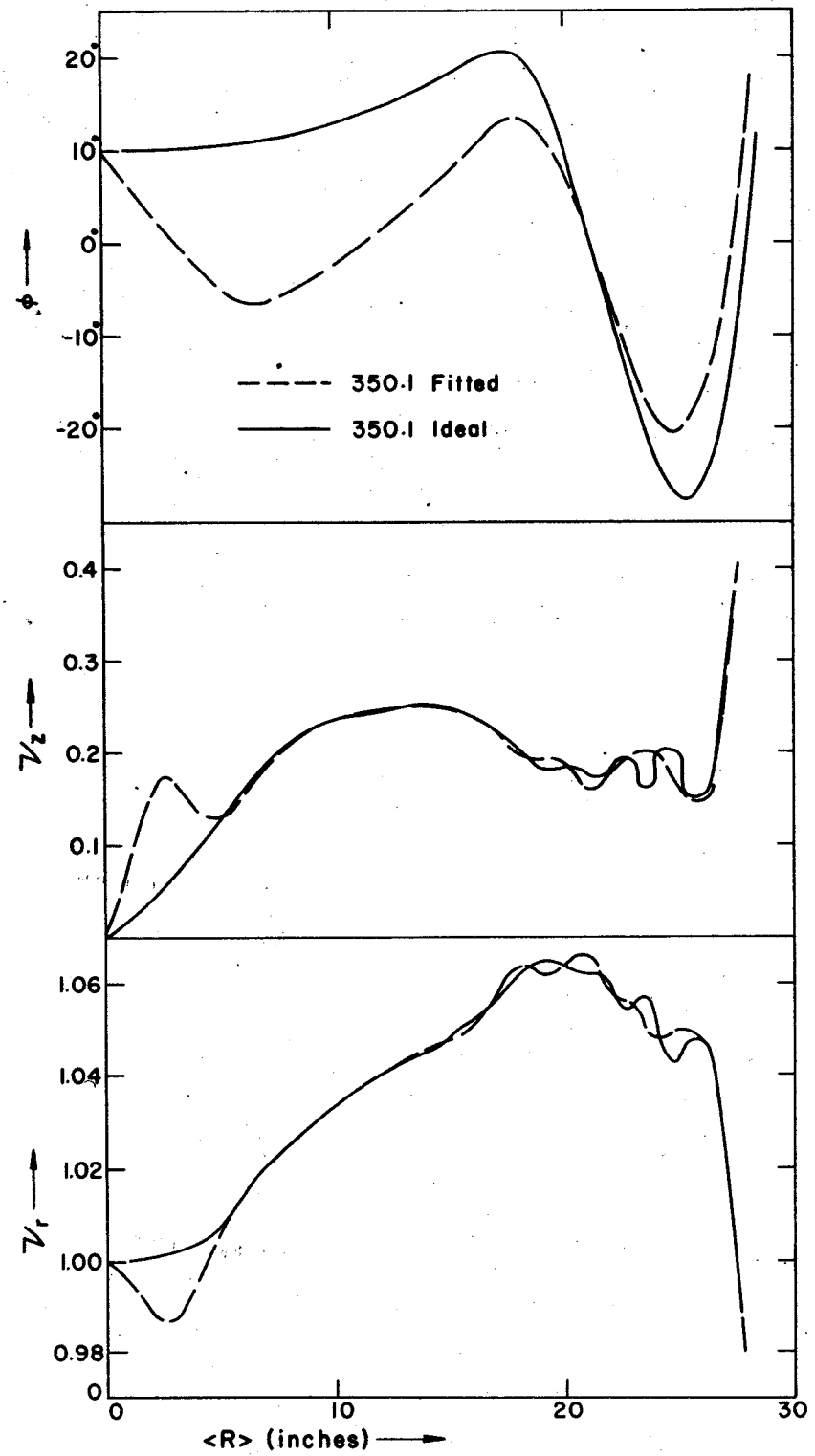

Figure 16. Comparison of ν_r, ν_z, and ϕ vs. radius with ideal average fields and fitted average fields for 52 MeV protons.

V. R.F. CALCULATIONS

The Michigan State University cyclotron is designed to operate with single-turn extraction, thereby achieving both high extraction efficiency and low energy spread in the extracted beam. Since the fields obtained by fitting are non-isochronous to varying degrees, it is necessary to redefine the RF frequency to obtain minimum energy spread—for a given non-isochronous field, a given final energy, and a given RF voltage, an RF frequency is uniquely defined such that for a given band of starting phases, the energy spread in the final turn is minimized. Mathematical details of this energy-spread minimization are given in a paper by M. M. Gordon[9]; the RF (longitudinal motion) calculations are carried out by an MSU computer code "PHINAL", devised and programmed by M. M. Gordon and Werner Joho[24]. Procedures will be outlined here only as necessary for an understanding of the basic principles involved.

The computations are based upon the assumption that the equations for longitudinal and transverse motion may be separated. This assumption is valid if the orbits are well-centered; in the limit of small dee voltage, the orbits between acceleration gaps would then become segments of the equilibrium orbit at the appropriate energy. Verification of these RF calculations can be obtained by comparing with numerical integrations of the complete equations of motion; results of such studies are discussed in Section 8.

Defining the phase of the particle ϕ with respect to the RF accelerating voltage:

$$d\phi = \omega_o dt - h d\theta \tag{5-1}$$

where ω_o is the RF angular frequency, h is the harmonic number, t is absolute time and θ is particle angle, the phase change per turn is given by:

$$\frac{d\phi}{dN} = 2\pi\left(\frac{\omega_o}{\omega} - h\right) , \tag{5-2}$$

where N is the turn number. The energy gain per turn is related to the phase through the equation:

$$\frac{dE}{dN} = E_1 \cos\phi(E) \tag{5-3}$$

where E_1 is the maximum energy gain per turn, which is a function of dee voltage and RF mode. Combining equations (5-2) and (5-3), one obtains the longitudinal differential equation of motion relating E and $\phi(E)$:

$$\frac{dE}{d\phi} = \frac{dE/dN}{d\phi/dN} = \frac{E_1 \cos\phi(E)}{2\pi\left(\frac{\omega_o}{\omega} - h\right)} . \tag{5-4}$$

Integrating this differential equation yields:

$$\sin\phi(E) = \sin\phi_o + \frac{2\pi h}{E_1} \int_0^E \left(\frac{\omega_o}{h\omega} - 1\right) dE , \tag{5-5}$$

or, in terms of the function F(E):

$$\sin\phi(E) = \sin\phi_o + \frac{hF(E)}{E_1} \quad , \tag{5-6}$$

where ϕ_o is the extrapolated, or "nominal", phase at E = 0. The function F(E) is obtained from numerical equilibrium orbit calculations. If the RF frequency is changed by a small fraction ϵ, such that a new RF frequency is defined:

$$\omega_o \rightarrow \omega_o(1+\epsilon) \tag{5-7}$$

equation (5-5) becomes:

$$\sin\phi(E) = \sin\phi_o + \frac{2\pi h}{E_1} \int_o^E \left[\frac{\omega_o(1+\epsilon)}{h\omega} - 1\right] dE \quad , \tag{5-8}$$

or, in terms of F(E):

$$\sin\phi(E) = \sin\phi_o + \frac{h(1+\epsilon)F(E)}{E_1} + \frac{2\pi h\epsilon E}{E_1} \quad . \tag{5-9}$$

The fractional frequency variation may then be adjusted to achieve an optimum phase history curve, where the function F(E) is obtained from equilibrium orbit data. In the case of the MSU cyclotron, it was desirable to obtain energy-spread minimization in the extracted beam. This procedure gives frequency and phase history results which are quite similar to those obtained by balancing the phase curve,

i.e., by requiring:

$$\int_{\infty}^{E} \sin\phi(E)dE = 0 \qquad (5\text{-}10)$$

However, as will be seen from data presented later, in order to obtain strictest control over the energy spread, it is necessary to carefully adjust the frequency beyond this first approximation obtained by balancing the phase integral.

For an arbitrary field, for a band of phases symmetrical about a starting phase ϕ_o the energy vs. phase for a sequence of turn numbers defines a series of so-called "energy parabolas", and the problem of minimizing energy spread is reduced to the problem of computing a fractional frequency correction ε such that the central ray lies at the position of the peak of the energy parabola for a given final energy. Mathematically, an ε must be found such that:

$$\left(\frac{\partial E}{\partial \phi_o}\right)_{\varepsilon,N} = 0 \qquad (5\text{-}11)$$

This is equivalent to maximizing the energy for a given number of turns, or to minimizing the number of turns in the central ray to obtain a given final energy. In particular, for single turn extraction, the energy spread should be much less than the energy gain per turn in the extraction region. Following the rules for partial derivatives, after considerable manipulation the following relation may be derived:

$$\left(\frac{\partial E}{\partial \phi_o}\right)_{\varepsilon,N} = -\cos\phi_o \cos\phi(E) \int_o^E \frac{\sin\phi(E)}{\cos^3\phi(E)}\, dE \qquad (5\text{-}12)$$

Using successive approximations for ε, the phase history $\phi(E)$ is obtained by integrating equation (5-9). The integral $(\partial E/\partial \phi_o)_{\varepsilon,N}$ may then be evaluated: the desired ε is reached when the integral vanishes.

For a strictly isochronous field operated at the isochronous frequency, the phase of a beam of particles remains constant over the entire acceleration region; in this situation the final energy of the particles assumes a $\cos\phi_o$ dependence upon the starting phase ϕ_o:

$$E = NE_1 \cos\phi_o \ , \qquad (5\text{-}13)$$

where N is the number of turns. The condition for minimization of energy spread is then identical to the condition for balancing the $\sin\phi$ curve about $\phi = 0^o$: the $\sin\phi$ curve is a straight line, where the central ray starts at phase ϕ_o, crosses $\phi = 0^o$ at turn N/2, and is extracted at turn N with a phase of $-\phi_o$. The phase dependence of the final energy is then given by:

$$E(\phi_o + \delta\phi) = NE_1 \frac{\sin\phi_o}{\phi_o} \cos\delta\phi \ , \qquad (5\text{-}14)$$

where $\delta\phi$ gives the phase deviation of a given ray from the central ray. The energy dependence of a beam of particles

thus lies on a cosine curve, where the position of the energy peak of the curve is a function of turn number; after N turns the central ray attains the position of peak energy, with symmetrical distribution of the energy about the central ray, and the energy spread for a phase distribution of $\pm \delta\phi$ about starting phase ϕ_o is a minimum.

Figure 17 shows the results obtained from the computer program "PHINAL" for the energy of a beam of particles of 6° phase width centered about a central ray of $\phi_o = 30^\circ$ as a function of turn number for the 25 MeV and 52 MeV fields previously discussed. The frequency has been adjusted to yield minimum energy spread at the indicated energies; the energy parabolas can be clearly observed to peak at the appropriate energy. The result of the energy spread minimization is most striking for 52 MeV protons, since the field deviates considerably from isochronism; the 25 MeV field is essentially isochronous to the edge region. With a band of starting phases of 6° width, which is readily attainable on the MSU machine using the central slit mechanism, energy spread in the extracted beam may be reduced to the design value of 0.1%. It should be noted that minimization of the energy spread at a given final energy does not preclude the possibility of an absolute minimum in the energy spread at a later turn number; however, the geometry of the extraction region as well as the diminishing energy separation between successive turns necessitates extraction at the earlier energy.

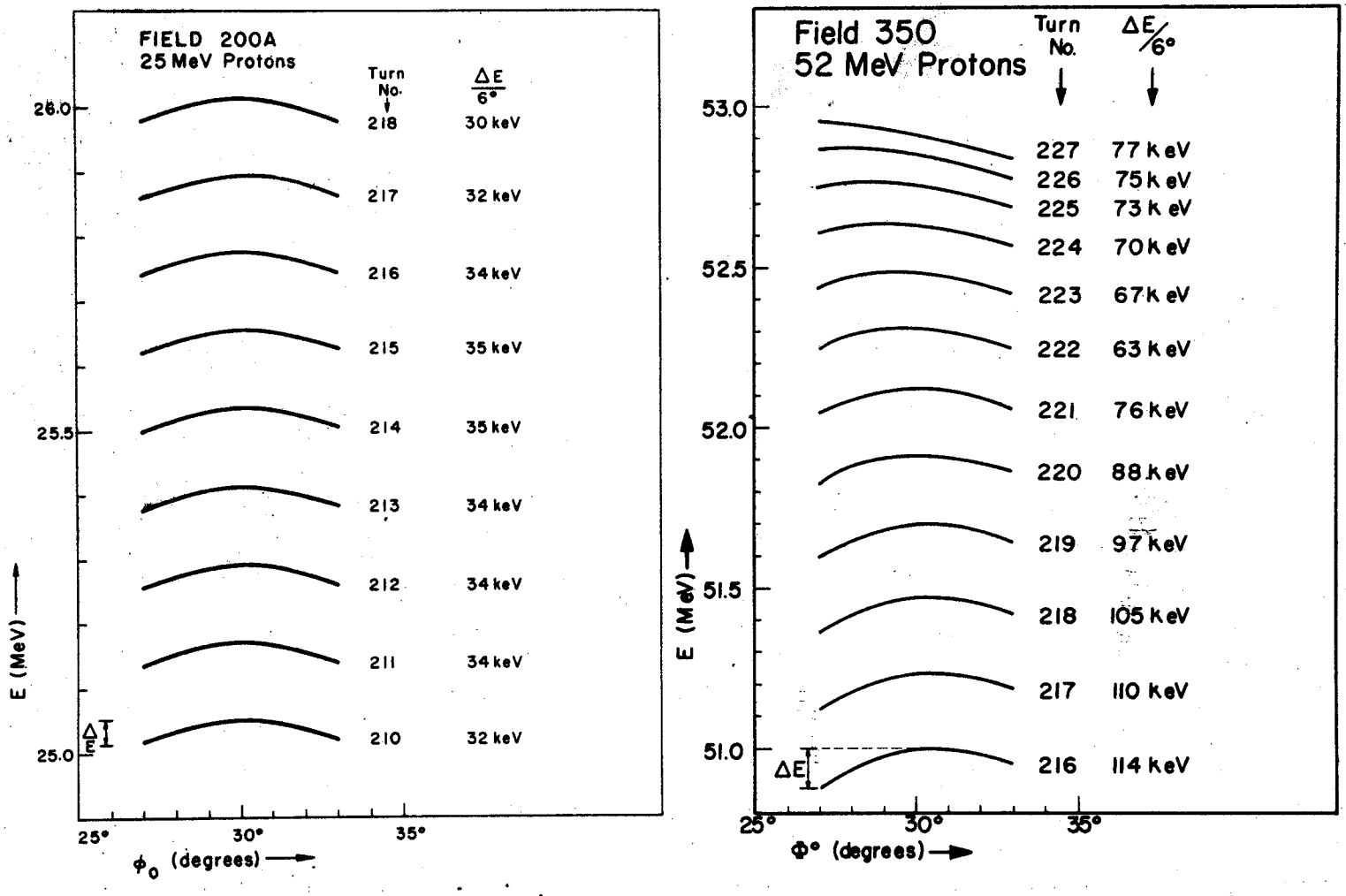

Figure 17. Energy vs. starting phase for turns near the extraction energy for a beam of 6° phase width about a central ray of nominal starting phase +30°. The energy spread has been minimized for 25.63 MeV (turn 212.9) and 51.97 MeV (turn 220.4), respectively.

Another important feature of the "PHINAL" code is the calculation of a set of frequency limits which drive the central ray of the beam out of phase with the RF accelerating voltage at various energies. From equation (5-9), it is clear that if the frequency is varied such that the phase is allowed to go to $\pm 90^{\circ}$, then $\sin\phi(E) = \pm 1$, and since E_1, $\sin\phi$ and $F(E)$ are known, for a given final energy E, the frequency correction ε, and thus the frequency, is uniquely defined. Validity of these results and their use are discussed in later sections.

VI. SUMMARY OF SETOP FEATURES

The computer program, SETOP, calculates complete control settings for the magnetic fields and RF system[25]. To use the program one specifies the desired particle and energy—the code then proceeds to compute the required control settings. In addition, along with each calculation, the program gives intermediate results necessary to perform additional orbit studies and diagnose problems in beam behavior.

The particle desired can be chosen from: $^{1}P^{+1}$, $^{2}D^{+1}$, $^{12}C^{+4}$, $^{3}He^{+2}$, or a "non-relativistic" heavy ion of mass 108 amu and charge of one electron unit. These operating point data can be used to accelerate any of the family possessing the same charge-to-mass ratio to roughly the same final energy per nucleon; for example, with only a few tenths of one percent change in frequency or main field, the deuteron operating point settings can be used to obtain alpha particles of twice the final energy of the deuteron.

Another device allows computation of operating points for particles of arbitrary charge-to-mass ratio. Using deuteron, $^{12}C^{4+}$, and "heavy ion" ideal average fields, interpolation in charge-to-mass ratio is used to obtain an ideal average field for the desired particle. These ideal average fields are then used in the operating point calculation.

The program consists of several sections, which are

discussed sequentially below—basic theoretical considerations have been discussed previously.

1. Magnetic Field Interpolation

All magnetic field data are stored as tables of Fourier coefficients at each measured main field excitation. The Fourier components at the desired intermediate excitation are computed by interpolation in the measured field data using the specified energy as the independent variable for the interpolation, where an energy value has previously been assigned to each measured field on the basis of orbit computations in the fitted fields. A complete set of Fourier coefficients for the resulting field is provided for possible use in independent orbit studies as well as to check the accuracy of the field computations and data handling. The set of cyclotron units are defined by taking the ideal field at machine center as the field unit.

2. Average Field Fitting

A modified least squares fit of the trim coil average fields to the difference field between the ideal average field and the main magnet average field is performed to determine trim coil currents for the eight sets of concentric circular trim coils; the fit covers the region from 5 inches

to 28 inches. Limitations on the trim coil power supply are imposed; no current may exceed a given maximum in absolute value, nor may any current be less in absolute value than the minimum current allowed for adequate power supply regulation. The effective field is then obtained by summing the Fourier coefficients of the main field and the average field components of the trim coils, scaled by their computed currents. The output includes the residual error fields over the radius region where the fit was performed.

3. Equilibrium Orbits

The MSU equilibrium orbit code ("CYCLOPS") is used as a subroutine to compute equilibrium orbits and their properties over the entire acceleration range; at each chosen energy the radial phase space coordinates (r,p_r) of the equilibrium orbit, the radial and axial focusing frequencies, and the fractional phase lag or lead per revolution are computed, along with other data not of direct interest in the operating point calculation. Data for equilibrium orbits are given at three angles: 0°, 180°, the angle of the beam probe, and $-22\ 1/2^\circ$, the angle of the entrance to the electrostatic deflector.

The extraction energy E is chosen to be the energy at which $\nu_r = 0.8$; the maximum energy gain per turn E_1 is fixed at E/210 to maintain uniform orbit geometry for all energies.

The RF harmonic number is taken to be the lowest possible within the frequency limits of the RF system using the cyclotron unit of frequency as a first approximation; the dee voltage is then computed:

$$h = 1: \; V_D = \frac{E_1}{4\cos 21^\circ}$$

$$h = 2: \; V_D = \frac{E_1}{4\sin 42^\circ}$$

$$h = 3: \; V_D = \frac{E_1}{4\cos 63^\circ}$$

4. Adjustment of RF Frequency

Using the equilibrium orbit orbital frequency data, and a given starting phase, a correction to the RF frequency is computed which minimizes the energy spread in the beam for a single turn at the extraction energy. A table of minimum and maximum frequencies as a function of energy for reducing the beam to half amplitude when the RF voltage is held constant is also provided as an aid in beam diagnosis using RF variation. (This is equivalent to driving the central ray out of phase with the RF as discussed in Section 5.)

5. Energy-Phase History Table

The energy and phase history of a "beam" of seven rays centered in phase about the central ray are tabulated as a function of turn number with the corrected RF frequency. These data are useful in checking the accuracy of the frequency calculation and field fitting processes, or as a source of initial conditions for other computations. The computer code "PHINAL", which is built in as a subroutine to the SETOP program, is used to calculate these data as well as the information described in the preceding subsection (4).

6. Valley Coil First Harmonic Calculations

A set of valley coil currents is given which a) cancels the existing first harmonic component near the $\nu_r = 1$ resonance, and b) produces the first harmonic necessary for resonant extraction. The amplitude and azimuth of the desired first harmonic must be computed in independent studies with exact orbit programs to yield the correct radial turn separation at the angle of the entrance to the electrostatic channel, and input to the operating point program.

7. Trim Coil Current Limits

A set of trim coil currents which drive the beam to half amplitude at various specified radii are computed; these data are useful in setting up the cyclotron main field and can be compared to experimental data taken in phase measurements.

8. SETOP Sheet

A final output sheet contains cyclotron control settings arranged in a manner convenient for use by an operator in setting up the cyclotron.

VII. RESULTS OF OPERATING POINT COMPUTATIONS

The information given by the SETOP program consists of two segments: (1) a series of results of intermediate calculations useful in cyclotron orbit studies and in diagnosis of any eminent problems, and (2) a summary sheet which enables the individual experimenter to successfully operate the machine by tabulating the various operational parameters in terms of simple dial settings. The results of intermediate calculations have been given previously in discussion of the various sections of the program.

A sample of the cyclotron operating point summary sheet is shown in Fig. 18. Each sheet is labeled by the particle and energy of interest. The main field is given in terms of the main magnet current and the voltage obtained by a rotating coil fluxmeter used to monitor the magnetic field. RF data includes frequency, harmonic and mode, and the dee voltage; the number of turns is given as an aid in obtaining the correct dee voltage. Trim coil "cut-off" currents at 24 inches are given as a method of setting the main field more accurately than is possible with the fluxmeter. Trim coil and valley coil data are given in terms of dial readings on their respective panels. First harmonic data are given in terms of the cyclotron control settings, bump amplitude and azimuth, in two parts. The first harmonic necessary to cancel the intrinsic first harmonic at the $\nu_r = 1$ resonance is used in setting up the operating point. For extraction the

52.000 MEV PROTON (52.009) 08/12/66

R. F. DATA

R. F. FREQUENCY = 21.0393940 MC., 1 HARMONIC
DEE VOLTAGE = 64.32 KV.
NUMBER OF TURNS= 217.0

MAIN FIELD DATA

MAIN COIL CURRENT = 649.48 AMPS
DEUT NMR FREQUENCY = 12097.01 MC.
HILL GAUSSMETER = 18507.22 GAUSS (TRIM COILS OFF)

SET MAIN FIELD BY TRIM COILS--PROBE AT 24 INCHES

	TC2	TC8
PHI=+90 DEGREES	-1.90	-7.66
OPERATING VALUE	-2.49	-5.56
PHI=-90 DEGREES	-2.83	+4.33

TRIM COIL DATA

TRIM COIL NUMBER	POT READING	CURRENT (AMPERES)
1U	2.08	41.51
1L	2.08	41.51
2	-2.49	-49.73
4	-4.17	-83.40
5	-4.00	-80.06
6	0.92	18.43
7	-5.89	-117.79
8	-5.56	-111.15

VALLEY COIL DATA

TOTAL FIRST HARMONIC DESIRED
AMPLITUDE = 0.55 GAUSS = 5.25 AMPS
POT READING= 0.26
AZIMUTH = 61.5 DEGREES

CANCELLATION OF INTRINSIC FIRST HARMONIC
AMPLITUDE = 1.81 GAUSS = 21.84 AMPS
POT READING= 1.09
AZIMUTH = 164.2 DEGREES

APPROXIMATE EXTRACTION FIRST HARMONIC
AMPLITUDE = 2.00 GAUSS
AZIMUTH = -0.2 DEGREES

Figure 18. SETOP data sheet, showing information necessary to tune up the cyclotron at the given energy.

vector sum of the cancellation first harmonic and the desired extraction first harmonic is used, thus producing the stated desired value as the net first harmonic.

When the cyclotron has been properly adjusted, turn structure is clearly visible out to the extraction region, which indicates the accuracy of the calculations, stability of the RF voltage, and the small beam phase width obtained by the use of central region slits. In each case the computed values of the operating parameters have allowed acceleration of the beam to full radius without additional adjustment, and in no case has deviation of any of the operating parameters from their computed values resulted in better beam properties[26].

Of particular interest in a variable energy cyclotron is attainment of a uniform beam over a continuum of energy range, or by small energy increments over the range. It has been found that use of the procedure described results in a series of operating points where the parameters vary smoothly with energy. As an example, Fig. 19 shows the currents in the eight trimming coils as a function of field number for proton fields over the entire range of excitation. From this data it can be seen that it is possible to obtain essentially a continuum of proton fields while performing only a limited number of complete operating point calculations. It is clear from the data given in Fig. 19 that the smoothness of the trim coil currents will give continuous energy variation by interpolation in a relatively small num-

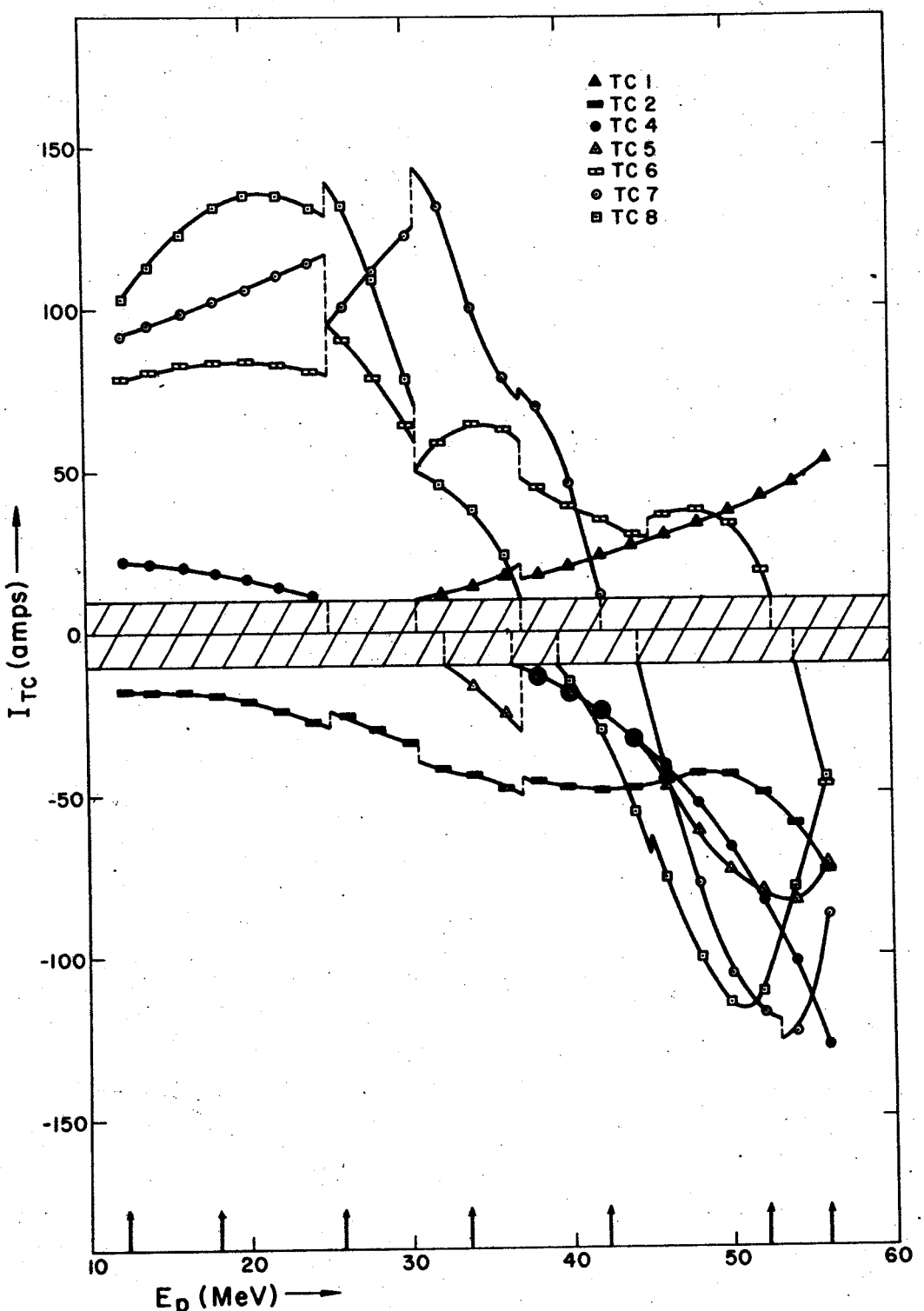

Figure 19. Trim coil currents as a function of proton energy over the entire magnetic field range of the MSU cyclotron. Discontinuities occur at points at which one of the trim coil currents drops below the minimum (10 amperes) imposed by the power supply regulator. Trim coil 3 has been eliminated from the fitting procedure. Arrows indicate measured field excitations.

ber of fully calculated points; an appropriate system is now being installed in the MSU cyclotron laboratory computer[27]. Other parameters such as the RF frequency and dee voltage and the main magnetic field are found to vary equally smoothly and are similarly adaptable for interpolation. Small discontinuities enter because of the minimum current limit requirements, but such discontinuities are small and can be dealt with in a relatively straightforward manner.

Through adequate prior calculations of ideal fields (and ultimately through model magnet studies), acceptable beam properties have been obtained over the entire excitation range. The smooth variation of both the extraction energy and the position of the $\nu_r = 1$ resonance with field excitation indicates the uniformity which the field shape retains. The small phase gain or lag per turn indicates the accuracy of the field fitting procedure, and is further evidence that the quality of the interpolated ideal average field data is essentially as good as that of the computed data at the measured excitations. In summary, Figs. 20, 21, and 22 show, respectively, radial focusing frequency ν_r, axial focusing frequency ν_z, and phase history as a function of radius for a rather complete family of proton operating points including both measured and interpolated fields.

Results of beam measurements are in excellent agreement with pre-computed data, and confirm the quality of the calculations, as is discussed in the following section.

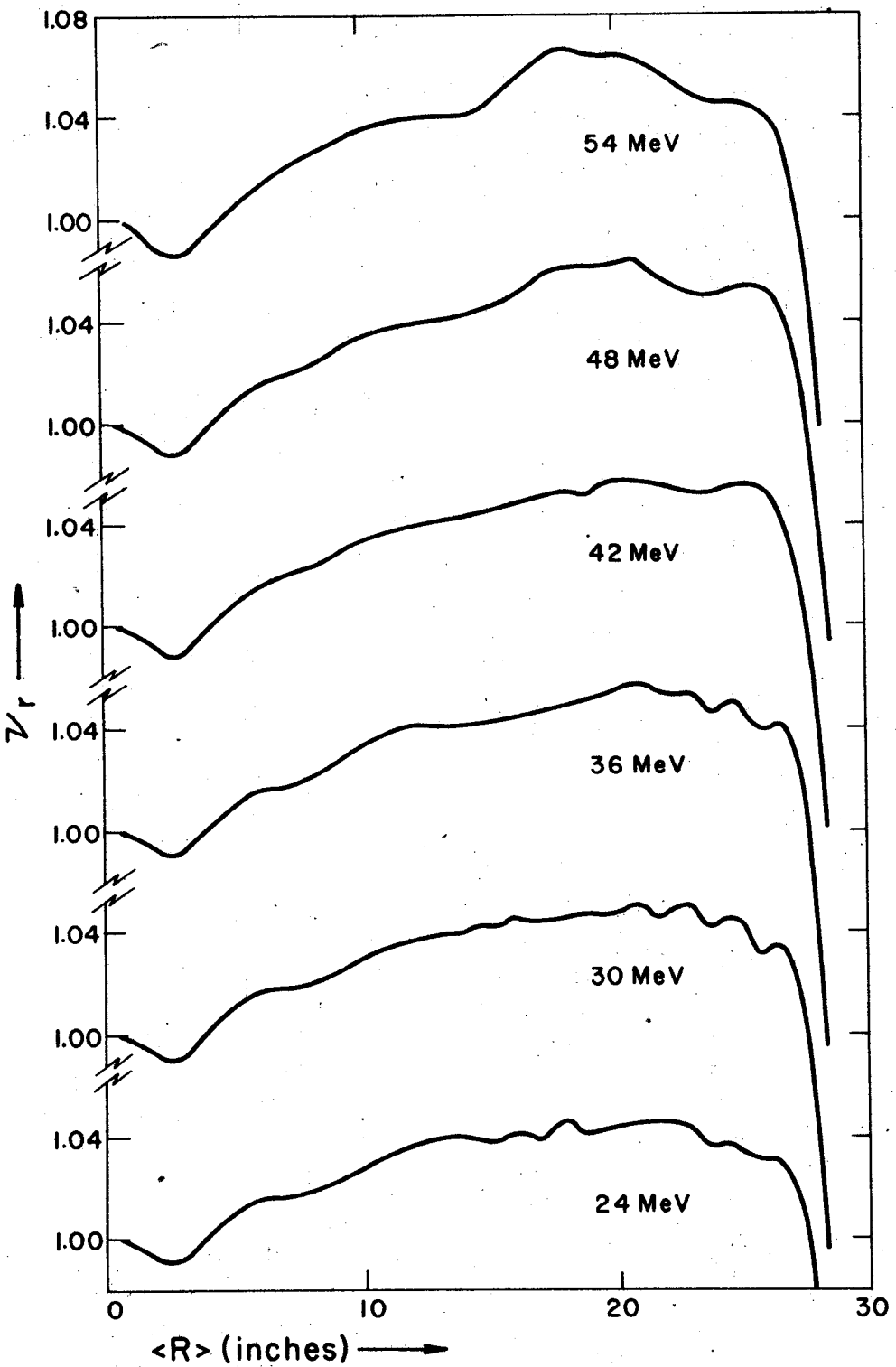

Figure 20. ν_r vs. radius for computed proton fitted fields covering the energy range accessible using rf first harmonic acceleration.

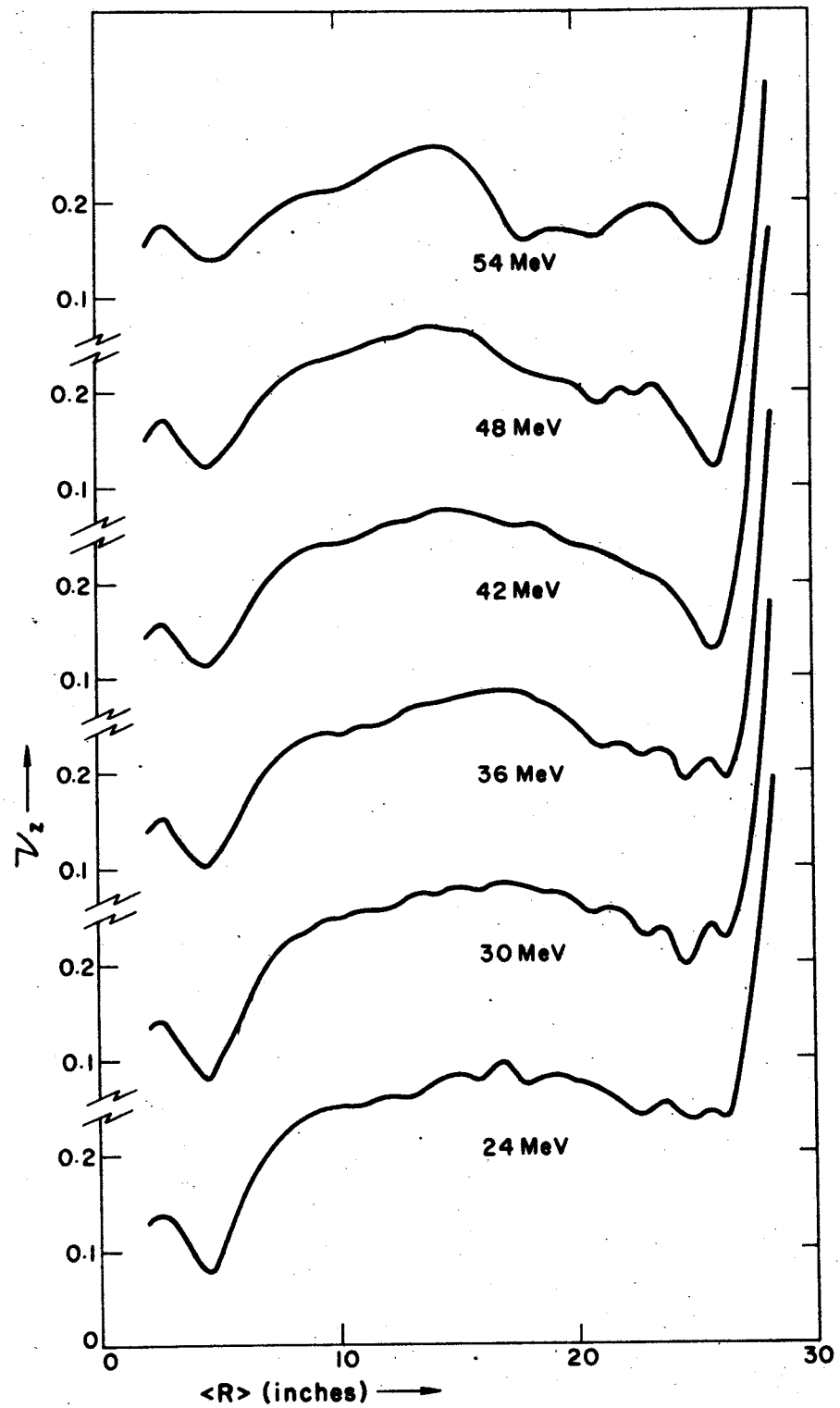

Figure 21. ν_z vs. radius for computed proton fitted fields covering the energy range accessible using rf first harmonic acceleration.

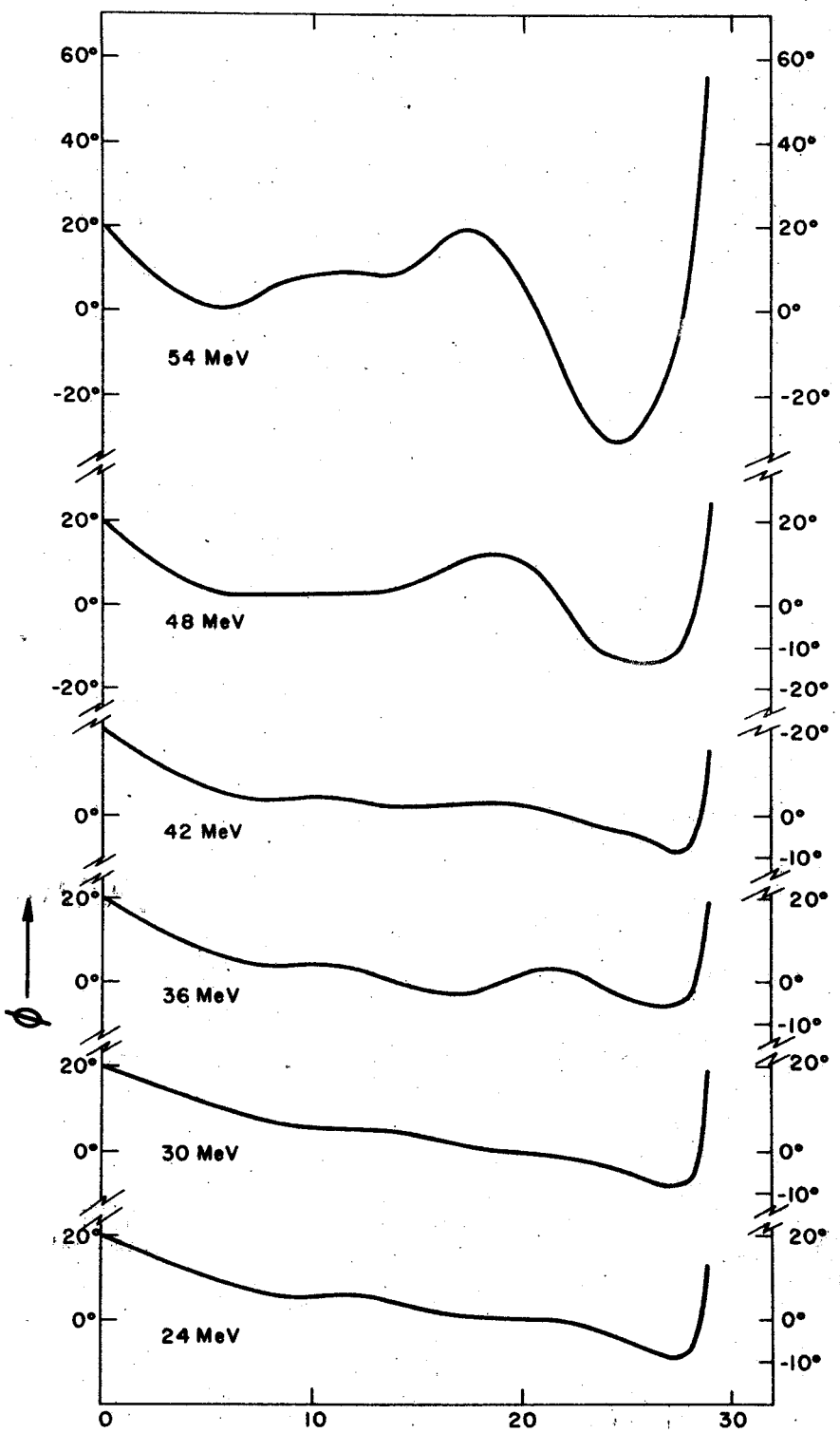

Figure 22. Phase vs. radius for computed proton fitted fields covering the energy range accessible using rf first harmonic acceleration.

VIII. ORBIT STUDIES

Properties of orbits in MSU cyclotron fields have been investigated using a very precise orbit integration program known as CYCLONE[28]; orbit properties obtained from CYCLONE are compared with results from the approximate methods used in SETOP. CYCLONE utilizes exact median plane equations of motion to track accelerated orbits in the magnetic field specified by SETOP. Details of the electric field are accounted for in three ways, depending on the level of significance of the electric field: (1) source-to-puller region, in which the electric field is obtained from a large-scale model electrolytic tank including exclusively the source-to-puller region; (2) "RF focusing" region, in which the finite width of the accelerating gaps is obtained by using a more complete electrolytic tank to obtain the electric fields covering approximately the first four turns; (3) the outer region, in which the electric field is approximated by a time-dependent step-function potential. CYCLONE also includes provisions for both an electrostatic deflector and a magnetic channel, and thus is capable of demonstrating behavior of orbits in the cyclotron from ion source through the complete extraction system.

Using CYCLONE in combination with various other orbit programs, a theoretical investigation has been made of several of the procedures used regularly for beam diagnostic work. Particular attention has been devoted to problems

involved in use of the Smith-Garren phase measurement procedure[29] and modifications thereof. Several important beam properties may be obtained through analysis of such measurements:

1) Phase history of the beam as a function of radius.

2) Phase width of the beam as a function of radius.

3) Dee voltage variation with radius.

Also, from the phase history data, a value of the nominal starting phase may be obtained by extrapolation. The procedure of phase analysis may also be used "in reverse" to carefully set the main magnetic field. Results of numerical investigations of procedures involved in such analysis are presented here along with results of experimental beam measurements.

Of particular interest are the limitations on the validity of the separated longitudinal equations of motion imposed by actual conditions of cyclotron operation. In many cases it is more convenient to use the longitudinal equations than to resort to more detailed and tedious integration of the exact equations, and the limitations of the approximate theory are therefore significant. (See Section 5 for derivation of the longitudinal equations of motion.) Errors in the approximate theory arise primarily from the off-centeredness of the orbits which leads to: (1) effects of coupling between the radial and longitudinal motion; and (2) failure of the normal radius vs. energy relation, which becomes quite evident when the ions gain negligible energy

during a precession cycle. These errors will be shown to be exceedingly small for conditions of normal operation of the MSU cyclotron. Discrepancies between the approximate theory and exact orbit integration arise primarily from coupling effects which are essentially incalculable except through such orbit integrations; these discrepancies lead to limitations in the application of the methods discussed only in certain circumstances.

Possible errors in actual practice arise from: (1) encounter of resonances or, in the case of trim coil adjustment, introduction of additional resonances, which results in large centering errors, and violates the assumptions necessary to separate the longitudinal equation of motion by introducing coupling terms and non-uniqueness of the radius-energy function, and (2) in the case of trim coil variations, further deviation is introduced into the radius-energy function due to average field variation.

The problems outlined here are of special concern to the operating point calculations described for two primary reasons: (1) the operating point set-up procedure makes use of the device of trim coil detuning to set the main field, and (2) in order to set the main field precisely and determine the RF frequency precisely, it is necessary to know the starting phase with substantial precision.

An example indicating the accuracy of the longitudinal equations under ideal circumstances is given in Table 1 for a 42 MeV proton field; energy and phase are tabulated as a

Table 1. Comparison of energy and phase versus turn number for central ray particles in a 42 MeV field using a) separated longitudinal equations of motion (PHINAL) and b) numerical integration of the exact radial equations of motion (CYCLONE).

	PHINAL		CYCLONE		
Turn	E(MeV)	ϕ(degrees)	E(MeV)	ϕ(degrees)	ΔF(E)(keV)
0	0.000	12.0	0.000	———	———
10	1.991	-5.1	1.962	-5.4	-1.0
20	3.975	-7.8	3.948	-7.8	0.0
30	5.952	-8.9	5.927	-8.8	+0.4
40	7.919	-11.1	7.897	-10.6	+1.8
50	9.871	-13.4	9.852	-13.1	+1.0
60	11.808	-14.6	11.792	-14.2	+1.4
70	13.740	-14.9	13.727	-14.6	+1.0
80	15.669	-15.4	15.658	-14.9	+1.8
90	17.591	-16.2	17.582	-16.0	+0.6
100	19.504	-17.2	19.497	-16.8	+1.4
110	21.406	-18.6	21.399	-18.4	+0.6
120	23.290	-20.3	23.283	-20.0	+1.0
130	25.154	-21.8	25.147	-21.7	+0.2
140	27.001	-22.8	26.993	-22.6	+0.8
150	28.841	-22.9	28.831	-22.9	0.0
160	30.688	-21.7	30.675	-21.6	+0.4
170	32.558	-19.2	32.542	-19.3	-0.4
180	34.466	-14.9	34.447	-15.0	+0.4
190	36.419	-8.4	36.399	-8.5	-0.4
200	38.411	+2.7	38.392	+2.5	-0.6
210	40.356	+23.0	40.348	+22.8	-0.6

function of turn number (at 10 turn intervals) for actual integrated orbits obtained from CYCLONE, and compared to the energy and phase obtained from SETOP by integrating the separated longitudinal equations (from Section 5):

$$\sin\phi(E) = \sin\phi_o + \frac{2\pi}{E_1}\int_o^E \left(\frac{\omega_o}{\omega} - 1\right) dE = \sin\phi_o + \frac{F(E)}{E_1} \quad , \quad (8\text{-}1)$$

and:

$$\frac{dE}{dN} = E_1 \cos\phi \quad , \quad (8\text{-}1a)$$

where the $\frac{\omega_o}{\omega} - 1$ values are obtained from the equilibrium orbit code. The integrated orbit in this case possessed a radial oscillation amplitude of approximately one millimeter; this behavior can be obtained on the MSU cyclotron by proper adjustment of central region parameters. Also given is the quantity $\Delta F(E)$ which is the difference between the F(E) values obtained from the two methods of integration. The small amplitude of $\Delta F(E)$ indicates the quality of the agreement; the fact that $\Delta F(E)$ oscillates with a period corresponding to the radial precession cycle indicates that the small errors present result from centering effects, particularly in the central region and at large radii. Errors as small as those in the table are of negligible effect in setting up the cyclotron. This result and the results of other examples verify the validity of the longitudinal equation under ideal

conditions, and validate its use in diagnostic procedures.

8.1 Frequency Detuning

The actual cyclotron beam consists of particles with phase distributed about some central ray whose phase is $\phi_c(r)$. When equation (8-1) is valid, the width of the beam in $\sin\phi(r)$ is constant (since F(E) depends only on the energy and not on the initial phase). This is illustrated for a 42 MeV MSU cyclotron field in Fig. 23. If the phase of any part of the accelerating beam reaches the limits $\pm 90^\circ$ ($\sin\phi = \pm 1$), it is lost, decelerating inward to machine center. In particular, when the central ray of a beam just reaches the 90° limit at a given radius, this is observed using an integrating beam probe as a reduction of the beam to half amplitude at that radius.

Use of frequency variation as a tool in determination of beam phase history was first proposed by Garren and Smith[29]. Writing the longitudinal equation, and introducing a new RF frequency ω', the following relation is obtained:

$$\sin\phi'(E) = \sin\phi_o + \frac{2\pi}{E_1}\int_o^E \left(\frac{\omega'}{\omega} - 1\right) dE \qquad (8\text{-}2)$$

or:

$$\sin\phi'(E) = \sin\phi(E) + \frac{2\pi(\omega'-\omega_o)[E+F(E)]}{E_1\omega_o}, \qquad (8\text{-}3)$$

where $\phi'(E)$ is the phase obtained with the new RF frequency,

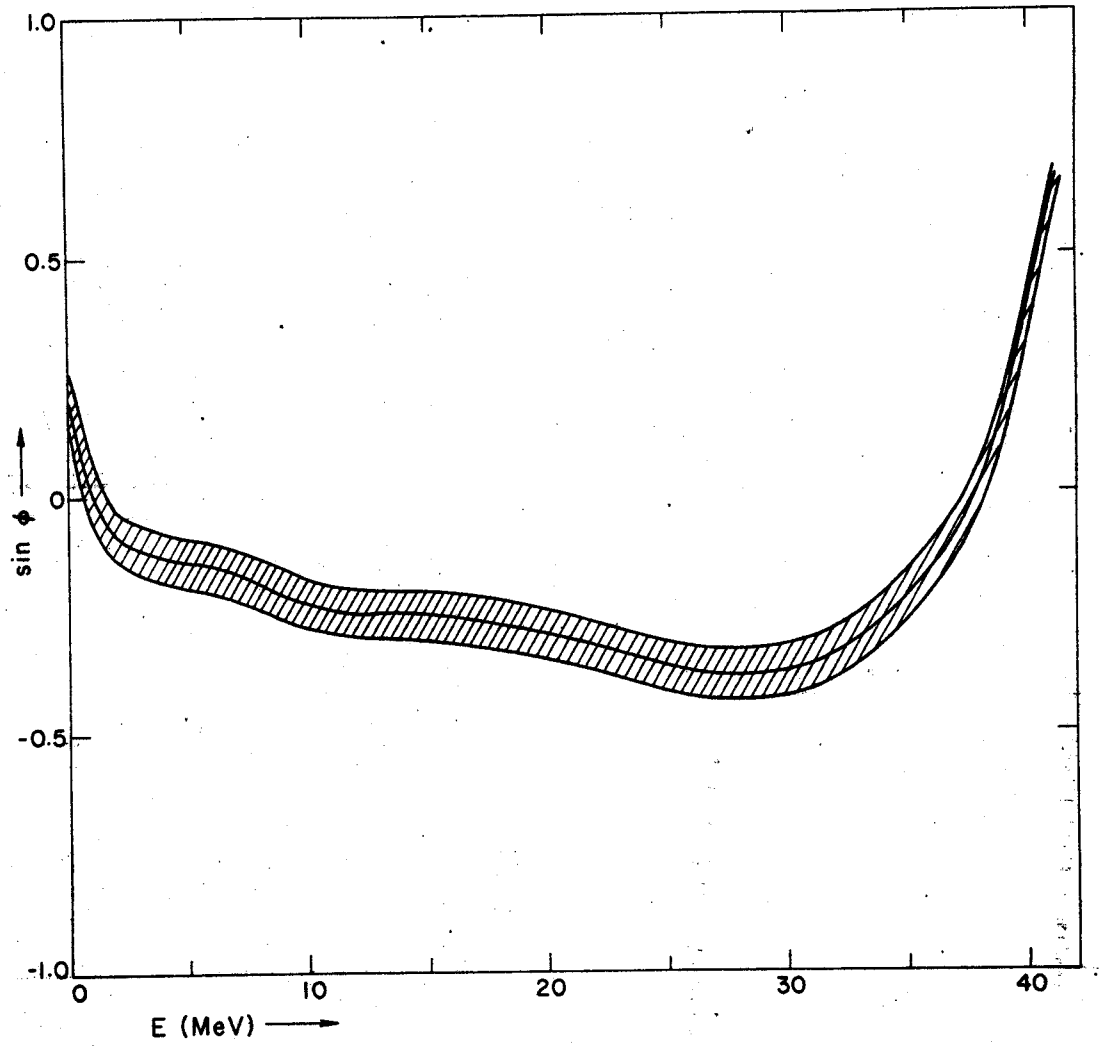

Figure 23. Sinφ vs. E for a phase group of 6° width in Field 300 (42 MeV protons).

and $\phi(E)$ is the undisplaced phase with the operating frequency ω_o. If frequencies ω_+ and ω_- are defined, which drive the phase to $\sin\phi = +1$ and -1 respectively, one can write equation (8-3) as:

$$+1 = \sin\phi(E) + \frac{2\pi(\omega_+ - \omega_o)[E+F(E)]}{E_1\omega_o}, \qquad (8\text{-}4a)$$

$$-1 = \sin\phi(E) + \frac{2\pi(\omega_- - \omega_o)[E+F(E)]}{E_1\omega_o}, \qquad (8\text{-}4b)$$

Combining equations (8-4):

$$\sin\phi(R) = \frac{2\omega_o - \omega_+(R) - \omega_-(R)}{\omega_+(R) - \omega_-(R)} . \qquad (8\text{-}5)$$

Thus, at a given radius, determination of the frequencies which drive the central ray out of phase with the RF accelerating voltage (or, equivalently, which reduce the beam to half intensity) allow calculation of the phase of the undisplaced central ray at that radius. Ideally, determination of the phase in this manner depends only upon the condition that all quantities (such as starting phase, dee voltage, and fields) are constant in time. However, several limitations appear in practice. First of all, centering of the beam places stringent limits on the accuracy of the method. For a beam with six millimeter radial oscillation amplitude, the phase at which the orbit reaches its maximum radius at the angle of the probe can be as small as 65°. Reduction

of the radial oscillation amplitude to below one millimeter raises the phase at which the orbit reaches its maximum radius to above 85°. One assumption used in obtaining equation (8-5) is that the radius is a function of energy alone, and not of turn number or frequency; this assumption is checked in calculations summarized by Table 2, for the same 42 MeV proton field, from results of a family of CYCLONE orbits. The effect of the small radial oscillation can be seen directly in the variation of radius at a particular energy, and the necessity of minimizing this effect becomes apparent. The conditions shown here are essentially identical to those obtained in the operation of the cyclotron. It should be noted that the oscillation is introduced through the starting conditions, and is not amplified by detuning of the system. It should also be noted that due to the gap crossing resonance[30], it is not possible to center the beam at all radii simultaneously; therefore, starting conditions should be used which center the beam at large radii, where the turn density is greatest.

Another limitation in applying the frequency detuning method at large radii arises from the particular shape of the $\sin\phi$ versus radius curve and its effect on the minimum frequency ω_- as a function of radius. Figure 24 shows the envelope of maximum and minimum frequencies as a function of radius for a 33.5 MeV proton field. Because the phase curve rises rapidly at large radii, the frequency required to drive the phase of the central ray to -90° is a constant

Table 2. Energy versus radius as a function of RF frequency in the 42 MeV field; such data establish the uniqueness of the radius as a function of energy within limits of experimental measurement, and validate the method of frequency detuning described.

R.F. Frequency →	19.06 Mc.	19.07 Mc.	19.09 Mc.	19.11 Mc.	19.12 Mc.
E(MeV)	R(inches)	R(inches)	R(inches)	R(inches)	R(inches)
10	13.560	13.561	13.529	13.508	13.524
15	16.458	16.464	16.461	16.457	16.456
20	———	18.912	18.876	18.838	18.861
25	———	21.033	21.040	21.028	———
30	———	———	23.024	———	———

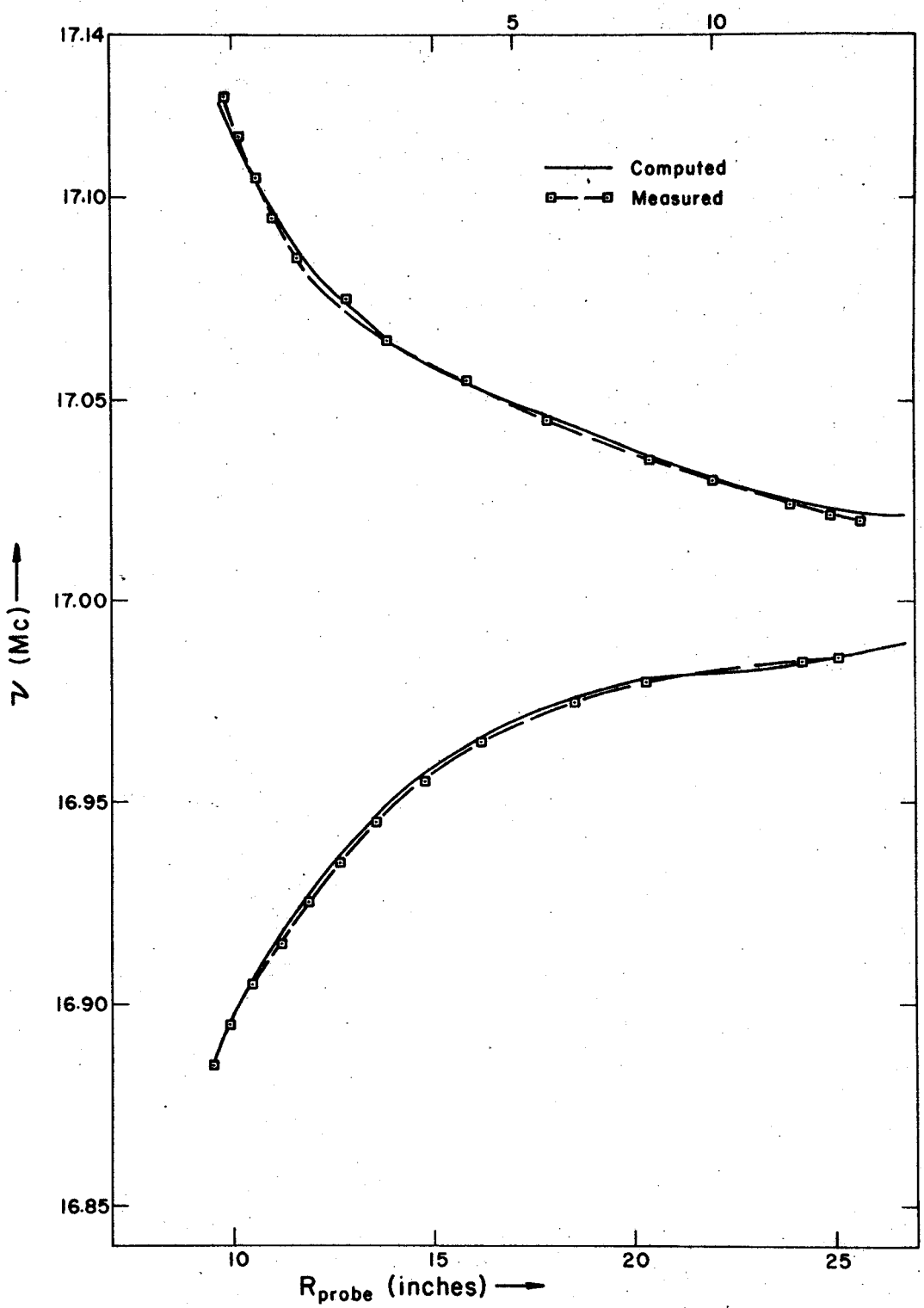

Figure 24. Envelope of frequency versus radius required to drive beam to half amplitude ($\sin\phi = \pm 1$ for central ray). Computed values obtained from SETOP are shown along with measured data for Field 200 (25 MeV protons).

for all radii greater than a certain value characteristic of the particular phase curve. This feature renders the phase measuring procedure invalid at large radii. Such behavior is observed in all fields of the MSU cyclotron to varying degrees, and care must thus be exercised in applying the method.

Also shown on Fig. 24 are the results of experimental measurements of this envelope of frequency cutoffs. Such an experimental determination of the frequency cutoff envelope was obtained for several fields, and the data used to compute experimental phase curves. Phase curves obtained for 25, 33, and 42 MeV fields are shown respectively in Figs. 25 and 26, along with the predicted values obtained from SETOP.

A more complete comparison of phase versus energy between use of the longitudinal equation (with phase slip per turn data from equilibrium orbit calculations) and use of actual orbit integration is shown in Fig. 27. The extremely good agreement reflects the adequacy of the approximations under the conditions obtained in the MSU cyclotron. The larger deviation apparent in the 19.082000 Mc. run is probably the result of a coupling term proportional to (x/R) which enters the longitudinal equation, where x is the displacement from the equilibrium orbit radius R; such terms become especially significant in the region where the phase curve approaches -90° very slowly, and a large number of turns results.

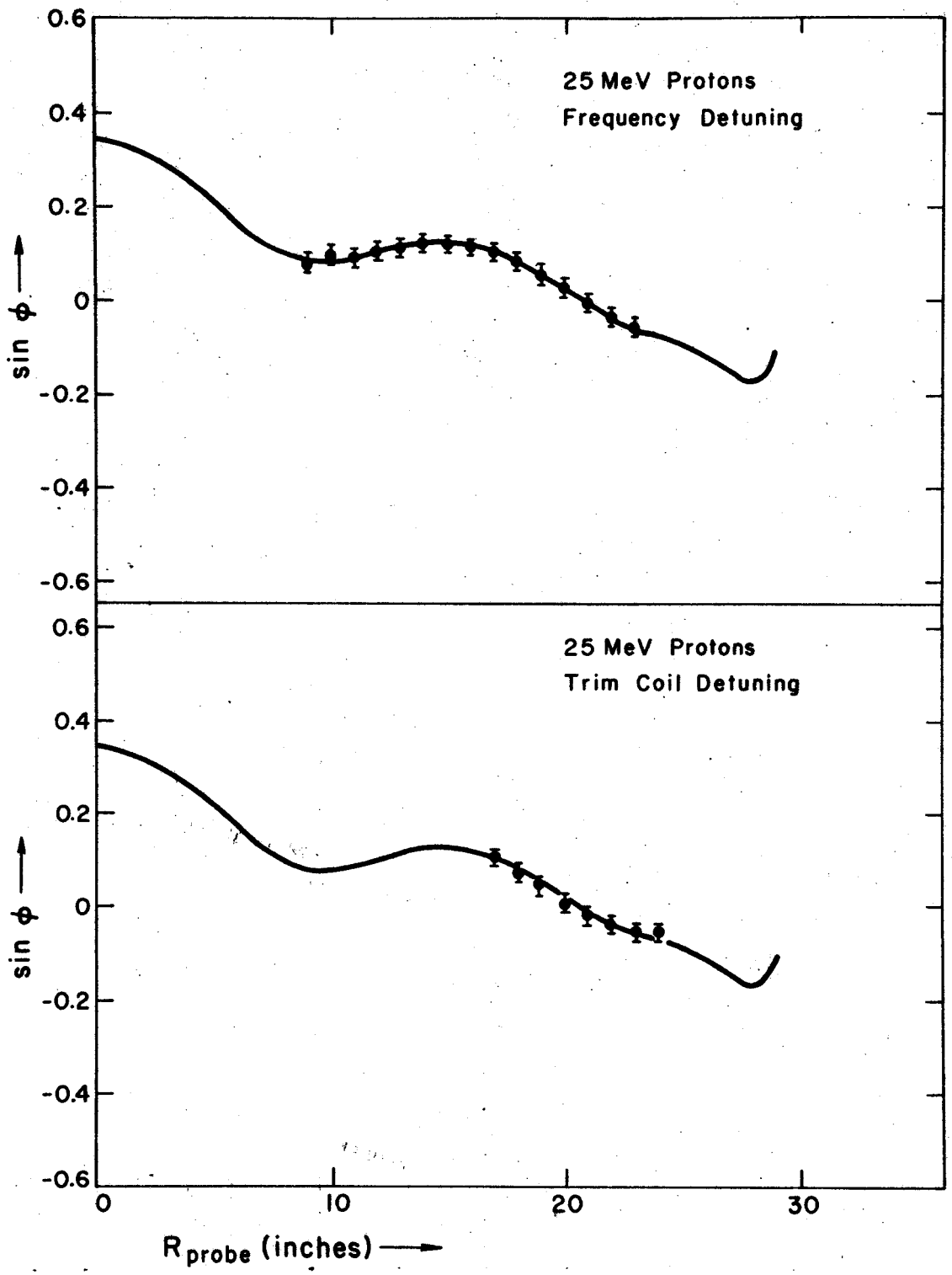

Figure 25. Sinϕ vs. probe radius for the 25 MeV proton field. Experimental data, obtained by frequency detuning and trim coil detuning, respectively, are compared to computed data obtained from SETOP.

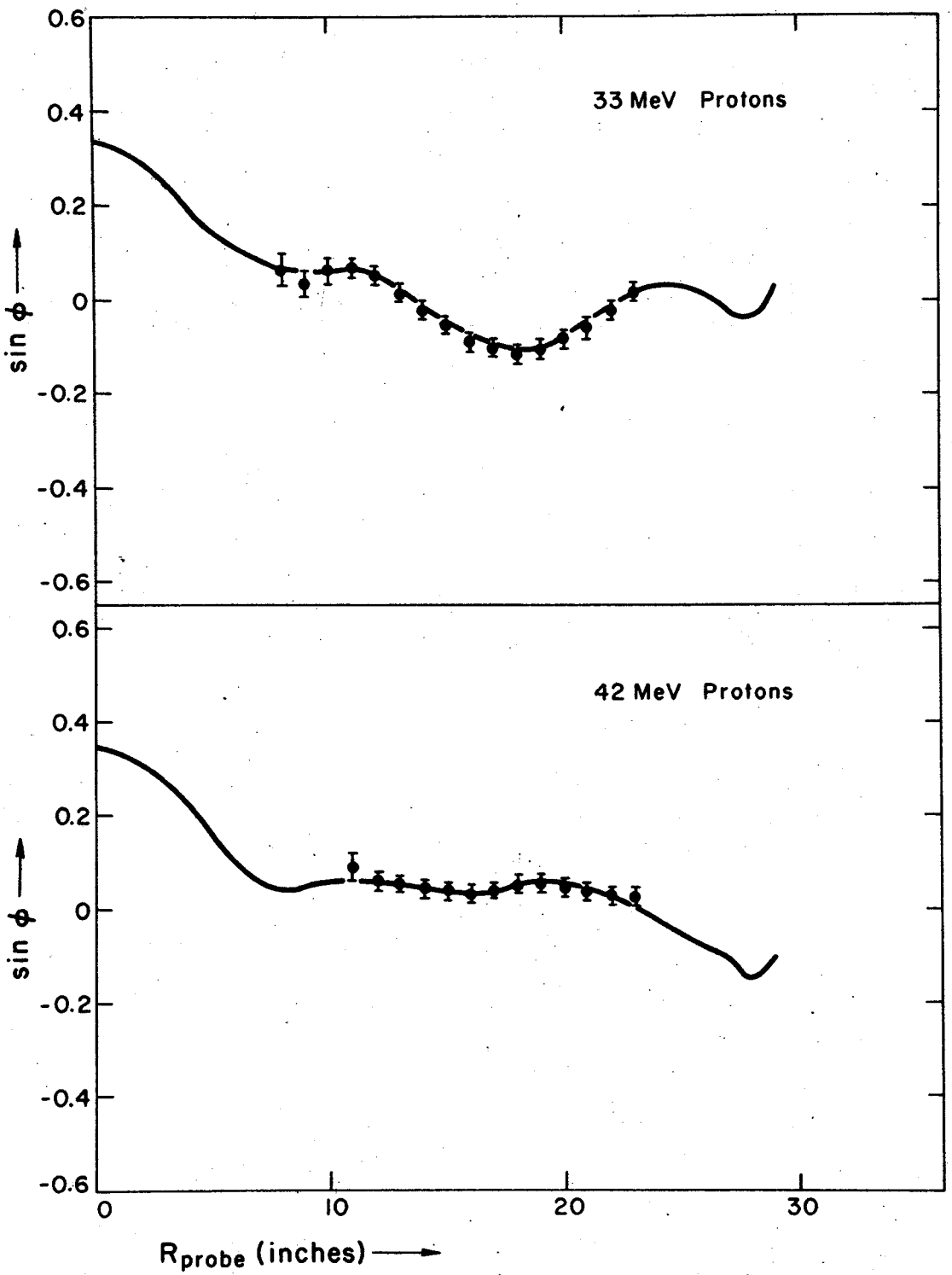

Figure 26. Sinϕ vs. probe radius for 33 MeV and 42 MeV protons. Computed values from SETOP are shown with experimental data obtained by frequency detuning.

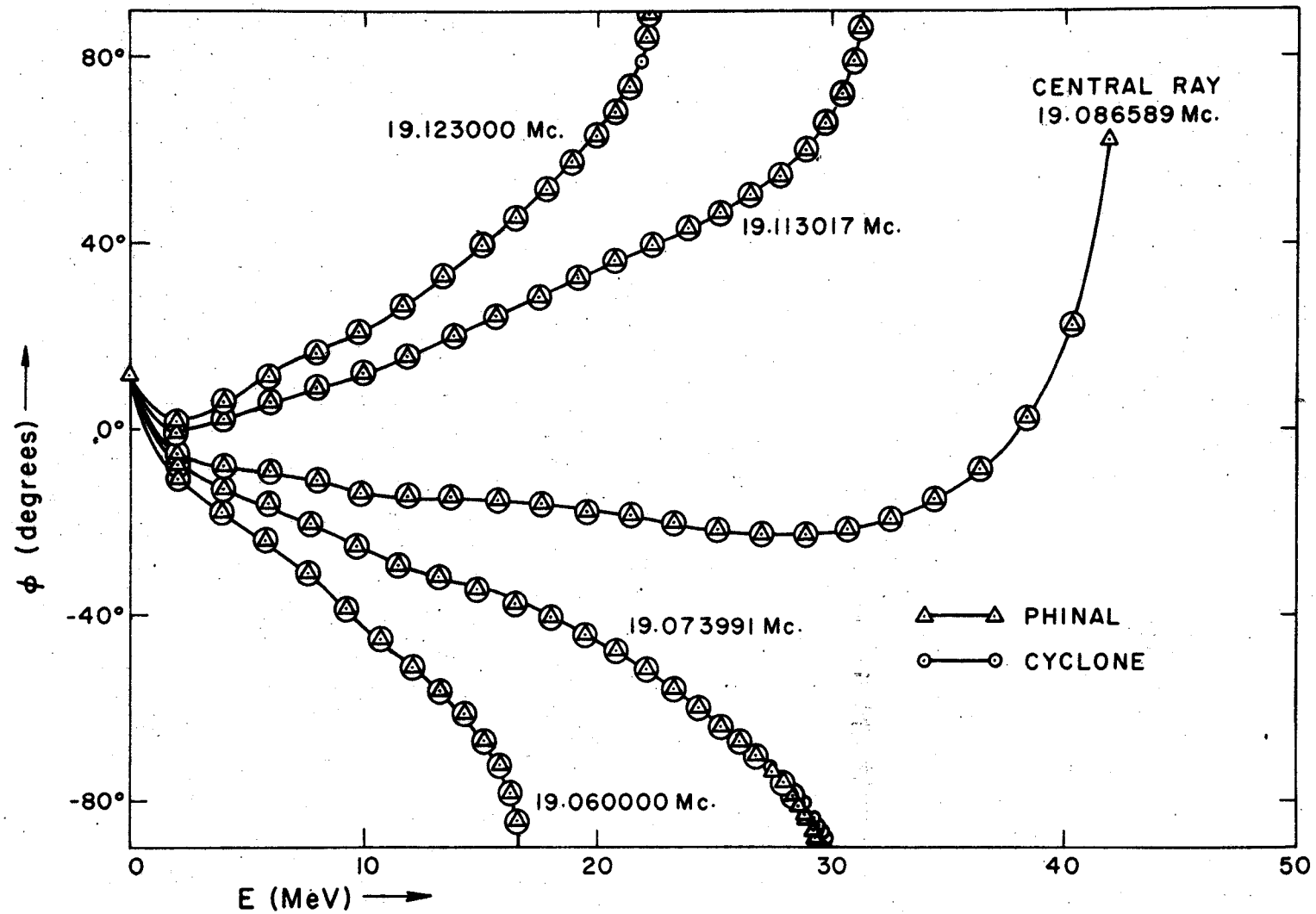

Figure 27. Comparison of sinφ vs. E for a 42 MeV field using a) the separated longitudinal equations as given in SETOP (PHINAL) and b) exact integration of the median plane equations of motion.

One result of use of the longitudinal equation is linearity of $\sin\phi$ versus ω at a given radius. Equation (8-3) can be written in the standard slope-intercept form as:

$$\sin\phi(\omega) = A\omega + B \qquad (8\text{-}6)$$

where A and B are functions only of the magnetic field, dee voltage, and initial phase. This has been checked by examination of computed accelerated orbits, and linearity has been established to well within the accuracy of the experimental measurements.

8.2 Field Detuning

A less frequently used method for phase diagnosis employs detuning of the magnetic field by using trim coils. This method involves several additional approximations; however, careful analysis has shown the method to be essentially identical in accuracy to the frequency detuning method. In addition, trim coil detuning possesses several operational advantages for the MSU cyclotron.

Assuming that the particle orbital angular velocity is related to the average field by the equation:

$$\omega(R) = \frac{q\langle B(R)\rangle}{m(R)} , \qquad (8\text{-}7)$$

equation (8-1) becomes:

$$\sin\phi(E) = \sin\phi_o + \frac{2\pi h}{E_1} \int_o^E \left[\frac{B_o - \langle B\rangle}{\langle B\rangle}\right] dE \ , \qquad (8\text{-}8)$$

where B_o is the isochronous average field.

Since in this case it is more convenient to work directly with radius than energy, the relation:

$$E = \frac{p^2}{2m} = \frac{q^2 \langle B\rangle^2 R^2}{2m} \ , \qquad (8\text{-}9)$$

may be used to convert to a radial integral, with the final result:

$$\sin\phi(R) = \sin\phi_o + \frac{2\pi h q \omega_o}{E_1} \int_o^R [B_o - \langle B\rangle] R dR \ . \qquad (8\text{-}10)$$

Thus, introduction of deviations in the average field B(r) from the isochronous average field $B_o(r)$ results in deviations in the sine of the phase which are proportional to the weighted integral of the field differences. The derivation given above is not rigorous; however, the result is valid for small (first-order) field deviations—relativistic effects actually cancel out and flutter effects can be minimized by taking R as the mean radius of the equilibrium orbit.

If this equation is written twice, where in one of these the field of a trim coil is introduced specifically, subtracting the two equations yields:

$$\sin\phi'(R) = \sin\phi(R) - \frac{2\pi h q \omega_o}{E_1} \int_o^R (\Delta B)_{TC} R dR \qquad (8\text{-}11)$$

where $\phi'(R)$ is the phase resulting from the introduction of a change in the trim coil field $(\Delta B)_{TC}$. If a change in trim coil current ΔI reduces the beam to half amplitude, knowledge of the field per unit current in the trim coil allows calculation of the original beam phase as a function of radius. Since the half-amplitude cutoffs correspond to $\sin\phi(R) = \pm 1$, equation (8-11) can be written for each case as:

$$+1 = \sin\phi(R) + \frac{2\pi q \omega_o}{E_1} \Delta I_+ \int_o^R (B)^i_{TC} R dR \ , \qquad (8\text{-}12a)$$

$$-1 = \sin\phi(R) + \frac{2\pi q \omega_o}{E_1} \Delta I_- \int_o^R (B)^i_{TC} R dR \ , \qquad (8\text{-}12b)$$

where $(B)^i_{TC}$ is the trim coil field per unit current. If ΔI_+ and ΔI_- are measured, equations (8-12) can be solved for $\sin\phi(R)$:

$$\sin\phi(R) = \frac{\Delta I_-(R) - \Delta I_+(R)}{\Delta I_-(R) + \Delta I_+(R)} \qquad (8\text{-}13)$$

An additional complexity enters in actual practice; in order not to disturb the path of the first turn through the central region radial slit, it is necessary to use two trim coils—a larger coil to produce the desired phase excursion to the $\pm 90^\circ$ limits, and a second smaller coil to cancel the field perturbation at the position of the central slit. Equa-

tion (8-11) then contains the difference between two trim coil field functions in the integral. However, since the trim coil fields are assumed to be linear with respect to current, the ratio of the currents in the trim coils required to produce zero net field at the position of the slit remains constant, and equation (8-13) remains valid, where I_+ and I_- refer to the currents in the outer trim coil.

Because it is necessary to use two coils in combination to maintain the field at a constant value at the slit position, the possibility of introducing additional resonances must be considered. In the trim coil detuning measurements thus far carried out on the MSU cyclotron, trim coils number eight and two have been used with their ratio always set to maintain the central field undisturbed. (See Figs. 5 and 6.) The resulting error field possesses large gradients in the edge region of the inner coil; this can lengthen the radial extent of the $\nu_r = 1$ resonance and thereby introduce large radial oscillations into an otherwise stable beam, or if the gradient is large, a region of axial instability can result.

The importance of such phenomena was investigated by calculating equilibrium orbits in various displaced fields using trim coil currents computed to drive the beam to $\pm 90^\circ$ phase limits at various radii. Figure 28 shows the radial focusing frequency ν_r as a function of radius for a widely varied set of such displaced magnetic fields, including the

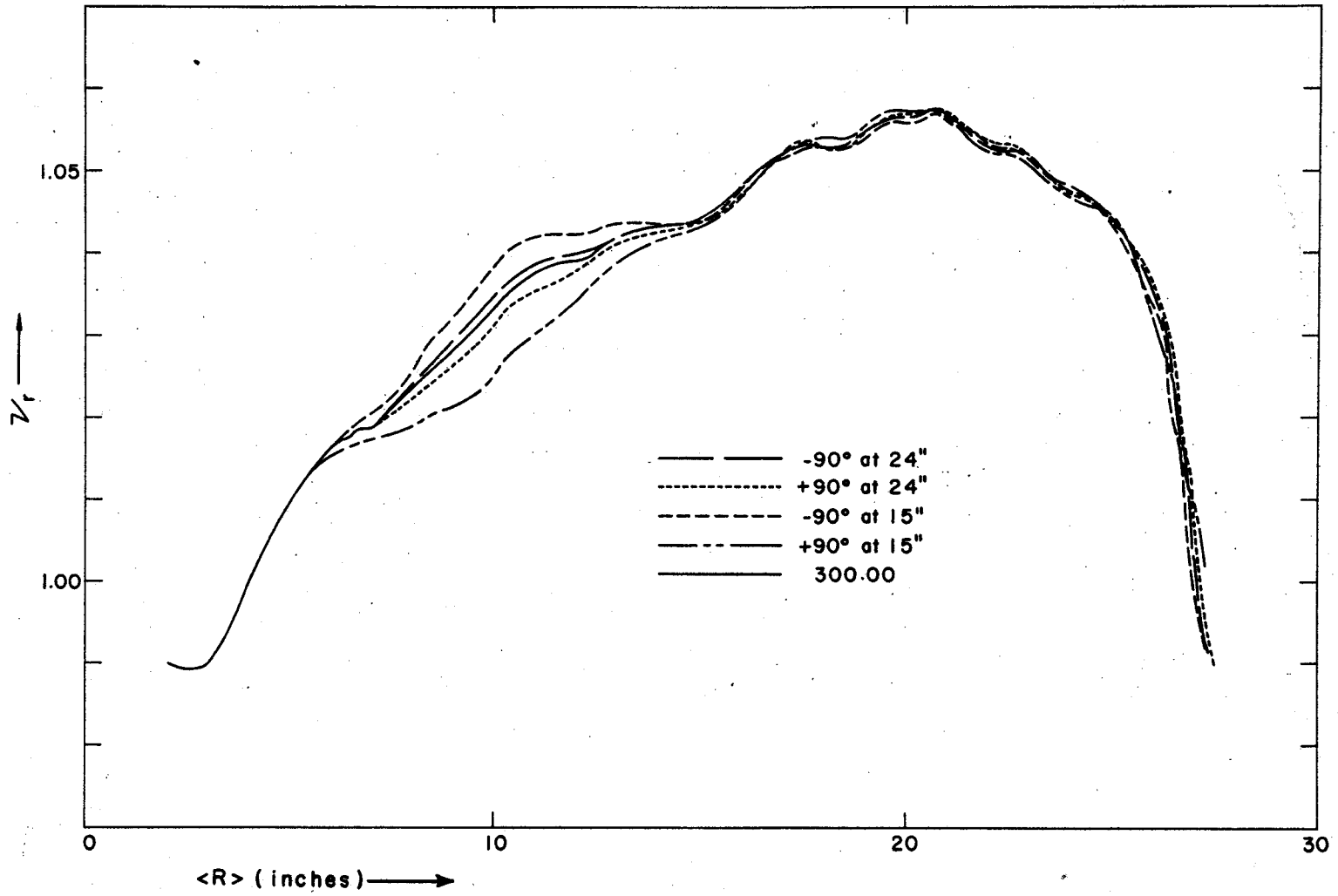

Figure 28. Computed ν_r vs. radius for the unperturbed 42 MeV field, along with that obtained when trim coils 2 and 8 are detuned to drive the phase of the central ray to $\pm$ 90° at 15" and 24", respectively.

undisplaced field; Fig. 29 shows the axial focusing frequency ν_z as a function of radius for the same fields. (The field used here is the same 42 MeV proton field discussed previously.) The general absence of unstable conditions indicates that resonance errors are unlikely.

Another source of error can arise if magnetic field changes lead to variation of energy with radius. The equilibrium orbit data show only small variations in radius versus energy for field displacements which drive the beam off resonance at about half of the extraction radius. In addition, centering errors described previously can create inaccuracies in resulting measurements. These problems were investigated by computation of accelerated orbits in CYCLONE; a table of radius versus energy for several displaced fields is given in Table 3. Using appropriate starting conditions, the amplitude of the radial oscillation was retained at the minimal value of about one millimeter, and no increase of oscillation amplitude was observed with variation of trim coil current. The uniformity of the radius versus energy function indicates that no errors result from the use of the method of trim coil detuning.

A result of the theory, analogous to the case of frequency adjustment, is linearity of $\sin\phi$ with trim coil current. Examination of computed accelerated orbits verified this assumption to essentially the same degree as in the case of frequency variation. The linearity of $\sin\phi$ with

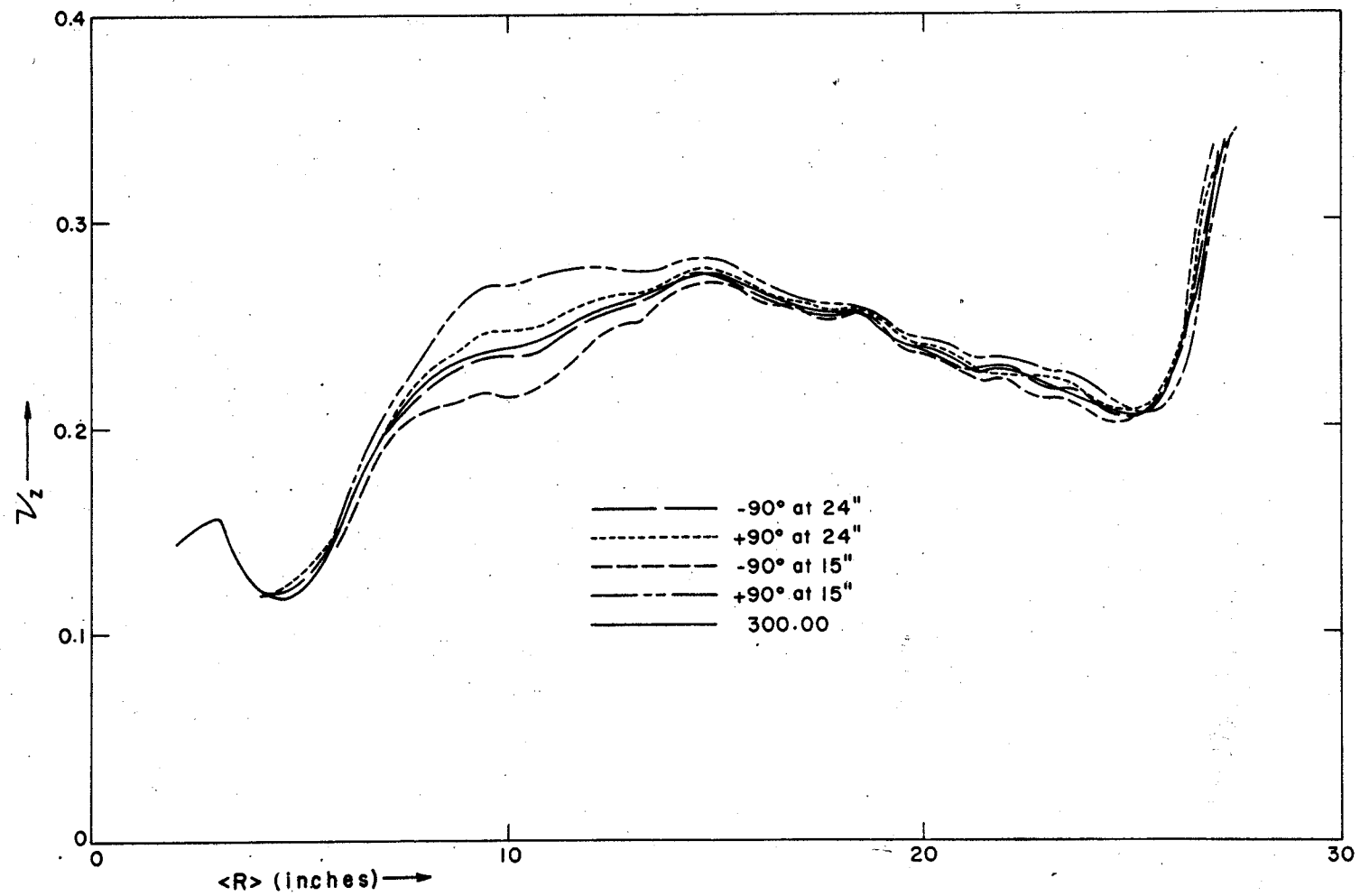

Figure 29. Computed ν_z vs. radius for the unperturbed 42 MeV field, along with that obtained when trim coils 2 and 8 are detuned to drive the phase of the central ray to $\pm$ 90° at 15" and 24", respectively.

Table 3. Energy versus radius as a function of trim coil current for the 42 MeV field; such data establish the uniqueness of the radius as a function of energy within limits of experimental measurement, and validate the method of trim coil detuning described.

	ΔI_{TC8}=-33.80amps	ΔI_{TC8}=-22.49amps	ΔI_{TC8}=0	ΔI_{TC8}=+13.63amps	ΔI_{TC8}=+15.24amps
E	$\phi \rightarrow$ +90° at 24"	$\phi \rightarrow$ +90° at 27"	central ray	$\phi \rightarrow$ -90° at 27"	$\phi \rightarrow$ -90° at 24"
(MeV)	R(inches)	R(inches)	R(inches)	R(inches)	R(inches)
10	13.521	13.520	13.523	13.518	13.519
15	16.480	16.474	16.463	16.464	16.455
20	18.883	18.911	18.876	18.882	18.891
25	21.041	21.051	21.046	21.042	21.016
30	———	23.032	23.026	———	———

current depends only on the assumption of a first-order change in field and is independent of the other assumptions made in deriving equation (8-12); since the field changes required to shift the phase to $\pm 90^{\circ}$ are quite small (of order 10^{-3} or less), it is not surprising that this linear relation is accurate.

As in the case of frequency detuning, it was found to be impossible to use the trim coil adjustment method at large radii due to the rapid rise in phase at the outer radii. This effect occurs at slightly larger radii for trim coil adjustment, although the critical radius moves inward as the particle energy becomes larger, as can be seen by inspection of Fig. 22.

Results of comparison of actual integrated orbits with data obtained from integration of the longitudinal equations are presented in Fig. 30 for the field discussed before. The good agreement between the two procedures again verifies the adequacy of the longitudinal equation; as in the case of frequency variation, shown in Fig. 27, discrepancy results in the region where the phase approaches -90° slowly, and coupling effects become significant. Furthermore, agreement between maximum radius obtained for given trim coil displacements pre-computed by equations (8-12) and that obtained by orbit integration indicates the accuracy of the assumptions involved in the derivation of these relations; these data are summarized in Table 4.

Further evidence of the over-all accuracy of the trim

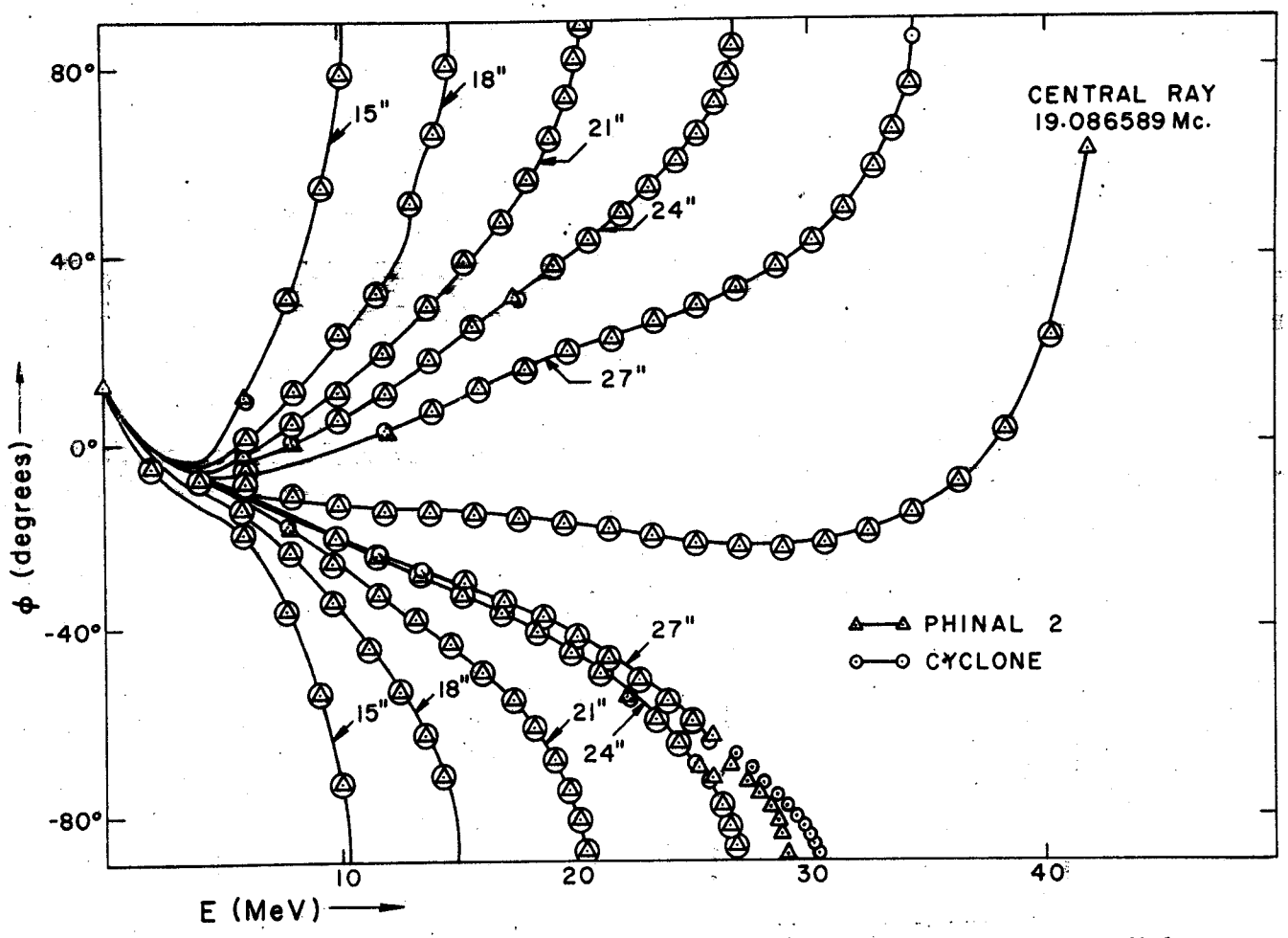

Figure 30. Comparison of sinφ vs. E obtained from a) integration of exact radial equations of motion (CYCLONE) and b) use of separated longitudinal equations in SETOP (PHINAL 2), for sets of detuned trim coil currents computed by the approximate relations used in SETOP to drive the central ray of the beam to ± 90° at several radii. The data for the 42 MeV proton field are illustrated.

Table 4. Comparison of central ray maximum radius and corresponding phase obtained by CYCLONE using trim coils detuned to drive the phase of the central ray to ± 90° at the indicated radii. The pre-computed trim coil currents were obtained from SETOP using simple approximations as described in the text.

Pre-computed	$\phi \rightarrow +90°$ ray			$\phi \rightarrow -90°$ ray		
Maximum Radius (inches)	$R(\phi=+90°)$ (inches)	R_{max} (inches)	$\phi(R_{max})$ (degrees)	$R(\phi=-90°)$ (inches)	R_{max} (inches)	$\phi(R_{max})$ (degrees)
15.00	14.964	14.976	93.1	14.950	14.965	-87.8
18.00	18.002	18.037	85.4	17.998	18.005	-89.0
21.00	21.047	21.061	91.7	20.950	20.985	-93.0
24.00	24.004	24.058	86.0	23.905	23.948	-92.7
27.00	27.096	27.097	89.2	———	———	———

coil detuning procedure lies in its use to set the main field; by adjusting the main field such that pre-computed trim coil currents drive the beam to half amplitude at a fixed radius, the main field excitation can be resolved to within five parts in 100,000. If the beam is well-centered and the starting phase is accurately known, the pre-computed phase history behavior is obtained to within $\pm$ 0.025 in $\sin\phi$ for all energies.

Similar to the case of frequency detuning, an envelope of trim coil displacement current necessary to drive the beam to half maximum is computed for each operating point. Such an envelope is plotted in Fig. 31 for a 25 MeV proton field, along with the experimentally determined curve. The trim coil displacement current envelope was used to determine the phase curve experimentally, and this data is plotted in Fig. 27 along with the phase curve obtained from frequency detuning. These results verify the validity of the procedure as well as the high quality of the magnetic field measurements and the computations.

8.3 Initial Phase

Using the measured phase data, it is possible to extrapolate back to zero energy by comparison with the computed phase data, and obtain the nominal starting phase ϕ_o. Corresponding to ϕ_o is a starting RF time τ_o at which the particles leave the ion source; τ_o is a function of the source-to-puller geometry, and is related to ϕ_o by the position

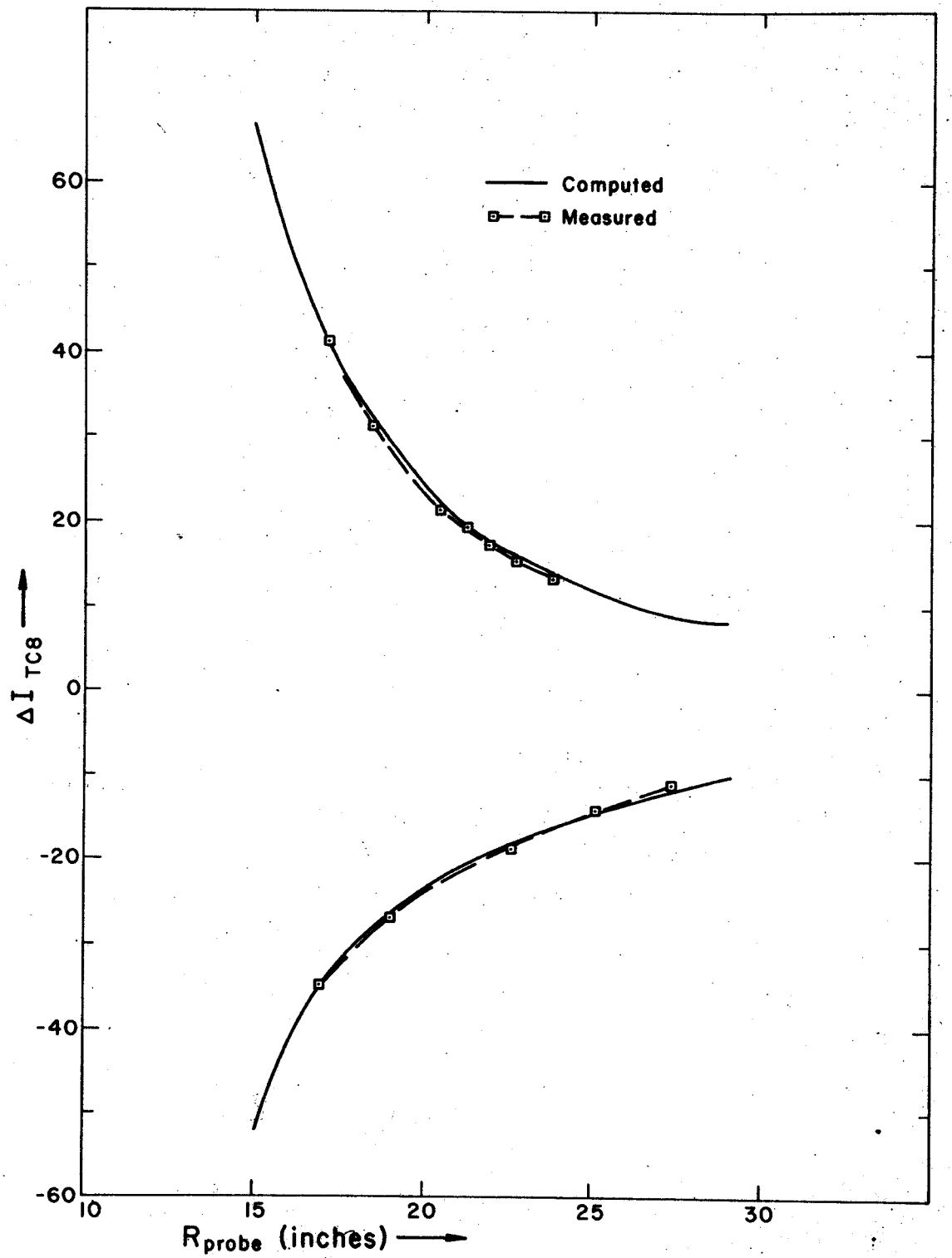

Figure 31. Envelope of trim coil 8 currents required to drive the central ray of the beam to ± 90° for the 25 MeV proton field (Run 200). Computed values obtained from SETOP are shown along with measured data.

of the source and puller with respect to machine center. It is desirable to determine starting time for which peak beam intensity is obtained. Since this starting time is an essentially incalculable quantity, it has been necessary to assume a reasonable value in order to perform detailed calculations of behavior of orbits in the central region[31]. Understanding of such behavior and knowledge of the starting phase is basic to the procedure of phase selection using an axial slit; thus it is of particular interest to determine the starting phase experimentally and verify the assumptions made in previous orbit calculations. It is necessary to determine τ_o very accurately, for the comparisons given, since a small starting phase error can introduce substantial error into the energy-phase history, especially near the region where $\sin\phi$ approaches -1 asymptotically, as in the examples of Figs. 27 and 30.

8.4 Phase Width

A useful variation of the phase measuring technique is to reduce the beam to quarter, eighth, tenth, etc., amplitude and determine the complete phase profile of an accelerating beam.

Such a profile of beam intensity as a function of trim coil current has been obtained experimentally, and is shown in Fig. 32 for the 25 MeV field at two radii. From these profiles the phase width of the beam is computed to be approximately 15° at the nominal starting phase $+20^\circ$.

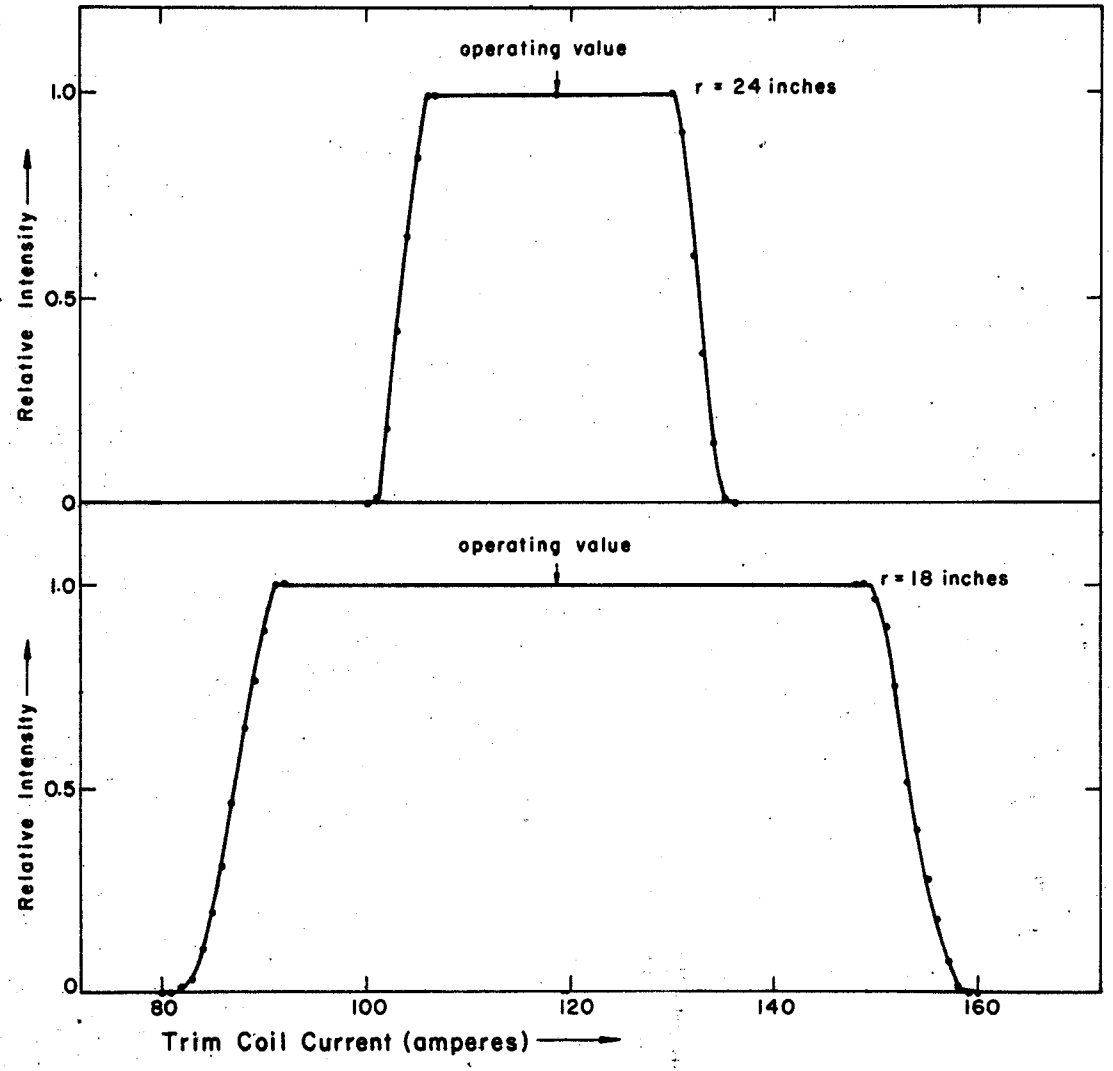

Figure 32. Beam intensity versus trim coil current at two radii in the 25 MeV proton field. These data can be used to obtain the central phase of the beam as a function of radius as well as the phase width of the beam.

With the aid of CYCLONE, the measured phase widths can be compared with widths inferred from turn patterns from a differential radial probe. Figure 33 shows a turn structure pattern obtained in the 25 MeV field using such a probe of 1/32 inch width. The pattern clearly shows the turn structure out to the extraction region, where the effect of the $\nu_r = 1$ resonance is observed. Using CYCLONE, a "beam" of fifteen particles, started at starting phases of one degree intervals about the central ray $\tau_o = -30^o$ (roughly equivalent to $\phi_o = +20^o$), was accelerated, and the radius of each particle plotted as a function of its starting phase over the region 100-130 turns is shown in Fig. 34. The "beam" was assumed to be continuous as a function of starting phase, and was given a radial width of one millimeter, the size of the slit in the ion source chimney. The resulting "turns" are indicated by the gray areas in Fig. 34. From this figure the density of particles in a radius interval of 0.030 inches, the width of the differential beam probe, was determined as a function of radius, and is also plotted in Fig. 34. Finally, at the top of Fig. 34 is the section of the experimental turn structure pattern corresponding to the computed pattern, on the same scale. The computed and measured turn structure patterns are similar in every respect: 1) both possess the same radial oscillation amplitude of about .120 inch, 2) the peak-to-valley ratio is essentially identical for all phases of the radial oscillation, 3) the characteristic sharp edge of each turn on the

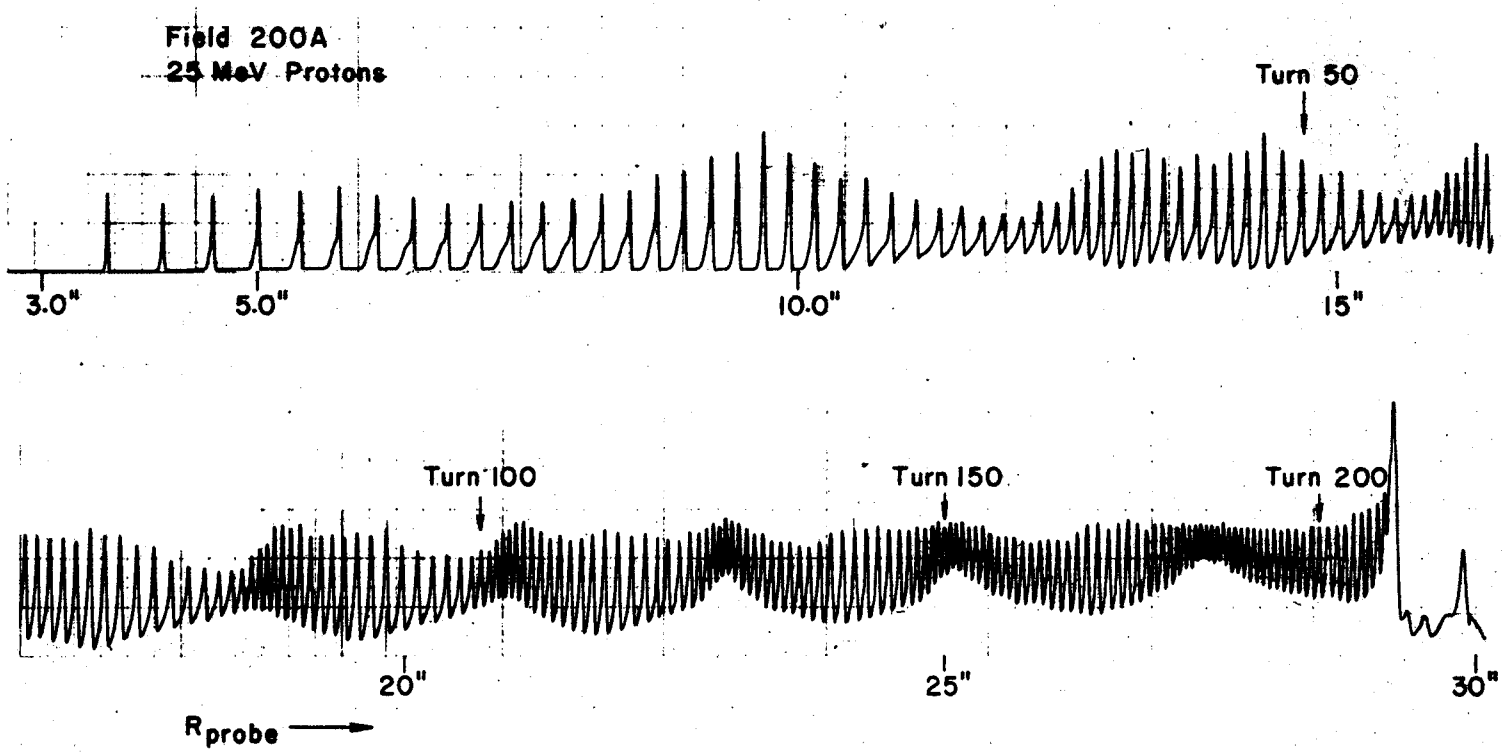

Figure 33. Radial differential probe pattern for 25 MeV protons.

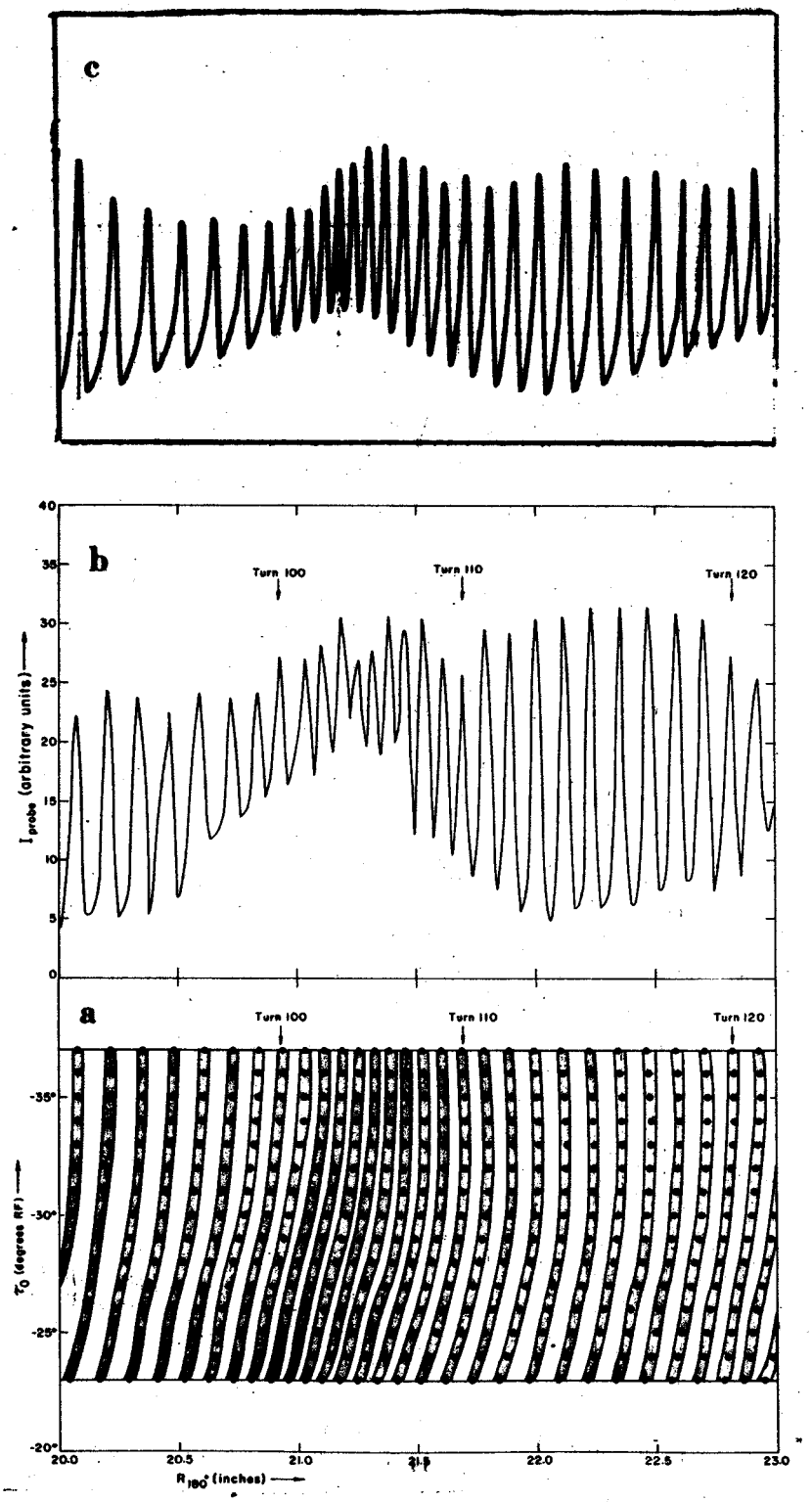

Figure 34. Comparison of "computed" and experimental radial probe patterns for the 25 MeV proton field near turn 100. Part (a) shows radius as a function of starting phase for successive turns, obtained by accelerating particles in CYCLONE, then introducing a radial width for the beam. Part (b) shows radial intensity contour obtained by summing the gray area in a small radial interval (regardless of turn number). This can be compared directly to the section of the 25 MeV radial differential probe pattern shown in part (c).

high-radius side resulting from the parabolic radial contour of the turns appears in both plots. This striking agreement between the computed and measured patterns confirms the high quality of the calculations performed in obtaining the operating point, and the accuracy with which CYCLONE computes accelerated orbits in actual cyclotron fields.

8.5 Dee Voltage

Equations (8-4a) and (8-4b) may be solved to obtain the maximum energy gain per turn E_1 as a function of radius, in terms of the measured frequencies ω_+ and ω_-:

$$E_1 = \frac{\pi(\omega_+ - \omega_-)}{\omega_o} [E+F(E)] \qquad (8\text{-}14)$$

where the dee voltage is a function of E_1 depending upon the RF mode. (See Section 6-3.) The radial dependence of the dee voltage obtained in this manner is given in Fig. 35 for the 25 MeV, 33 MeV, and 42 MeV proton fields. These data are in good agreement with results of calculations in which the dees are composed of short sections of transmission line. It should be noted that E_1 cannot be obtained without reference to the calculations; the energy E and F(E) at each radius must be obtained by inspection of equilibrium orbit data.

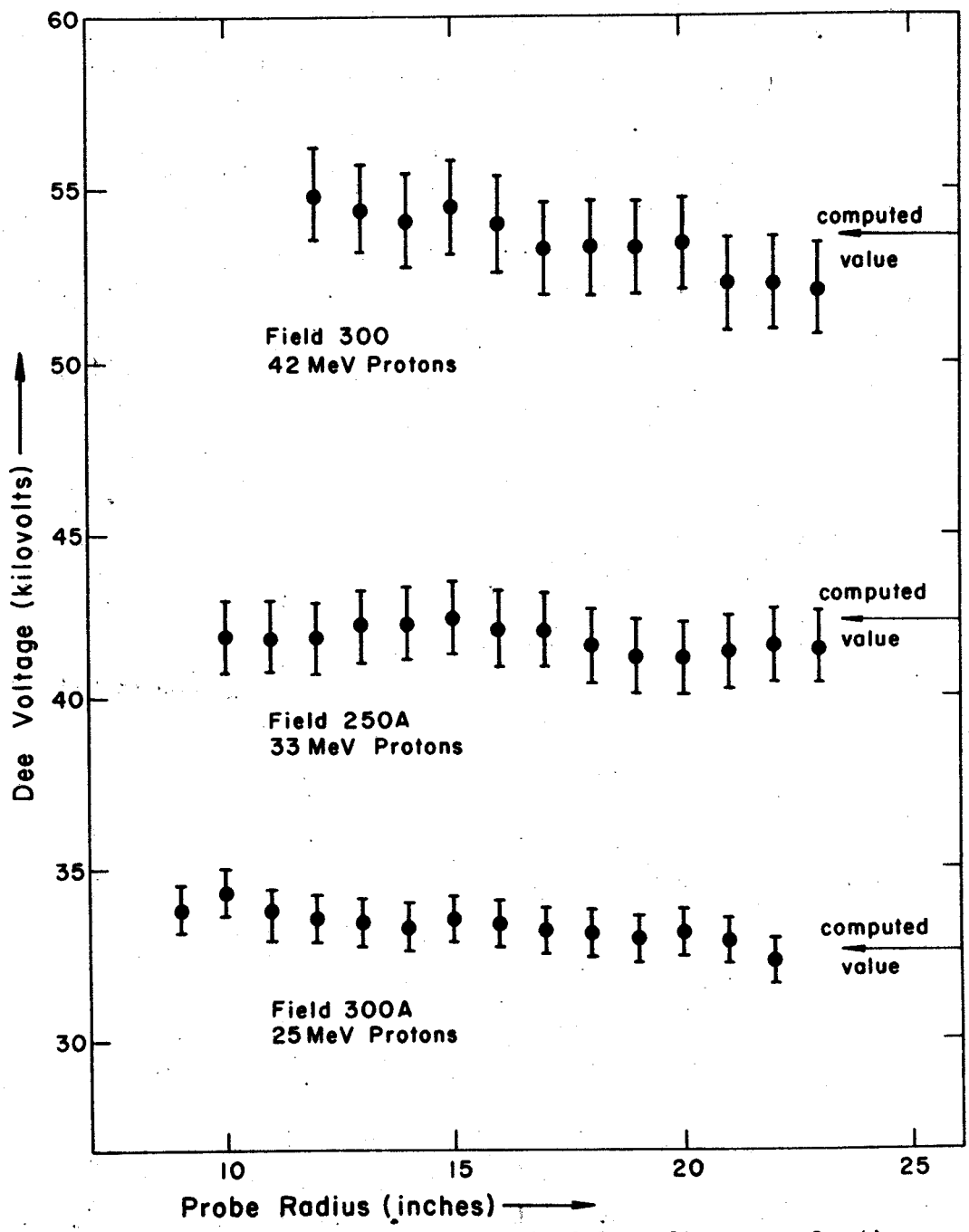

Figure 35. Experimentally determined dee voltage as a function of radius for three proton fields. Computed value is indicated by arrow on right.

8.6 Radial Focusing Frequency

It can be seen from Fig. 33 that the radial turn structure pattern possesses a periodic behavior; the radial focusing frequency is related to the number of turns in one precession cycle:

$$N_r = \frac{1}{|\nu_r - 1|} \quad . \tag{8-15}$$

The number of turns per cycle can be readily obtained from a turn structure pattern such as that of Fig. 33, and accurate experimental values for ν_r as a function of radius obtained. Figure 36 shows the computed ν_r versus radius curve for four magnetic fields, along with the experimental values obtained in the prescribed manner. The horizontal bars indicate the radial interval over which the turns were counted to obtain an average value of ν_r, and the vertical bars indicate the error in the average ν_r arising from inaccuracies in the number of turns counted. Note that for fields 200 and 300 both trim coil fields and main magnetic fields were measured. For field 250 the trim coil fields were obtained by interpolation, and field 280 was obtained entirely by interpolation in main magnet and trim coil fields.

8.7 Axial Focusing Frequency

A z-probe with a 1/8 inch square sensitive area which can be moved vertically over a 3/4 inch distance has been used to obtain data on axial motion. For these measurements

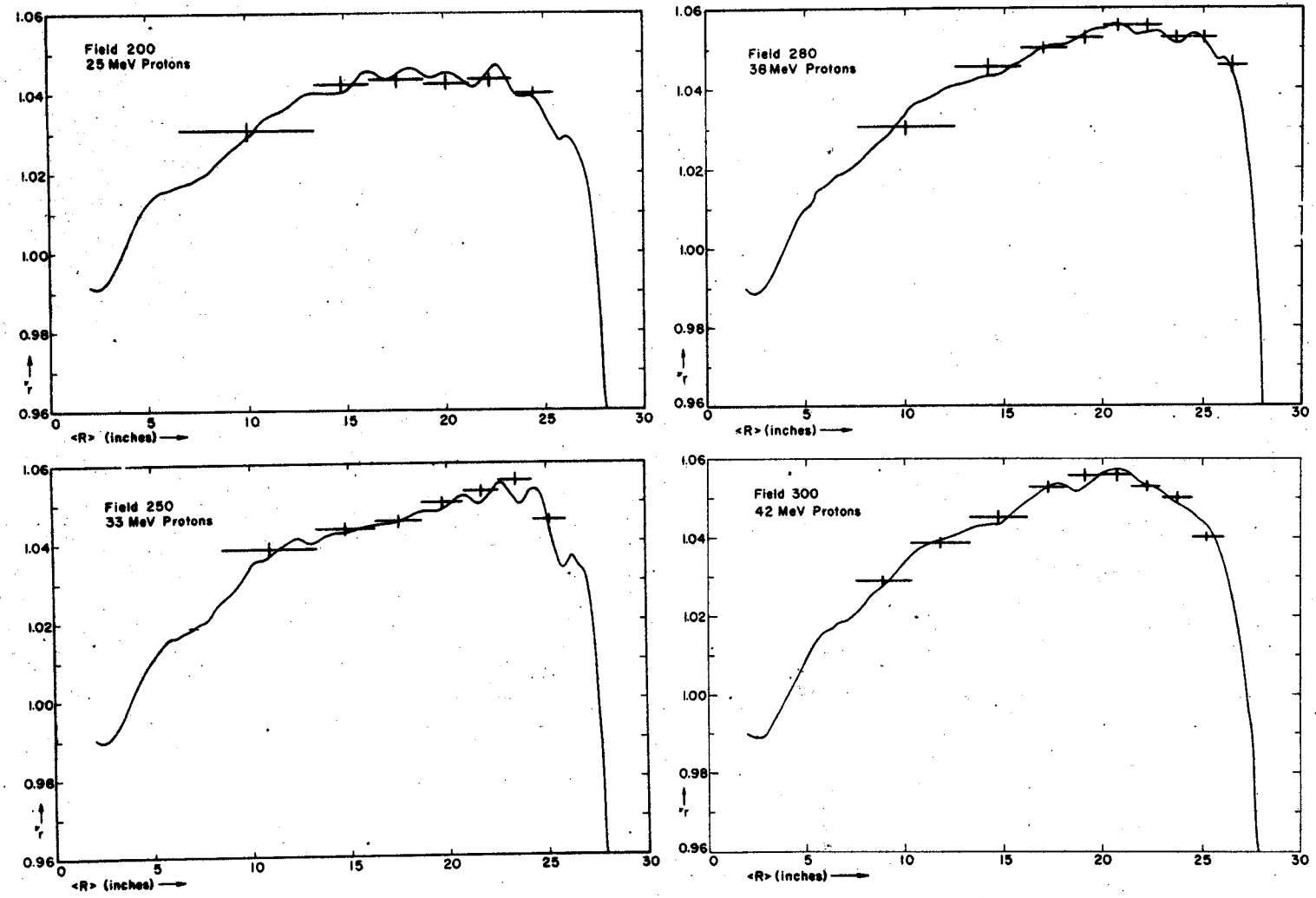

Figure 36. Radial focusing frequency as a function of average radius for four proton fields; computed values obtained from SETOP fitted fields are shown along with measured data. Field 280 is obtained entirely by interpolation and field 250 trim coil fields are obtained by interpolation.

a large coherent axial oscillation was induced in the beam using a thin slit 0.15 inches above the median plane at the position of the first quarter turn. Making successive radial scans with the probe at various z-values, an effective nine-finger axial probe was obtained. Analyzing such data, it is possible to follow the coherent axial oscillation out to the edge region of the magnetic field. The number of turns in a complete cycle of axial motion is related to the focusing frequency:

$$N_z = \frac{1}{\nu_z} \quad . \tag{8-16}$$

Following the oscillation, the number of turns per cycle can be accurately obtained, allowing precise determination of ν_z. The results of such measurements are shown in Fig. 37 for the same fields shown in Fig. 36 to illustrate radial focusing frequency. The radial interval over which each average value of ν_z was obtained is indicated by the horizontal bars; the vertical error bars arise from errors in counting the number of turns per cycle of axial motion.

8.8 Summary

The excellent agreement between the beam properties obtained through computation and properties obtained experimentally verifies both the high quality of the magnetic field measurements and the accuracy of the SETOP computations performed in obtaining operating points. The precise agreement between computed and experimental properties clearly

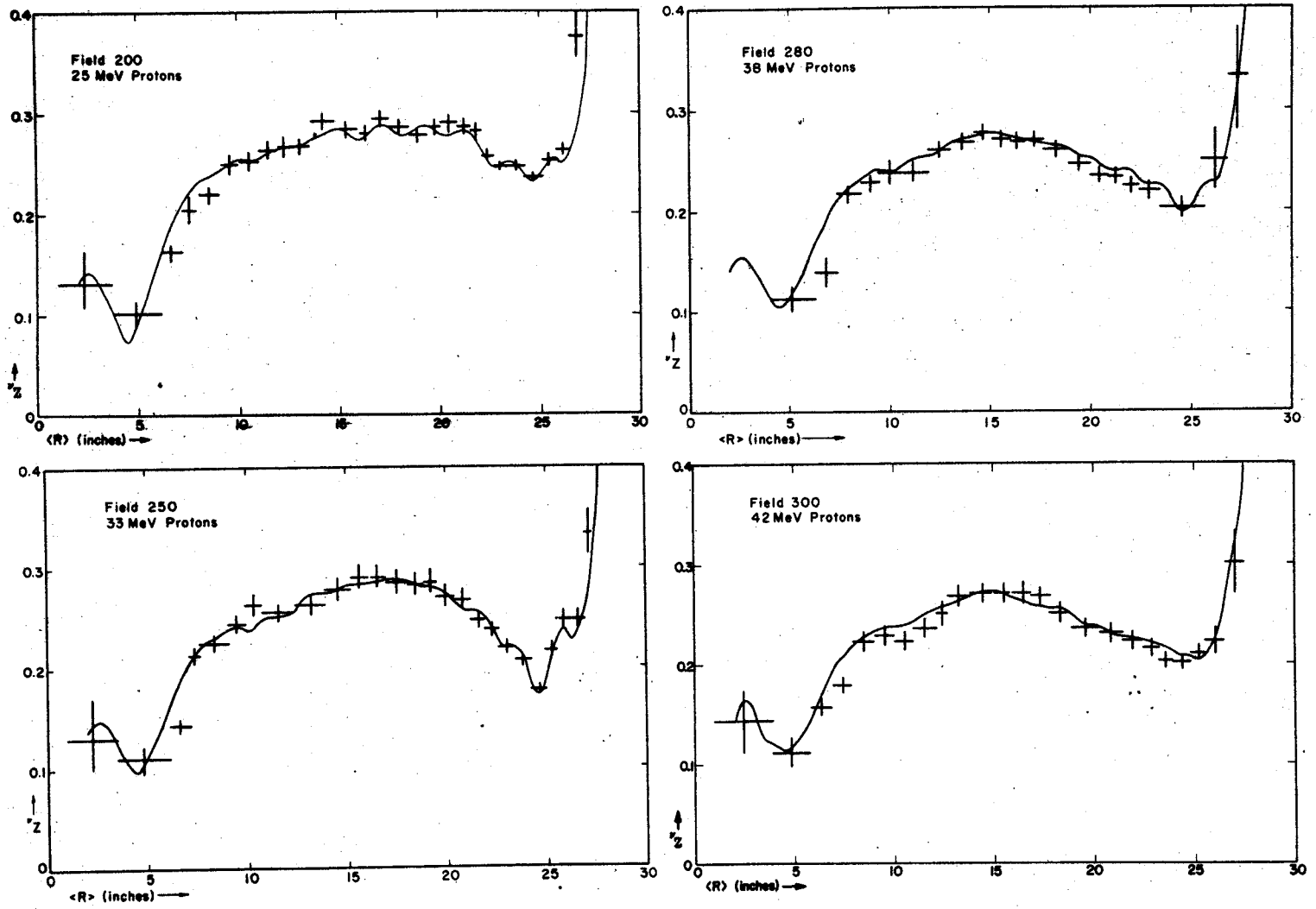

Figure 37. Axial focusing frequency as a function of average radius for four proton fields; computed values obtained from SETOP fitted fields are shown along with measured data. Field 280 is obtained entirely by interpolation and field 250 trim coil fields are obtained by interpolation.

demonstrates the power of the computer in predicting detailed behavior of orbits in cyclotrons.

REFERENCES

1. H. G. Blosser, Magnet Design for the MSU 50 MeV Cyclotron, Proceedings of the International Conference on Sector-Focused Cyclotrons and Meson Factories, CERN, April, 1963.
2. W. P. Johnson, Radio-Frequency System for the MSU Cyclotron, Proceedings of the International Conference on Sector-Focused Cyclotrons and Meson Factories, CERN, April, 1963.
3. "Sector-Focused Cyclotrons", Proceedings of the Sea Island Conference, February, 1958.
4. M. Reiser and J. Kopf, Michigan State University Cyclotron Project Report MSUCP-19, May, 1964.
5. J. W. Beal, Michigan State University Cyclotron Project Report MSUCP-21, August, 1964.
6. R. E. Berg and H. G. Blosser, The Focusing Air-Core Magnetic Channel for the MSU 55 MeV Cyclotron, IEEE Transactions on Nuclear Science, June, 1965.
7. E. Kashy, Beam Transport System for the MSU Cyclotron, Michigan State University Cyclotron Laboratory internal report, August, 1966.
8. H. G. Blosser, Problems and Performance in the Cyclotron Central Region, IEEE Transactions on Nuclear Science, August, 1966.
9. M. M. Gordon, Single-Turn Extraction, IEEE Transactions on Nuclear Science, August, 1966.

10. A. A. Garren, Nuclear Instruments and Methods 18, 19 (1962), 309-322.

11. H. G. Blosser, M. M. Gordon, and T. I. Arnette, Nuclear Instruments and Methods 18, 19 (1962), 488-519.

12. H. G. Blosser and M. M. Gordon, Nuclear Instruments and Methods 13 (1961),101-117.

13. R. E. Berg, H. G. Blosser, and W. P. Johnson, Michigan State University Cyclotron Project Report MSUCP-22, August, 1966.

14. J. A. Futhey, Michigan State University Cyclotron Project Report MSUCP-18, July, 1963.

15. D. A. Lind, M. E. Rickey, and B. M. Bardin, Nuclear Instruments and Methods 18, 19 (1962), 129-134.

16. K. R. Symon, D. W. Kerst, L. W. Jones, L. J. Laslett, and K. M. Terwilliger, Physical Review 103 (1956), 1837-1859.

17. J. E. Stover, Michigan State University Cyclotron Project Report MSUCP-3, August, 1960.

18. H. G. Blosser, M. M. Gordon, and M. Reiser, Central-Region Studies for the MSU Cyclotron, Proceedings of the International Conference on Sector-Focused Cyclotrons and Meson Factories, CERN, April, 1962.

19. M. M. Gordon and D. A. Johnson, private communication.

20. M. M. Gordon and T. A. Welton, Computational Methods for AVF Cyclotron Design Studies, ORNL-2765.

21. M. M. Gordon and W. Joho, Correction of Axial Focusing in a Cyclotron by Average Field Trimming, Michigan State University Cyclotron Laboratory internal report (1964).

22. Handbook of Mathematical Functions, Edited by M. Abramowitz and I. A. Stegum, National Bureau of Standards Applied Mathematics Series No. 55, June, 1964.

23. J. D. Young, A. S. Kenney, and A. A. Garren, Nuclear Instruments and Methods 18, 19 (1962), 323-326.

24. M. M. Gordon and W. Joho, Energy-Phase Analysis of a Cyclotron Beam, Michigan State University Cyclotron Laboratory internal report (1964).

25. R. E. Berg, H. G. Blosser, and M. M. Gordon, Control of the Michigan State University Cyclotron, IEEE Transactions on Nuclear Science, August, 1966.

26. H. G. Blosser and A. I. Galonsky, The Michigan State University 55 MeV Cyclotron: Progress and Status, February,1966, IEEE Transactions on Nuclear Science, June, 1966.

27. Scientific Data Systems: Sigma Seven.

28. T. I. Arnette, Program CYCLONE, Michigan State University internal report (1966).

29. A. A. Garren and L. Smith, Diagnosis and Correction of Beam Behavior in an Isochronous Cyclotron, Proceedings of the International Conference on Sector-Focused Cyclotrons and Meson Factories, CERN, April, 1963.

30. M. M. Gordon, Nuclear Instruments and Methods 18, 19 (1962), 268-280.

31. M. Reiser, Michigan State University Cyclotron Project Report MSUCP-15, February, 1963.

32. V. H. Rutishauser, Zur Matrizeninversion nach Gauss-Jordan, Z. angew. Math. Mech. 10 (1959), 281-291.